UNIVERSITY OF HAWAII
LIBRARY
JUL 14 '50

The
PHILOSOPHICAL MAGAZINE

FIRST PUBLISHED IN 1798

L. 41 SEVENTH SERIES No. 317 JUNE, 1950

A Journal of Theoretical Experimental and Applied Physics

EDITOR
PROFESSOR N. F. MOTT, M.A., D.Sc., F.R.S.

EDITORIAL BOARD
SIR LAWRENCE BRAGG, O.B.E., M.C., M.A., D.Sc., F.R.S.
ALLAN FERGUSON, M.A., D.Sc.
SIR GEORGE THOMSON, M.A., D.Sc., F.R.S.
PROFESSOR A. M. TYNDALL, C.B.E., D.Sc., F.R.S.

PRICE 10s.
Annual Subscription £5 2s. 6d. payable in advance.

TED AND PUBLISHED BY TAYLOR & FRANCIS LTD., RED LION COURT, FLEET ST., LONDON. E.C.4

Annals of Science

A QUARTERLY REVIEW OF THE HISTORY OF SCIENCE SINCE THE RENAISSANCE

EDITORS

D. McKIE, D.Sc., Ph.D.,
University College, London.

HARCOURT BROWN, M.A., Ph.D.,
Brown University, Providence, R.I., U.S.A.

H. W. ROBINSON,
Former Librarian,
Royal Society of London.

ANNUAL SUBSCRIPTION

£2 0s. 0d.

OR

10s. 6d.
PER PART
POST FREE

TAYLOR & FRANCIS, LTD., Red Lion Court, Fleet Street, LONDON, E.C.4

ALERE FLAMMAM

THE MATHEMATICAL WORKS OF JOHN WALLIS, D.D., F.R.S.

by

J. F. SCOTT, Ph.D., B.A.

"His work will be indispensable to those interested in the early history of The Royal Society. I commend to all students of the Seventeenth Century, whether scientific or humane, this learned and lucid book."—Extract from foreword by Prof. E. N. da C. Andrade, D.Sc., Ph.D., F.R.S.

Recommended for publication by University of London

12/6 net

Printed and Published by:

TAYLOR & FRANCIS, LTD.
RED LION COURT, FLEET STREET, LONDON, E.C.4.

XLVI. *The Refractive Index and Classical Radiative Processes in an Ionized Gas.*

By K. C. Westfold,
The Queen's College, Oxford*.

[Received March 10, 1950.]

Abstract.

The rôle of the refractive index in the classical theory of radiation in an ionized gas is investigated. The Lorentz formula for the macroscopic absorption coefficient is recovered from microscopic considerations, and the heuristic modification of the formula for the emissivity obtained in a previous paper is justified. The consequent modification of the free-free transition probabilities is indicated.

§1. Introduction.

So long as astronomical observations were confined to frequencies greater than the infra-red, astrophysicists have been able to interpret them in terms of a microscopic theory of radiative processes in a medium whose refractive index is always unity.

In recent years observations have been extended to radio frequencies which, although they allow an adequate interpretation within the classical theory of radiation, require a detailed study of the part played by a refractive index that is a function of the frequency of the radiation.

It is generally accepted that the solar atmosphere and interstellar space are populated by fully ionized atoms. Such a medium profoundly affects the propagation of radio-frequency radiation.

The classical theory of radiation in an ionized gas in the absence of magnetic fields has been considered in a recent paper by Smerd and Westfold (1949)†. They found it necessary to introduce the refractive index as a factor in the denominator, in building up the macroscopic absorption coefficient from the microscopic transition probabilities obtained by ignoring the refractive index, and again as a factor in the numerator of the formula for the emissivity.

The first was necessary to secure agreement with the classical Lorentz formula and the second so that the resulting formula for the intensity divided by the refractive index should agree with the Planck formula.

In this paper we shall justify this procedure by investigating the microscopic processes of absorption and emission, while taking into account the electromagnetic scattering by the other particles of the

---

* Communicated by the Author.

† This paper will be subsequently referred to as S.W.

medium. It is this latter effect which constitutes the macroscopic refractive index. Although many of the results obtained are not essentially new, it is necessary to state them in a form that shows their dependence on the refractive index explicitly.

§ 2. ELECTROMAGNETIC SCATTERING AND THE REFRACTIVE INDEX.

The relation between electromagnetic scattering and the refractive index has been considered extensively by Darwin (1924) and Hartree (1928, 1931). In an ionized gas, scattering, absorption and emission associated with the motions of the ions are negligible compared with those associated with electron motions.

The mean motion of a free electron, of charge e and mass m, in an electromagnetic field ($\mathbf{E}$, $\mathbf{H}$) is determined by the equation (see *e.g.* Burkhardt (1950))

$$m(\dot{\mathbf{v}}+\nu\mathbf{v})=e\left(\mathbf{E}+\frac{1}{c}\mathbf{v}\times\mathbf{H}\right),$$

where $\mathbf{v}$ is the mean velocity induced by the field. The units are Gaussian. The term $m\nu\mathbf{v}$ represents the average damping force due to elastic collisions, principally with ions. On free-path considerations ν is taken to be the collision frequency, but the kinetic-theory derivation of the absorption coefficient in S.W. indicates that $\frac{3}{4}\nu$ should be the collision frequency. Provided $v \ll c$, the velocity of light *in vacuo*, the second term on the right side may be neglected, leaving the linear relation

$$\dot{\mathbf{v}}+\nu\mathbf{v}=\frac{e}{m}\mathbf{E}. \qquad (2.1)$$

Now under the condition $v \ll c$ the scattered field due to the induced motion of the electron is equivalent to that of an elementary current of strength $e\mathbf{v}/c$. All the other electrons are similarly affected and their coherent scattered fields are together equivalent to that of a distribution of induced current of density

$$\mathbf{I}=ne\mathbf{v}/c, \qquad (2.2)$$

where n is the electron density. Moreover this is the only source distribution of the field. The scattered field must, therefore, be identical with the inducing field and satisfy Maxwell's equations,

$$\left.\begin{aligned}\operatorname{curl}\mathbf{E}+\frac{1}{c}\frac{\partial\mathbf{H}}{\partial t}&=0,\\ \operatorname{curl}\mathbf{H}-\frac{1}{c}\frac{\partial\mathbf{E}}{\partial t}&=4\pi\mathbf{I}.\end{aligned}\right\} \qquad (2.3)$$

The relations (2.1)–(2.3) determine the field in terms of one of the vectors. Since they are linear, it is sufficient to confine our attention to monochromatic fields of frequency

$$f=\omega/2\pi, \qquad (2.4)$$

such that the field vectors are the real parts of the complex vectors

$$\mathbf{E}=\mathbf{E}'\exp(-i\omega t),\text{ etc.} \qquad (2.5)$$

Then we find

$$\left.\begin{aligned} &\mathbf{I}=\sigma_f\mathbf{E},\\ \text{where}\qquad &\sigma_f=i\frac{ne^2}{m\omega c}\frac{1}{1+i\nu/\omega}\end{aligned}\right\} \qquad (2.6)$$

is the complex conductivity,

$$\mathbf{H}=-i\frac{c}{\omega}\operatorname{curl}\mathbf{E}, \qquad (2.7)$$

and **E** is subject to the condition

$$\left.\begin{aligned} &\left(\nabla^2+\frac{\omega^2}{c^2}q_f^2\right)\mathbf{E}=0,\\ \text{where}\qquad &q_f^2=1+4\pi i\frac{c}{\omega}\sigma_f.\end{aligned}\right\} \qquad (2.8)$$

The refractive index and absorption coefficient follow directly from consideration of plane-wave solutions of (2.8). A wave travelling in the direction of the unit vector **n** has the form

$$\mathbf{E}=\mathbf{E}''\exp\{-i\omega(t-q_f\mathbf{n}.\mathbf{r}/c)\}. \qquad (2.9)$$

Thus q_f is the complex refractive index which may be written

$$q_f=\mu_f+i\chi_f, \qquad (2.10)$$

where μ_f is the real refractive index and the absorption index, χ_f, determines the absorption coefficient. Both field vectors are normal to the direction of propagation, the magnetic vector being

$$\mathbf{H}=q_f\mathbf{n}\times\mathbf{E}. \qquad (2.11)$$

Writing

$$\begin{aligned} q_f^2&=\mathrm{M}_f+i\mathrm{N}_f\\ &=(\mu_f+i\chi_f)^2, \end{aligned} \qquad (2.12)$$

we find

$$\left.\begin{aligned} \mu_f^2&=\tfrac{1}{2}\mathrm{M}_f\{\sqrt{(1+\mathrm{N}_f^2/\mathrm{M}_f^2)}+1\},\\ \chi_f^2&=\tfrac{1}{2}\mathrm{M}_f\{\sqrt{(1+\mathrm{N}_f^2/\mathrm{M}_f^2)}-1\},\end{aligned}\right\} \qquad (2.13)$$

where, from (2.6) and (2.8),

$$\left.\begin{aligned} \mathrm{M}_f&=1-\frac{\omega_0^2}{\omega^2+\nu^2}, \\ \mathrm{N}_f&=\frac{\nu\omega_0^2}{\omega(\omega^2+\nu^2)}, \\ \omega_0^2&=4\pi ne^2/m. \end{aligned}\right\} \quad \ldots\ldots\ldots \quad (2.14)$$

The energy absorption coefficient is then

$$\kappa_f=2\chi_f\omega/c. \quad \ldots\ldots\ldots \quad (2.15)$$

These are the formula of the Lorentz theory.

If, as is usually the case, $\nu \ll \omega$, (2.13)–(2.15) yield the approximate results quoted in S.W.,

$$\left.\begin{aligned} \mu_f^2&=1-f_0^2/f^2, \\ \kappa_f&=\nu f_0^2/cf^2\mu_f, \\ \text{where} \qquad f_0&=\omega_0/2\pi. \end{aligned}\right\} \quad \ldots\ldots\ldots \quad (2.16)$$

§3. THE CROSS-SECTION FOR ABSORPTION BY A FREE ELECTRON AND THE ABSORPTION COEFFICIENT.

In this section we recover the Lorentz formula for the absorption coefficient by investigating the absorption cross-section of a free electron belonging to an ionized gas in a radiation field, taking account of the scattering properties of the medium.

The quantities in electromagnetic theory that are important in the theory of radiation are the energy density of the radiation field and the Poynting vector which corresponds to the radiative flux vector. Since a radiation field may be regarded as the linear superposition of monochromatic plane waves of all frequencies and travelling in all directions, we may restrict our consideration to plane-wave fields of the type (2.9). Burkhardt (1950) has pointed out that the energy of the radiation field together with the magnetic energy of the current distribution constitutes the total energy of the electromagnetic field. The energy density of the current distribution may be expressed in terms of the current density and the vector potential, **A**, of which it is the source function, as $-\frac{1}{2}(\mathrm{Rl}\,\mathbf{I})\,.\,(\mathrm{Rl}\,\mathbf{A})$. Then the energy density, U_f, and the Poynting vector, $\mathbf{S}_f$, are given by

$$\left.\begin{aligned} \mathrm{U}_f&=\frac{1}{8\pi}\{(\mathrm{Rl}\,\mathbf{E})^2+(\mathrm{Rl}\,\mathbf{H})^2+4\pi(\mathrm{Rl}\,\mathbf{I})\,.\,(\mathrm{Rl}\,\mathbf{A})\}, \\ \mathbf{S}_f&=\frac{c}{4\pi}(\mathrm{Rl}\,\mathbf{E})\times(\mathrm{Rl}\,\mathbf{H}). \end{aligned}\right\} \quad \ldots \quad (3.1)$$

Again, since the duration of the phenomena in which we are interested is large compared with the period of the light or radio waves observed, we may restrict ourselves further to consider time averages of U_f and $\mathbf{S}_f$ over a period $1/f$. These are given by (*cf.* Stratton 1941)

$$\left.\begin{aligned}\overline{U}_f &= \frac{1}{16\pi}\{|E|^2+|H|^2+4\pi \mathrm{Rl}(\mathbf{I}\,.\,\mathbf{A}^*)\},\\ \overline{\mathbf{S}}_f &= \frac{c}{8\pi}\mathrm{Rl}(\mathbf{E}\times\mathbf{H}^*),\end{aligned}\right\} \quad . \quad . \quad (3.2)$$

where a modulus sign denotes the complex modulus and an asterisk the complex conjugate.

Since the net charge density is zero, the electromagnetic field may be specified completely by **A**, whence

$$\mathbf{E}=i\frac{\omega}{c}\mathbf{A} \quad . \quad . \quad . \quad . \quad . \quad . \quad . \quad . \quad . \quad (3.3)$$

and **H** is given by (2.11). Substituting the results (2.6), (2.11) and (3.3) into (3.2), we get

$$\left.\begin{aligned}\overline{U}_f &= \frac{1}{8\pi}\mu_f^2|E'|^2,\\ \overline{\mathbf{S}}_f &= \frac{c}{8\pi}\mu_f|E'|^2\mathbf{n}.\end{aligned}\right\} \quad . \quad . \quad . \quad . \quad . \quad . \quad (3.4)$$

Thus
$$\overline{\mathbf{S}}_f=\frac{c}{\mu_f}\overline{U}_f\mathbf{n}, \quad . \quad . \quad . \quad . \quad . \quad . \quad . \quad . \quad (3.5)$$

showing that the phase velocity, c/μ_f, is the velocity of energy propagation.

This result is contrary to an assertion made in S.W. that the velocity of energy propagation is $c\mu_f$, a statement which is true only for the propagation of a group of waves such as a pulse.

The average rate of absorption of energy by an electron from the field is

$$\begin{aligned}\overline{W}_f &= e(\mathrm{Rl}\,\mathbf{v})\,.\,(\mathrm{Rl}\,\mathbf{E})\\ &= \tfrac{1}{2}e\,\mathrm{Rl}(\mathbf{v}\,.\,\mathbf{E}^*),\end{aligned} \quad . \quad . \quad . \quad . \quad . \quad . \quad . \quad . \quad (3.6)$$

as in (3.2). From (2.2) and (2.6) we find

$$\overline{W}_f=\frac{e^2}{8\pi m}\,\frac{\nu}{f^2+\nu^2/4\pi^2}|E'|^2. \quad . \quad . \quad . \quad . \quad . \quad . \quad . \quad (3.7)$$

It is clear from (3.7) that there is an overall extraction of energy from the field only by virtue of the collisions the electron makes with the other particles of the medium. During part of any period the rate of absorption of electromagnetic energy is negative. This represents the emission stimulated by the field. If no collision takes place, it is balanced by an equal amount of energy absorbed from the field during the other half of the period. Thus $\overline{W}_f$ is the net absorption over a period. It is, on the average, communicated to the ions with which an electron collides.

The cross-section for absorption by a free electron, a_f, is defined such that

$$\overline{W}_f = a_f \overline{S}_f. \qquad (3.8)$$

Then by (3.4) and (3.7)

$$a_f = \frac{e}{\pi c m \mu_f} \frac{\nu}{f^2+\nu^2/4\pi^2}. \qquad (3.9)$$

The absorption coefficient is now simply

$$\begin{aligned}\kappa_f &= n a_f \\ &= \frac{\nu f_0^2}{c f^2 \mu_f} \frac{1}{1+\nu^2/4\pi^2 f^2}.\end{aligned} \qquad (3.10)$$

This is identical with the exact result obtained from (2.13)–(2.15).

§4. THE EMMISSIVITY.

There remains to show that scattering introduces a factor μ_f in the formula for the emissivity, η_f.

In S.W., Kramers's procedure of making a Fourier analysis of the total radiation, Q, emitted during a free-free electron-ion encounter was followed, giving Q_f such that

$$Q = \int_0^\infty Q_f \, df. \qquad (4.1)$$

Then Q_f was summed over all types of encounter taking place in a volume element over a small time interval, to give the emissivity. The first part of this analysis will have to be done afresh, taking scattering into account from the outset.

The microscopic source of the field under consideration is an electron accelerating in a hyperbolic orbit about a positive ion. Its acceleration at any instant is $\mathbf{j}(t)$, and we may conveniently take the duration of the encounter as from $t=-\infty$ to $t=+\infty$. The Fourier transform of $\mathbf{j}$ is

$$\left.\begin{aligned} \mathbf{J}(\omega) &= \int_{-\infty}^{\infty} \mathbf{j}(t) \exp(i\omega t)\, dt, \\ \text{whence} \quad \mathbf{j}(t) &= \frac{1}{2\pi}\int_{-\infty}^{\infty} \mathbf{J}(\omega) \exp(-i\omega t)\, d\omega. \end{aligned}\right\} \qquad (4.2)$$

The Fourier transforms of **E** and **H** due to **j** are likewise

$$\left.\begin{aligned} \overline{\mathbf{E}}(\omega) &= \int_{-\infty}^{\infty} \mathbf{E}(t) \exp(i\omega t)\, dt, \\ \text{whence} \quad \mathbf{E}(t) &= \frac{1}{2\pi}\int_{-\infty}^{\infty} \overline{\mathbf{E}}(\omega) \exp(-i\omega t)\, d\omega, \text{ etc.} \end{aligned}\right\} \qquad (4.3)$$

Then the Maxwell-Lorentz equations (2.1)–(2.3) transform to

$$\left.\begin{aligned} \operatorname{curl} \overline{\mathbf{E}} - i\frac{\omega}{c}\overline{\mathbf{H}} &= 0, \\ \operatorname{curl} \overline{\mathbf{H}} + i\frac{\omega}{c} q_f^2 \overline{\mathbf{E}} &= 0, \end{aligned}\right\} \qquad (4.4)$$

where q_f^2 is given by (2.8) and (2.6).

These equations are formally identical with those conditioning a monochromatic field of frequency $f=\omega/2\pi$ such that $\mathbf{E}'=\overline{\mathbf{E}}df$.

We may, therefore, write down the formulæ for $\overline{\mathbf{E}}$ and $\overline{\mathbf{H}}$ is terms of $\mathbf{J}$ directly from the corresponding formulæ for the field vectors due to a harmonic Hertzian oscillator of moment

$$e\boldsymbol{\xi}=e\boldsymbol{\xi}'\exp(-i\omega t),$$

in a medium of dielectric constant q_f^2.

Only the acceleration field is significant and $\ddot{\boldsymbol{\xi}}$ corresponds to $\mathbf{J}$. Then at a position $\mathbf{R}$, with respect to the source, we have

$$\left.\begin{aligned}\overline{\mathbf{E}}&=\frac{e}{c^2\mathrm{R}}(\mathbf{J}\times\hat{\mathbf{R}})\times\hat{\mathbf{R}},\\ \overline{\mathbf{H}}&=q_f\frac{e}{c^2\mathrm{R}}\mathbf{J}\times\hat{\mathbf{R}},\end{aligned}\right\}\quad\ldots\ldots\quad(4.5)$$

where the circumflex denotes a unit vector.

The total contribution to the emissivity during an encounter is

$$\mathrm{Q}=\int_{-\infty}^{\infty}dt\int_0\mathbf{S}\,.\,\mathbf{n}\,d\mathrm{S},\quad\ldots\ldots\ldots\quad(4.6)$$

where $\mathbf{n}$ is the unit normal directed out from a closed surface surrounding the locality of the encounter. Now

$$\begin{aligned}\int_{-\infty}^{\infty}\mathbf{S}(t)\,dt&=\frac{c}{4\pi}\int_{-\infty}^{\infty}\mathbf{E}(t)\times\mathbf{H}(t)\,dt\\ &=\frac{c}{8\pi^2}\int_{-\infty}^{\infty}\overline{\mathbf{E}}(\omega)\times\overline{\mathbf{H}}(-\omega)\,d\omega,\quad\ldots\quad(4.7)\end{aligned}$$

by one of the Parseval formulæ for Fourier integrals. This is the analogue of the monochromatic relation (3.2).

It then follows from (4.1) and (4.6) that

$$\mathrm{Q}_f=\frac{c}{2\pi}\int_0\mathrm{Rl}\{\overline{\mathbf{E}}(\omega)\times\overline{\mathbf{H}}(-\omega)\}\,.\,\mathbf{n}\,d\mathrm{S}.\quad\ldots\ldots\quad(4.8)$$

By (4.5)
$$\overline{\mathbf{E}}(\omega)\times\overline{\mathbf{H}}(-\omega)=q_f\frac{e^2}{c^4\mathrm{R}^2}|\,\mathrm{J}\,|^2\sin^2\Theta,$$

where
$$\mathrm{J}\cos\Theta=\mathbf{J}\,.\,\hat{\mathbf{R}}.$$

Since the integral of $\sin^2\Theta$ over a complete solid angle is $8\pi/3$, we obtain finally

$$\mathrm{Q}_f=\frac{4e^2}{3c^3}\mu_f|\,\mathrm{J}\,|^2.\quad\ldots\ldots\ldots\ldots\quad(4.9)$$

This is the result S.W. (3.23) with the additional factor μ_f.

The determination of $|J|^2$ in terms of the initial velocity, g, and the distance of the interacting ion from an asymptote of the orbit, b, is the same problem as in S.W. With the same assumptions, that $fb/g \ll 1$ and that there have been sufficient collisions to bring about a Maxwellian distribution of the velocities of the particles, we shall arrive at the heuristic formula S.W. (3.53) which it was our purpose to justify.

§5. THE TRANSITION PROBABILITIES.

Although the emission of radiation by an electron in a classical (g, b) orbit is not (apart from possible modifications to the orbit) affected by the presence of the surrounding electrons, we have seen that these have the effect of scattering the radiation so that the contribution, Q_f, to the emissivity, η_f, in the frequency range $(f, f+df)$ is reduced according to the factor μ_f.

To interpret this statement in terms of the quantum theory, we may say that the probability, α_{21}, of the spontaneous emission of a quantum hf in the range $(f, f+df)$ accompanying a switch from an orbit (g_2, b_2) to an adjacent orbit (g_1, b_1) is reduced by the presence of the surrounding electrons according to the factor μ_f. The identification is such that (S.W.(3.43) and (3.45))

$$\left.\begin{aligned} Q_f df &= \alpha_{21} hf \\ \text{and} \qquad hf &= \tfrac{1}{2}m(g_2^2 - g_1^2). \end{aligned}\right\} \quad . \; . \; . \; . \; . \quad (5.1)$$

The probability coefficient, β_{21}, for a stimulated emission in a transition $2 \rightarrow 1$, and the coefficient, β_{12}, for an absorption in the converse transition $1 \rightarrow 2$, are both inversely proportional to α_{21}. They are given in S.W. (3.40) and (3.41). Since they contain the factor $1/\mu_f$, the consequent kinetic-theory derivation of κ_f will yield the heuristic formula S.W. (3.15).

This quantum-theory interpretation differs from the details suggested in S.W., where the refractive index was associated not with the transition probabilities but with the number of transitions taking place per unit volume and time. The final formulæ for η_f and κ_f involving μ_f are of course unaffected.

ACKNOWLEDGMENT.

This work was carried out during the tenure of a studentship from the Commonwealth Scientific and Industrial Research Organization, Australia.

REFERENCES.

BURKHARDT, G., 1950, *Annalen d. Physik*, **5**, 373–80.
DARWIN, C. G., 1924, *Trans. Camb. Phil. Soc.*, **23**, 137–67.
HARTREE, D. R., 1928, *Proc. Camb. Phil. Soc.*, **25**, 97–120; 1931, *Ibid.*, **27**, 143–62.
STRATTON, J. A., 1941, *Electromagnetic Theory*, (New York: McGraw-Hill), Section 2.20.

XLVII. *Investigation of Soft Radiations.*—VII. *Energy Expenditure per Ion-pair for Slow Electrons in Various Gases.*

By S. C. Curran, A. L. Cockroft and G. M. Insch,
Department of Natural Philosophy, University of Glasgow *.

[Received March 20, 1950.]

Summary.

The proportional counter is applied to the problem of determining the energy expenditure per ion-pair formed in argon, methane, ethylene, air, nitrogen, oxygen and carbon dioxide. Two different methods are applied. In the first the nearly homogeneous X-rays of Copper 64 are employed and the measurement of the number of disintegrations per minute occurring in a known fraction of the source is compared with the ion current through the same tube due to the whole source. Tritium gas is used likewise, in known relative amounts, to give rise to ion-currents and counting rates of easily measurable magnitudes. Hence the energy expenditure is obtained for the photo-electrons produced by Kα X-rays and for the slow β-rays of tritium (average energy$=5{\cdot}7$ Kev). The advantages obtained by using slow β-rays in counters are stressed.

Introduction.

The experimental determination of the energy expenditure per ion pair formed by different ionizing particles at various velocities has been the subject of many investigations (Compton and Allison 1936). Much of the earlier data was inaccurate owing to the limitations of the techniques available. There is however surprisingly little data directly obtained for electrons of known energy and which aims at reasonable standards of accuracy. Reviews of parts of the subject have been given by Gray (1944) and Binks (1936) and some more recent values are tabulated in MDDC-1017. We note particularly that investigations with mono-energetic electrons have been made by Eisl (1929) and Gerbes (1935) for air and by Nicodemus (1946) for argon. The accurate determination of the energy expenditure is a matter of considerable importance and the work described below was undertaken in an effort to obtain accurate values for electrons in a number of different gases. In particular it was essential that values should be measured for the gases employed in proportional counting tubes since the resolving power of the instrument was involved (Curran, Cockroft and Angus 1949). It was realized that the proportional counter offered a new and powerful tool for the accurate absolute measurement of energy expenditure for slow electrons.

---

* Communicated by the Authors.

Experimental Methods.

1. *Homongeneous X-rays.*

Studies of X-radiation performed with proportional tubes (Curran, Angus and Cockroft 1949) showed that they could be used to measure accurately the average energy of the quanta and to count the number of such quanta with small error. In principle therefore if the flux of quanta entering the tube is n-sec. and the average energy expended by the quanta is E electron-volts (obtained from the photo-electron and Auger electron liberated in the gas), the rate of production of ion pairs is $n\mathrm{E}/\mathrm{V}$. per sec. where V is the energy expended in producing each ion pair. If the tube is used to measure n and E by operating it as a proportional counter, and if it is then operated as an ionization chamber by reducing the applied voltage below the value for onset of gas multiplication, the current i produced by the ions can be measured. Hence since

$$i=n\mathrm{E}/\mathrm{V}. \quad \text{. . . . .} \quad (1)$$

the value of V can be calculated. In actual practice the determination of V is not quite so straightforward as suggested here. Thus counting rates n of the order of 50,000/min. could be easily measured but the electrometer valve circuit used to observe the absolute value of i was not sufficiently sensitive to give the corresponding current i accurately. The source of radiation can however be adjusted by a known fraction upwards or downwards in intensity. If a fraction f of the source gives n quanta/sec. then we have

$$fi=n\mathrm{E}/\mathrm{V}. \quad \text{. . . . .} \quad (2)$$

To make the current measurement accurate and stable a value of of $f\sim1$ per cent was usually arranged.

2. *Beta-rays of Tritium.*

The use of X-rays as the primary agents responsible for the ionizing electrons is not ideal in practice since the fractional absorption of these in the gases investigated makes it necessary to maintain the same pressure throughout the experiment. Moreover the measurement of n involves the proper quantitative operation of the counter with all of the gases employed. It is not possible to obtain good plateaus on the characteristic curves of tubes filled with such gases as air, oxygen or carbon dioxide. For this reason an alternative proceedure was adopted. This depended on the use of the slow β-rays of tritium gas, H^3, as the ionizing electrons. A small quantity of tritium was taken and the rate of disintegration measured. It is to be noted that any filling gas with good counting features (*e. g.* argon+methane mixture) could be used in this part of the experiment. Indeed a suitable Geiger tube might perform satisfactorily. Then a much larger quantity of tritium, together with the gas or mixture of gases being investigated, was used to fill the counter which was subsequently operated as an ionization chamber. The larger quantity of tritium was of course accurately related to the smaller quantity used when counting was done. The ratio of the two quantities was either determined by measuring volumes of the gas or by measuring pressures.

The average energy of the β-rays forming the spectrum of tritium is accurately known and recent work with the proportional tube (Curran, Angus and Cockroft 1949) shows that it is 5·7 keV. (See also Slack *et al.* 1949) and Jenks *et al.* 1949). Clearly this second method offers some considerable advantages. Any gas which gives a saturation current in an ionization chamber can be investigated. Thus air, oxygen and other gases with appreciable electron-attachment coefficients are not excluded. Again the absolute value of V can be measured for one gas and the values of V for other gases obtained by using definitely related quantities of tritium in each gas in turn. It is to be noted that the partial pressure of the tritium can be kept very small and below a value likely to affect the accuracy of the results. Moreover the short range of the β-rays means that very little error (∼1 per cent) is involved in assuming that all of their energy is expended in the gas even when chambers of moderate dimensions (∼2 in. diameter) are employed and pressures ∼1 atmosphere. The transparency problem involved with X-rays is thus eliminated.

ABSOLUTE VALUE OF V FOR ARGON.

1. *X-ray Method.*

The choice of argon as the gas receiving most attention is justified in view of its widespread use in counters, ion chambers and cloud chambers. It was decided at the outset that the accurate measurement of the fraction f (equation (2) above) was of crucial importance. Various procedures could have been adopted but it seemed best to the authors to use radioactive decay. Fortunately a suitable source of soft X-rays exists in the form of Cu^{64} and the half-life (12.8 hrs.) was such that a period of only 3 days separated the measurements of ion-current and counting rate.

The small piece of radioactive copper was rigidly attached to the aperture of a proportional counter (4 in. diameter, 20 in. long) filled to atmospheric pressure with a 60/15 mixture of argon and methane. The ionization current through the tube was measured under conditions assuring good saturation. The source was allowed to decay and after a suitable interval the rate of counting was observed. The plateau obtained for the counter was fairly good although not entirely free from ambiguity. At the lower edge of the plateau the counting rate was higher than on its main stretch but it was thought that this was a spurious effect. After measurement of the counting rate the spectrum of the pulses was analysed as described elsewhere (Curran, Angus and Cockroft 1949). A good prominent peak corresponding to the Kα radiations of nickel was found (as shown in fig. 1) but the high-energy tail of low intensity produced by the annihilation γ-radiation from the source (which was covered with polythene to absorb β-particles) formed a large contribution to the total energy. The 60/15 mixture was not too fortunate a choice in this instance and a higher total pressure of argon would have been preferable.

The spectrum could be analysed over the entire energy range however, and it was found that $\bar{E}$, the average energy expended by the quanta in the gas was 12·7 keV. With this value, V for argon/methane in the ratio of 60/15 by pressure was 29·5 eV.

Regarding the experimental error this is difficult to assess. No account is taken of end-effect but absorption of the X-rays in the argon renders this less disturbing than usual—the source was placed at the centre of the tube. It is more likely that the total count was achieved than that complete saturation of the current was reached. (There was small but definite slope on the curve for current as a function of voltage.) In this way the authors consider that it is probably safe to express V in the form.

$$V=29{\cdot}5^{+0{\cdot}5}_{-1{\cdot}0}\text{ eV}.$$

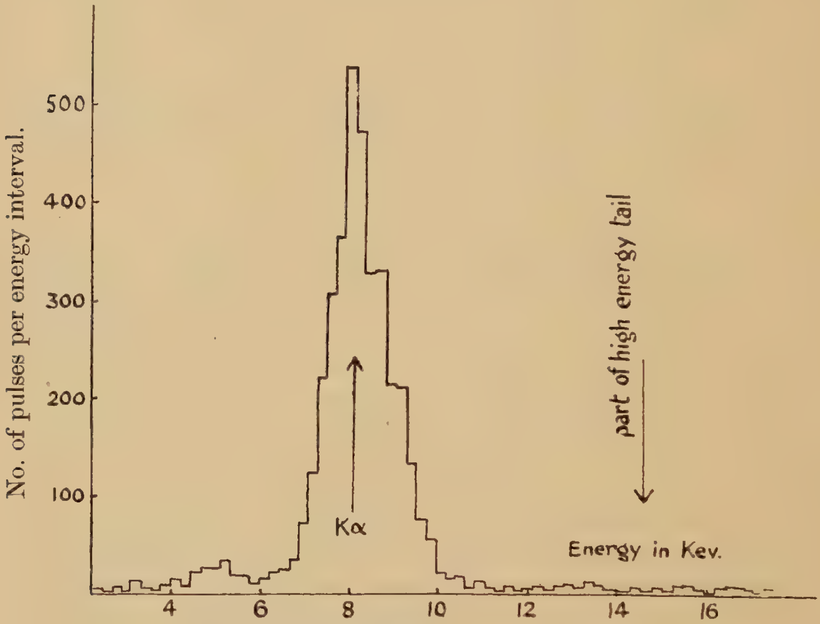

X-ray and γ-ray spectrum of Copper 64.

2. *Use of Tritium.*

Tritium was mixed with a little hydrogen as diluent and carrier. Experience gained in various attempts to define the fraction *f* which was counted led the authors to the conclusion that it was best to have two vessels identically constructed, one which acted as a counter and one which performed as an ion chamber. A supply of radioactive gas was prepared and a known fraction (by volumes) drawn off. This could be diluted further if required. The gas mixture containing the smaller activity was passed into the counter and the larger quantity into the ion chamber. The counter was then filled with a suitable counting mixture (frequently 7 cm. of CH_4 70 cm. of argon) while the ion chamber was filled with the main quantity. Usually the two vessels were very long (72 in.) and of relatively small diameter ($1\frac{1}{4}$ in.). The counter contained a thin wire (0·1 mm. diameter) and the chamber a thick one (2 mm. diameter). By using two vessels in this way the counter remained essentially free of contaminant after experimentation since the radioactive content was always small and the fraction sticking to the wall was found to be $\sim$1 per cent. Moreover the thick central wire of the chamber permitted easy attainment of saturating current conditions even at high pressure. On the other hand, lower pressures in the counter facilitated the search for a good plateau for complete counting. The large ratio of length/diameter assured us that end-effect, even if somewhat different for counter and chamber, did not appreciably affect the evaluation of V.

The values obtained for V in the two experiments which seemed to be most satisfactory were as follows :—

Press in cm. of Hg.		V in electron-volts.
CH_4	Argon	
15	135	28·5
10	138	28·4

These two values are not considered to be significantly different and the error limits on the value obtained for X-rays makes it consistent with them. It will be shown below that argon and methane agree closely in V values and we are of the opinion that the V value of the mixture is effectively the same for the β-rays of tritium (average energy 5·7 keV.) and photo-electrons of Cu^{64}. This conclusion is drawn from our earlier curve[7], showing constancy of V as a function of the energy of the electron. We conclude finally then that our work indicates that the value of V for argon containing about 10 per cent CH_4 and for electrons of energy between a few keV. and say 50 keV. is given by

$$V = 28{\cdot}5 \pm 0{\cdot}5 \text{ eV.}$$

Other Gases.

To extend the work to other gases it was only necessary to subidivde a supply of tritium into a number of volumes of accurately known relative values. These were made nearly equal and added to the ion chamber in turn, together with the gas or mixture under investigation. Fairly consistent values of V for several gases were measured in this way but the procedure was not entirely satisfactory, mainly on account of the appreciable difficulty of " sticking " of tritium to the walls of the glass containers. However, the value for air given below was obtained by this method, the standard reference gas being argon. Taking the value of V for argon as 28·5 eV. the value for air was by comparison 31·0 eV. Next an ion chamber containing some tritium was filled to atmospheric pressure with nitrogen and the current measured. Oxygen was added to the vessel and the current re-measured. Hence the value for nitrogen was deduced, viz., 32·0 eV. Finally, V for oxygen was found by adding oxygen to give a 50/50 mixture of oxygen and nitrogen, noting the current in the mixture and assuming that the change in the current from the value for nitrogen was proportional to the percentage oxygen content of the mixture. Among the values listed below the oxygen result is the least trustworthy in view of this assumption and the difficulty of measuring accurately the small changes.

Gas	V in eV.
Air	31·0
Nitrogen	32·0
Oxygen	28·8

The value for carbon dioxide was obtained by noting the current passing in a chamber filled to atmospheric pressure with argon. Carbon dioxide was added to raise the pressure to two atmospheres. Great care was taken to measure the true saturation current through the tube in both conditions and it was separately verified that there was no appreciable effect which could be ascribed to mere pressure increase. Thus at pressures of argon between 30 cm. Hg and 150 cm. Hg no change was noted in the same counter used in a similar fashion. To deduce the value of V for CO_2 it was necessary to assume the fall in current produced by adding CO_2 to argon was proportional to the amount added. In this way the value V=33·5 eV. was measured for CO_2.

Methane and Ethylene.

The determination of V for these organic gases was done in more detail. The current due to some tritium in pure argon at one atmosphere was measured, then the current was measured as increasing amounts of methane were added till a total pressure of two atmospheres was reached. Next, starting with methane at one atmosphere, argon was added in increasing amounts. It was found that throughout the range pure methane to pure argon there was no appreciable alteration in the ion current. We can therefore deduce that methane has the same V-value as argon, namely 28·5 eV. and that this value holds for any mixture of argon and methane.

Similar examination of the behaviour of ethylene and argon gave the value V=30·6 eV. for ethylene and indicated that the addition of C_2H_4 to argon raised V from 28·5 eV. to 30·6 eV. linearly with increasing percentage of ethylene.

The complete list of values for the gases investigates is thus as below :—

Gas	V in electron–volts
Argon	28·5
Air	31·0
Nitrogen	32·0
Oxygen	28·8
Carbone dioxide	33·5
Methane	28·5
Ethylene	30·6

DISCUSSION.

With regard to the results listed in the table we have to note that no special effort was made to purify the gases thoroughly. Indeed in all cases the values were obtained with a small amount of tritium and hydrogen present (at partial pressures $\gtrsim$1 cm. Hg). The gases were of commercial purity which meant that there was ~1 per cent nitrogen in the argon and ~2 per cent in the methane. Other contaminations were considerably less in quantity. There was some indication that the value for very pure argon could differ appreciably from 28·5 eV. but no serious attempt was made to establish this observation.

Concerning air, the experiments do not support the variation of V with energy as given by the formula of Gerbes (1935). The value of 31·0 eV. is indeed remarkably close to his value of 31·6 eV. for high speed electrons (60 keV.) and would seem to suggest that V is almost constant for air throughout the range from ~3 keV. to ~300 keV. since the measured value for fast β-rays (energy=·3 MeV.) is 32·0 eV. The best mean value in this large range would appear to be 31·5 eV. It is hoped that future work will improve the accuracy of the value given here. The same method can be extended to include the nearly homogeneous photo-electrons of A^{37} (energy 2·8 keV.) and thus to examine more thoroughly the question of possible variation of V with energy.

We have to note some measure of disagreement with the result of Nicodemus (1946) for electrons of energy 17·4 keV. in argon. His value of 26·9 eV. and our value of 28·5 eV. give a mean value of about 27·7 eV. which is probably just outside the estimated limits of error (believed to be about 0·5 eV.). (We are indebted to Dr. Nicodemus for private communication on his measurements.) It is possible that there is some slight variation of V with electron energy in the range 5·7 keV. (tritium) to 17·4 keV. but this would appear unlikely in view of previous work by the authors and by Hanna, Kirkwood and Pontecorvo (1949). It is hoped that further more extensive measurements will resolve this difficulty.

Regarding some comparable measurements with α-rays (and protons) it appears that the above values for electrons are smaller (Gray 1944) in the case of air (and presumably nitrogen), but larger for ethylene and argon (Schmeider 1939). The values for carbon dioxide are nearly the same. Apparently there is no change of a regular nature involved here.

FURTHER REMARKS ON APPARATUS.

The absolute value of current through the ion chambers was determined by measuring a high resistance in terms of a standard one of 1 megohm. The actual resistance used in the grid circuit of the electrometer triode was $1{\cdot}8\times10^{11}$ ohms. Currents of about 10^{-12} amps. were passed through this and the anode current of the triode was measured with a sensitive micro-ammeter. In practice the standing anode current was cancelled and the meter was reset to zero during ion current measurement by applying a biassing voltage. This bias voltage was the actually observed quantity and it was measured on a standardized voltmeter.

In the course of the work various forms of counters and ion chambers were tried in a search for the most stable design. The later more accurate work was done with ion chambers constructed entirely of glass except for the central wire and its grounding shield. The glass envelopes were coated with aquadag externally and this coated glass was found to serve admirably as cathode. Even pyrex glass of specific resistance 5×10^{16} ohms could be used (at least in thicknesses up to 1·3 mm.). Long term operation brought polarization effects into evidence but these were not serious and the effective capacity of the chamber was such that in short-term operation ($\sim$1 hr.) it was almost negligible. Excellent saturation curves were obtained. Further information (Cockroft and Valentine) will be published separately. Meanwhile it is to be noted that such vessels are well adapted for outgassing in work with gases of high purity or with gases or vapours which tend to be absorbed by the metals in common use.

Further work.

The method of using slow β-sources such as H^3 is well suited to the investigation of the energy expendure in nearly all gases and vapours; the measurements will be extended soon to cover some specially interesting ones such as hydrogen, helium and water vapour. Knowledge of V for the first two would assist in deriving a theoretical explanation of the results. Moreover any variation of V with energy of the ionizing electrons can be readily investigated with the proportional counter since the spectra of pulses produced by various sources of β-radiation can be analysed and the average energy of the β-particles deduced.

We thank Professor P. I. Dee, F.R.S., for his advice and interest in the work described here.

REFERENCES.

COMPTON, A. H., and ALLISON, S. K., 1936, *X-rays*.
GRAY, L. H., 1944, *Proc. Camb. Phil. Soc.*, **40**, 72.
BINKS, W., 1936, *Reports on Progress in Physics*, **3**, 347.
EISL, A., 1929, *Ann. Phys. Leipzig.*, **3**, 277.
GERBES, W., 1935, *Ann. Phys.*, **23**, 648.
NICODEMUS, D. B., 1946, *Thesis*, Stanford University.
CURRAN, S. C., COCKROFT, A. L., and ANGUS, J., 1949, *Phil. Mag.*, **40**, 929.
CURRAN, S. C., ANGUS, J., and COCKROFT, A. L., 1949, *Phil. Mag.*, **40**, 36.
CURRAN, S. C., ANGUS, J., and COCKROFT, A. L., 1949, *Phys. Rev.*, **76**, 853.
SLACK, L., OWEN, G. E., and PRIMAKOFF, H., 1949, *Phys. Rev.*, **75**, 1448.
JENKS, G. H., GHORMLEY, J. A., and SWEETON, F. H., 1949, *Phys. Rev.*, **75**, 701.
HANNA, G. C., KIRKWOOD, D. H. W., and PONTECORVO, B., 1949, *Phys. Rev.*, **75**, 985.
SCHMEIDER, K., 1939, *Ann. d. Phys.*, **35**, 445.

XLVIII. *Magnetic Spectrometer of Large Solid Angle.*

By E. R. Rae,
Department of Natural Philosophy, University of Glasgow *.

[Received February 7, 1950.]

[Plate XIII.]

Summary.

An account is given of a magnetic spectrometer of large solid angle and good resolution which should find applications in the study of complex beta-ray spectra by the method of beta–gamma coincidences. The original apparatus, consisting of a segmented annular G.M. counter set round a radioactive source in a magnetic field is described, the method of use being to select from the output of the counter, large pulses which correspond to the simultaneous triggering of several sections by the passage of an electron tangentially to the annular counter. The performance of the instrument is discussed and modifications are described which rectify the defects in the earlier design and give a solid angle of 2·5 per cent of 4π with a resolution of 5 per cent.

The geometry of this type of spectrometer is considered and the performance which might be obtained with good design is discussed. It is concluded that collecting angles up to the order of 50 per cent of 4π are possible with good resolution.

§ 1. Introduction.

An account has recently been published by Siegbahn and Slätis (1949) of an instrument for the determination of the energies of beta and gamma radiations. The device consists of an arrangement for placing the source of the radiations at the centre of an annular G.M. counter whose plane is at right angles to the direction of the magnetic field. Considerable work has been done here on an apparatus which is superficially very similar to that of the above authors, but which in fact has several advantages over it. For this reason it has been decided to place on record this short account of our method which confirms some of the results of Siegbhan and Slātis and which also leads to the design of a magnetic spectrometer of very large solid angle which should prove a valuable tool in the examination of complex beta-ray spectra by the method of beta–gamma coincidences.

---

* Communicated by the Author.

§2. DESCRIPTION OF ORIGINAL APPARATUS.

The device as originally designed by Dr. S. C. Curran consisted of an annular counter with the wire supported on a large number (about 40) of small insulating pillars which had the effect of splitting the main counter into a large number of small counters acting in parallel (Stever 1942, Curran and Rae 1947). A sketch of the apparatus is given in fig. 1 and it will be seen that the counter had no window, the whole apparatus being filled with the counting mixture. The intention was to use the device to measure the energy of hard gamma-rays by detecting the positron–electron pairs ejected from a thin lead foil placed round the source, for in the case of equipartition of energy, and for the correct value of the magnetic field, both positron and electron could trigger four or five sections of the counter, thus giving a pulse eight to ten times as large as the background single section pulses.

Fig. 1.

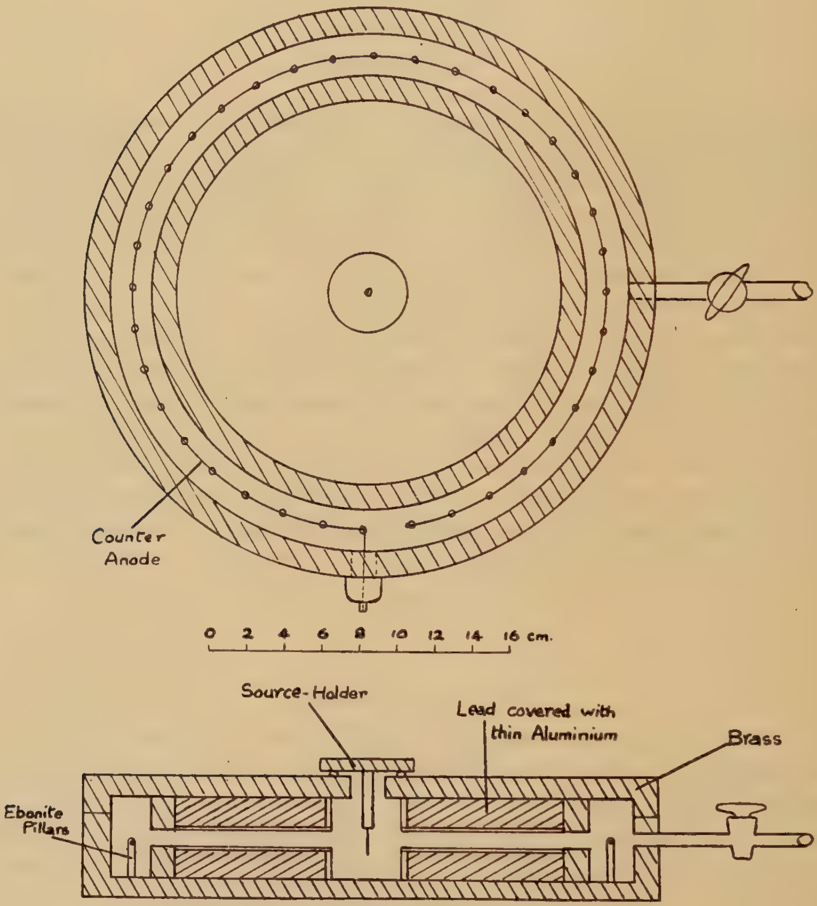

Schematic diagram of original apparatus.

Unfortunately this simple and elegant arrangement did not yield the expected results, for two main reasons: firstly because the background was found in fact to contain a large number of double and multiple pulses owing to bad geometry which made it highly probable that a particle entering one section of the counter would be scattered into at least one more. This meant that there was a considerable number of four and five-fold pulses when a strong gamma-ray source was being used, and so the number of accidental coincidences between these, giving eight to ten-fold pulses was not negligible. The second difficulty was that because the counter sections were so short relative to their length, they had very serious end effects which caused them to have only a very short plateau. This meant that even on the plateau the pulse size was a steep function of the high tension voltage, and so it was difficult to get stable working and reproducible results, since the method depended on selecting pulses of a particular size with a discriminator. These same two difficulties also prevented the device from being used satisfactorily in a similar manner to determine ordinary beta-ray and secondary electron spectra. It was at this point that the method of removing the discriminator and counting all the pulses of all sizes was tried, since though it does not give the spectrum of the source directly, it does overcome the difficulties mentioned above. This is of course the same method as that used by Siegbahn and Slätis, and though it was not studied here in detail, the results obtained were very similar to those published by them. For comparison the curves obtained for the secondary electrons ejected from a thick lead foil by the gamma-rays of Co^{60} and the annihilation radiation of Cu^{64} are shown in fig. 2. From these results and a number of others, an empirical calibration curve was constructed for the device as used in this way.

This method is however subject to several serious disadvantages. Firstly, even when one has obtained the experimental integral spectrum there is no explicit way of obtaining the true spectrum of the source because of the fact that for any setting of the magnetic field the solid angle of the device is a function of the energy of the particles detected. Thus when used in this way, the device is only suitable for determining end-points, unless one is prepared to carry out long and tedious successive approximations. Secondly, because of the high background in the counter, photo-electron lines and any other kind of fine structure are quite invisible, and thick convertors must be used for the determination of gamma-ray energies, which makes the resolution of the device poor. For instance, it will be noted that in the curves for Co^{60} given by Siegbahn and Slätis and by the present author, in neither case was it possible to resolve the lower energy line at 1·1 MeV. from that at 1·3 MeV. Thirdly, as stressed by Siegbahn and Slätis, the effect of scattering in the gas is such as to produce counts at values of the magnetic field much higher than that corresponding to the true end-point of the spectrum being examined, and this causes difficulties in the interpretation of the curves. In addition to these criticisms it should be mentioned that since one of the obvious uses for a large solid angle spectrometer of this sort would be the separation of complex beta-ray spectra by the method of beta–gamma coincidences, it would be a great advantage if the device could be made to give the true spectrum instead of an integral one, since the former would reduce the background of accidental coincidences by a very large factor near the end-point, that is, in the region of the greatest interest. For these reasons it was decided that it was worth while to attempt to overcome the difficulties in the original design in a different way.

Fig. 2.

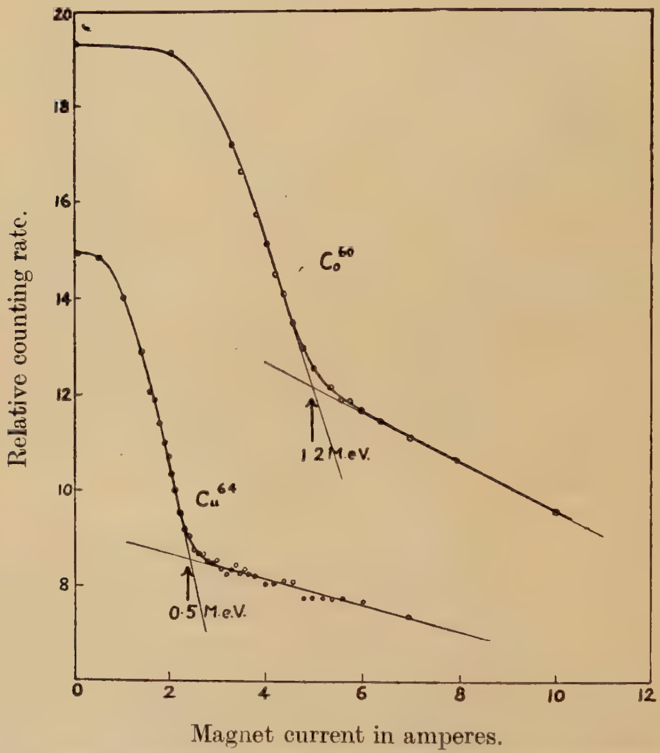

Integral momentum spectra of electrons ejected from a thick lead foil by the gamma-rays of Co^{60} and the annihilation radiation of Cu^{64}.

§ 3. THE IMPROVED APPARATUS.

A photograph of the improved apparatus is shown in fig. 3 (Pl. XIII.) and it will be seen that the number of sections into which the counter was divided has been reduced, thus giving longer sections and very much improved electrical performance. It will also be noted that the sections are separated by polythene partitions instead of the pillars of the original design, and that these partitions have openings in them just large enough to permit the passage of electrons within the desired momentum range.

RAE

Fig. 3.

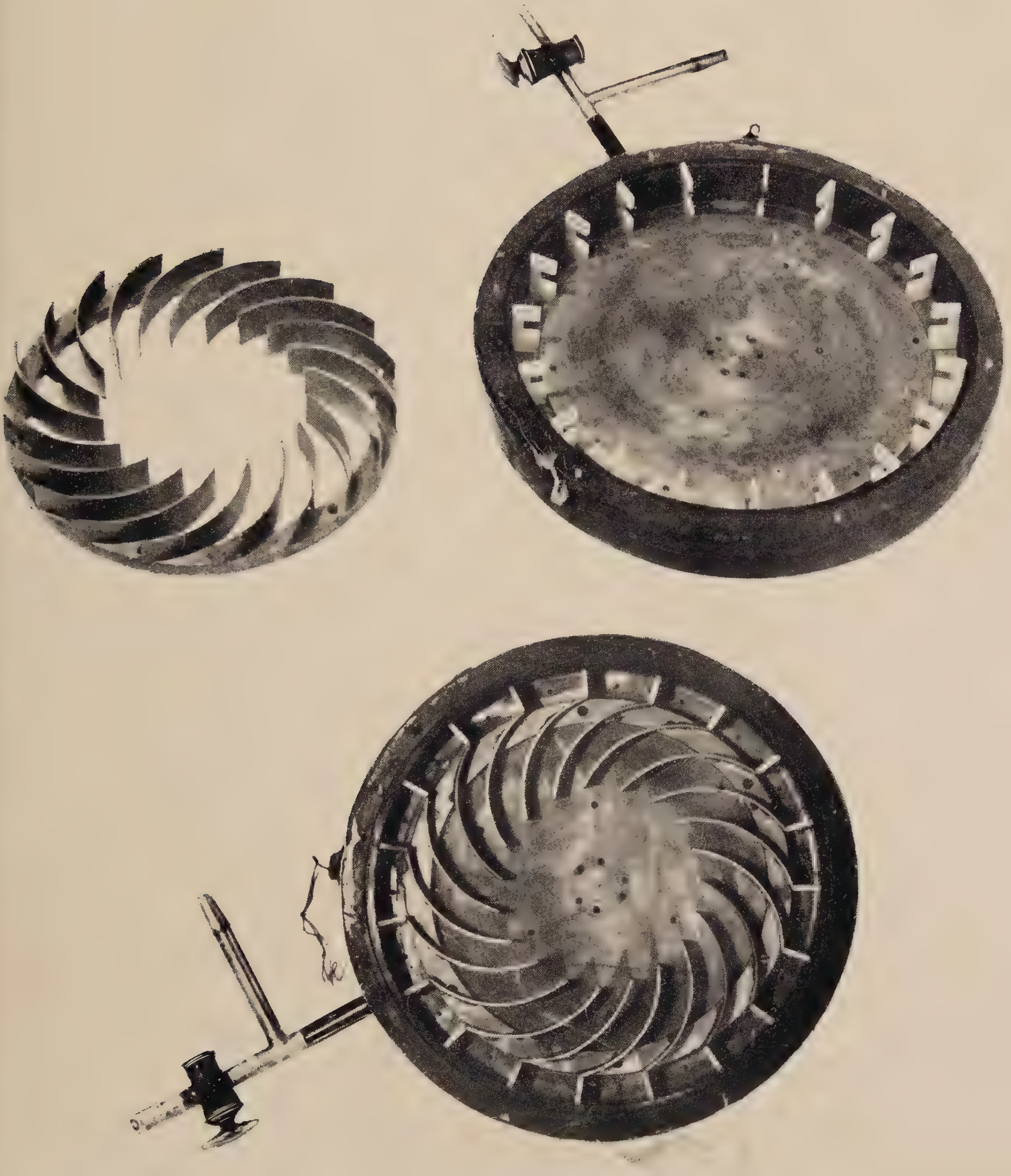

Photograph of improved apparatus.

To face page 528

This has the effect of cutting down to a very large extent the number of particles which are accidentally scattered into more than one section. Finally, the device has been fitted with a set of baffles which permit only particles of the correct sign of charge and the correct momentum range to enter the counting system, and which together with the partitions ensure that only those particles are detected which have not been seriously scattered in the gas.

With these improvements it was found possible to take spectra with the discriminator set to count single, double, or triple section pulses with good reproducibility. The single section spectra contained a large number of spurious counts at low energies because of scattering, but the spectra obtained from the double and triple section pulses were very similar. The spectrum of RaE as obtained from an old thin-walled radon seed with triple section pulses is shown in fig. 4 and it will be observed that the shape is good apart from a displacement of the number maximum towards higher energies because of the scattering of the softer beta-rays in the gas filling. The filling for this run was 3 cm. argon+1 cm. alcohol, the working voltage about 1100 V. and the estimated resolution (for triples) of the order of 5 per cent.

Fig. 4.

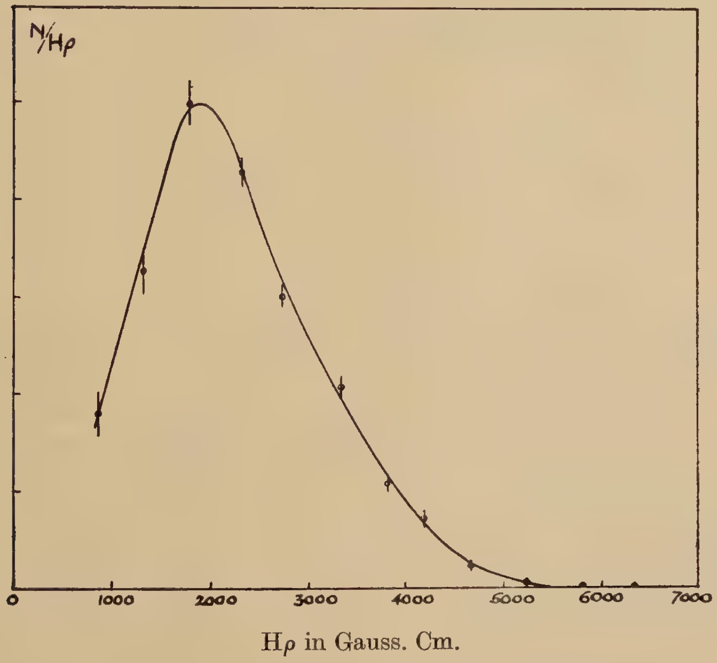

The beta-ray spectrum of an old radon seed.

These modifications to Curran's original apparatus thus produced a 360° spectrometer with a resolution of about 5 per cent and a solid angle of 2·5 per cent of 4π as compared with 1 per cent of 4π for a corresponding semicircular focusing spectrometer. It can however easily be shown that by altering the type of counting system and so obtaining a much wider slit, an instrument can be built which will give a solid angle of 20 per cent of 4π with a 5 per cent geometrical resolution, and further, that if the apertures in the partitions between the counters and the corresponding baffle systems are specially shaped, then solid angles up to the order of 50 per cent of 4π might be obtained with 5 per cent resolution. The design considerations for such an instrument both in the restricted and general form are discussed in the next section.

§ 4. Design Considerations for Spectrometer of very large Solid Angle.

Fig. 5.

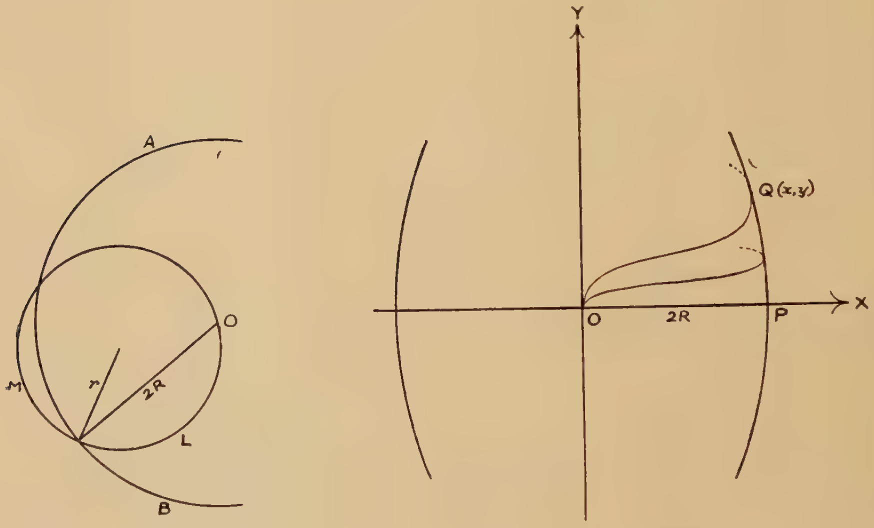

(*a*) Section by median plane.

(*b*) Section by plane containing the axis of symmetry.

Geometry of 360° spectrometer.

If we consider the diagram in fig. 5(*a*) which shows a section of the spectrometer by the median plane, then the circle AB represents the inner edge of the counting area which has radius 2R. OLM represents the path of a particle, radius r, where r is just great enough to ensure that it intersects n counter sections. Now it can easily be shown that if α is the angle subtended at O by a single section, then

$$r/\mathrm{R}=\sec(\overline{n-1}\,\alpha/2).$$

Hence we can draw up a table of values of r/R as a function of n and α, which table will tell us how wide we must make the counting area and what order of pulse size we must record to obtain a given resolution with a given value of α. With $\alpha=15°$, which is a suitable value for ease in construction, we find that the values of r/R for $n=1, 2, 3, 4, 5$ are 1·000, 1·009, 1·034, 1·082 and 1·154. This means that if we set the limit of our counting area at $2R_1=1{\cdot}07\times 2R$ and count triples, then we have a resolution of the order of 5 per cent.

If we now consider fig. 5 (*b*) which represents a section of the spectrometer by a plane containing the axis of symmetry, then the magnetic field lies along OY and O represents, as in fig. 5 (*a*), the position of the source which in this case is assumed to be emitting mono-energetic particles. Then OP represents the projection in the plane of the paper of the semicircular trajectory of a particle emitted normally to the plan of the paper. The sine curve OQ represents the projection on the plane of the paper of the helical trajectory of a particle emitted in a plane through O perpendicular to OP but whose direction of emission makes and angle θ with the normal to the plane of the paper. Then if Q has coordinates (x, y) with respect to O as origin, it is clear that if $OP=2R$, the locus of Q is the ellipse given by the freedom equations $x=2R \, . \cos\theta$, $y=\pi R \, . \sin\theta$, *i. e.* the ellipse

$$x^2/(2R)^2+y^2/(\pi R)^2=1.$$

This means that the locus of the points of maximum distance from the axis of symmetry, of the particles emitted from O, is the ellipsoid of revolution :—

$$(x^2+z^2)/(2R)^2+y^2/(\pi R)^2=1.$$

Now it can easily be shown that if we consider only those particles which are emitted with angles θ lying between $\theta=\pm\phi$ then the solid angle into which they are projected is $4\pi \sin\phi$. Hence for a geometry to collect 10 per cent of all the particles from the source $\sin\phi=1/10$, and for a limiting particle $x/2R=\cos\phi=1-1/200$. That is, the substitution of a right circular cylinder of radius 2R for the ellipsoid would introduce an error of only ½ per cent in the momentum of the particles registered. For 20 per cent collection the error would be about 2 per cent and for larger solid angles would increase rapidly. Thus where an overall resolution of the order of 5 per cent is desired, a spectrometer of solid angle 20 per cent of 4π could be built on the same principle as that described in the last section with simple cylindrical construction and rectangular apertures in the partitions. For larger solid angles, the partitions would have to be shaped, the shape being given by the envelope of the family of sine curves corresponding to the plot of the actual distance of the particle from the axis of symmetry against y. The general shape of this curve is shown in fig. 6 and it has freedom equations given by

$$x^2=-4R^2 \sin^3 X/\cos X(X-\tan X),$$

$$y^2= \quad 4R^2X^3/(X-\tan X),$$

where X is a parameter whose values are confined to those that make tan X/X negative.

It is clear, however, that for these large solid angles the original scheme for having a common anode for all the counters running round the median plane would have to be abandoned since the depth of the counting space has become so great. The difficulty can be overcome by using counters of roughly square section when viewed along the axis of symmetry, and fitting separate anodes parallel to the magnetic field.

Fig. 6.

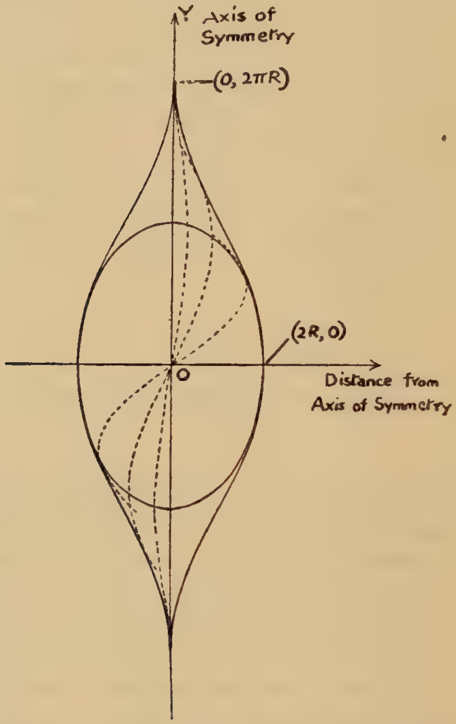

Section by plane through axis of symmetry, of envelope of trajectories.

Even with this method of construction, however, a reference to fig. 6 will show that solid angles in excess of about 50 per cent of 4π would produce counters of such a shape that their efficiency might be rather poor for particles intersecting them near their ends. For this reason and because of the difficulty of constructing a baffle system or thin window of the correct shape, it seems probable that 50 per cent collection would be about the practical maximum. It should of course be realized that these figures represent the ideal collecting fractions which might be obtained with perfect design ; in practice any baffle system would obstruct part of the solid angle and any windows would cause the loss of particles by scattering as would also the gas filling. Nevertheless, the figures given above represent such an improvement on the collecting fractions available by any of the conventional methods of beta-ray spectroscopy that it is felt that the development of this method would provide a powerful tool in the study of complex beta-ray spectra by the method of beta–gamma coincidences.

I must acknowledge the help given me in this work by Dr. S. C. Curran who designed the original apparatus and with whom I had many dicussions which were of the greatest value in suggesting ways of overcoming the faults in the early design. I must also thank Mr. D. L. Pursey for deriving the freedom equations to the envelope of the electron trajectories.

REFERENCES.

CURRAN, S. C. and RAE, E. R., 1947, *J. Sci. Instrum.*, **24**, No. 9, 233.
SIEGBAHN, K. and SLÄTIS, H., 1949, *Arkiv for Mat., Astr. o. Fysik*, **36** A, No. 22, p. 1.
STEVER, H. G., 1942, *Phys. Rev.*, **61**, 38.

XLIX. *The Influence of Exchange and Correlation Forces on the Specific Heat of Free Electrons in Metals.*

By E. P. Wohlfarth, Ph.D.,
Department of Mathematics, Imperial College, London*.

[Received March 1, 1950.]

Summary.

The effect on specific heat of including exchange terms in the expression for the electronic energy of a free electron gas is discussed. Previous work is considered ; the only full discussion (Koppe 1947) contains a number of algebraical errors. When these are corrected the theoretical expression for specific heat becomes, for sodium,

$$C_e = \gamma T / (8{\cdot}9 - 1{\cdot}7 \log_{10} T),$$

over a wide temperature range, γ being the Sommerfeld factor (§ 2). This relation is in disagreement with observation, due to the approximation implied in the use of a one-electron wave function. In § 3 Landsberg's tentative suggestion (1949) for estimating the effects of correlation forces is considered in relation to the present problem, a screened rather than a simple Coulomb potential being used in the exchange integral. The value of the screening constant required to restore approximate agreement with observed specific heats is found to be of the same order of magnitude as that derived from the soft X-ray emission spectrum.

§ 1. Introduction.

The well known Sommerfeld treatment of the electronic specific heat of metals leads to a linear temperature dependence at low temperatures. This result agrees with experiment not only for metals for which the operative electrons may be assumed very nearly free (*e. g.* sodium and copper) but also for the transition metals (*e. g.* nickel and palladium), the specific heat of which is due largely to the holes in an incompletely filled energy band (*cf.* Jones and Mott 1937). In the former case the observed linear temperature coefficient usually differs only slightly from Sommerfeld's value (for copper the ratio is about 1·5) ; such discrepancies may be justifiably ascribed to slight deviations of the electron distribution from that of perfectly free electrons. For the transition metals the ratio is much larger (about 30 for palladium), consistent with the fact that the density of states near the Fermi limit in the incompletely filled band is very high. In all cases, however, the observed temperature dependence is strictly linear.

---

* Communicated by the Author.

A closer examination of the electron theory of metals reveals at once, however, that the simple treatment is incomplete, owing to the neglect of the exchange terms, which have to be included in the expression for the electronic energy as a consequence of the exclusion principle. This omission is inconsistent with the application of theory to ferromagnetism (*cf.* Wohlfarth 1949) and to the calculation of cohesive energies (*cf.* Seitz 1940), where the exchange terms play a vitally important part. If the treatment is extended to include the exchange terms it is found that the agreement between calculated and observed specific heats is to a large extent invalidated. This situation is discussed in the present paper. It has been discussed previously, and a brief account of the history of this aspect of electron theory may be of interest.

Perhaps the first mention of the anomaly was made by Brillouin (*e. g.* 1934), who showed that on applying to metals the methods of Fock and Dirac, in which exchange is taken into account, the dependence of the energy on momentum is modified considerably as compared with that given by Sommerfeld, in that the $\epsilon(k)$ curve has an infinite slope, so that the density of states vanishes, at the top of the Fermi distribution. The effect of this modification on specific heat was first mentioned by Bardeen (1936), who found that the specific heat of free electrons is given, as a result of including the exchange terms, by

$$C_e = \gamma T / |\ln T| \quad . \quad . \quad . \quad . \quad . \quad . \quad . \quad . \quad . \quad (1.1)$$

at very low temperatures, instead of the usual linear relation. At higher temperatures the specific heat is stated to be smaller than the Sommerfeld value by a large factor of about 3–7. Bardeen never fully published his findings (presented in an Abstract of some 300 words), and in a later paper by Wigner (1938) little more is done than to give a *resumé* of the essential ideas and to quote an explicit relation for the ratio of the Sommerfeld specific heat to that calculated by Bardeen (*cf.* § 2). The first *full* discussion of the problem was given by Koppe (1947). Unfortunately Koppe's paper contains a number of algebraical errors which almost entirely destroy the significance of his final conclusions. Although obtaining relation (1.1) at very low temperatures, Koppe states that it is valid only below 10^{-4} °K. and that at higher temperatures $C_e = \gamma T$, with γ only slightly less than the Sommerfeld value, the calculated ratio being 1·58 for sodium at 1° K. as compared with the much larger value obtained by Bardeen.

In the present paper Koppe's calculations are corrected and the amended results briefly discussed (§ 2). In § 3 a possible method of circumventing these difficulties is considered, based essentially on a suggestion due to Landsberg (1949). Briefly, the suggestion concerns the possibility of estimating by a tentative empirical method the effects on the properties of the electron gas of the correlation energy terms (arising from the fact that the initial total wave function contains terms depending on the interelectronic distances and is thus more complicated than that based on the usual one-electron approximation). That these correlation terms might restore the agreement with experiment was in fact first suggested by Wigner (1938).

§ 2. CORRECTION OF KOPPE'S CALCULATIONS.

Koppe derives an expression (1947, (2)) for the free energy of an assembly of free electrons, including the exchange energy. This is derived in the ususal way (*cf.* Sommerfeld and Bethe 1933); in considering thermodynamic properties of the assembly at finite temperatures it is, however, necessary to introduce the Fermi distribution function $f(k, T)$ and the free energy expression becomes

$$\begin{aligned}F(T)=&\frac{h^2V}{16\pi^4m}\int_0^\infty f(k,T)k^4\,dk\\&-\frac{e^2V}{4\pi^3}\int_0^\infty\int_0^\infty f(k_1,T)f(k_2,T)k_1k_2\ln\frac{k_1+k_2}{|k_1-k_2|}\,dk_1\,dk_2\\&+\kappa T\frac{V}{2\pi^2}\int_0^\infty\{f\ln f+(1-f)\ln(1-f)\}k^2\,dk,\qquad(2.1)\end{aligned}$$

the second term representing the exchange energy, k denoting wave number (related to Koppe's p by $p=kh/2\pi$) and V the volume of the assembly. By minimizing F subject to constancy of the total number of particles, Koppe finds

$$\frac{h^2}{8\pi^2m}k_1^2-\frac{e^2}{\pi k_1}\int_0^\infty k_2f(k_2,T)\ln\frac{k_1+k_2}{|k_1-k_2|}\,dk_2-\zeta=\kappa T\ln\frac{1-f(k_1,T)}{f(k_1,T)},\qquad(2.2)$$

ζ being the usual statistical parameter. This is a functional equation of considerable complexity, and Koppe approximates to the solution by the discontinuous function

$$\left.\begin{aligned}f(k,T)&=1, && 0\leqslant k\leqslant a\\f(k,T)&=\alpha-\beta k, && a\leqslant k\leqslant b\\f(k,T)&=0, && b\leqslant k\end{aligned}\right\},\qquad(2.3)$$

with

$$a=(\alpha-1)/\beta,\qquad b=\alpha/\beta.$$

The parameters α and β are eliminated through the relation for the total number of particles (if each state is occupied by two particles with opposite spin,

$$N=\frac{V}{\pi^2}\int_0^\infty k^2f(k,T)\,dk),\qquad(2.4)$$

and by minimizing F. For $T=0$, $\alpha\rightarrow\infty$ and Koppe evaluates the various terms in (2.1) in series form in α^{-1} to cover the low temperature range, neglecting α^{-3} and higher powers. The subsequent development shows that the trial function (2.3) probably represents a very close approximation to the solution of (2.2).

Koppe's main error arises in evaluating the double integral in (2.1); on carrying through the calculation correctly this is found to be

$$\frac{1}{2}\left(\frac{\alpha}{\beta}\right)^4\frac{e^2V}{4\pi^3}\left\{1-2\alpha^{-1}+\frac{119}{72}\alpha^{-2}-\frac{1}{6}\alpha^{-2}\ln 2\alpha+O(\alpha^{-3})\right\}, \quad . \quad (2.5)$$

instead of Koppe's expression (6, 2). Using (2.5) and eliminating (α/β) through (2.4), the expression for F becomes

$$F(T)/N=\frac{3}{5}\epsilon_0\left(1+\frac{5}{12}x^2\right)-\frac{3}{4}\epsilon_j\left(1-\frac{13}{72}x^2+\frac{1}{6}x^2\ln\frac{x}{2}\right)-\frac{3}{2}\kappa Tx\ldots, \qquad (2.6)$$

with $x=\alpha^{-1}$ and

$$\epsilon_0=(h^2/8m)(3N/\pi V)^{2/3}, \qquad \epsilon_j=e^2(3N/\pi V)^{1/3}.$$

Koppe's corresponding quantities (his (9,1) and (9,2)) are related to ϵ_0 and ϵ_j by

$$\theta=3\kappa T/\epsilon_0, \qquad q=3\epsilon_j/2\epsilon_0\,;$$

in employing them he makes a further error in that his relation (10) should read

$$\theta=\left(1+\frac{97}{3}q\right)x-\frac{5}{3}qx\ln\frac{x}{2},$$

using his (incorrect) relation (7) for F. The correct relation between x and T is obtained through $(\partial F/\partial x)_T=0$, giving, from (2.6),

$$3\kappa T/\epsilon_0=\left(1+\frac{7}{24}\frac{\epsilon_j}{\epsilon_0}\right)x-\frac{1}{2}\frac{\epsilon_j}{\epsilon_0}x\ln\frac{x}{2}, \quad . \quad . \quad . \quad . \quad (2.7)$$

and the specific heat expression becomes

$$C_e=-T\left(\frac{\partial^2F}{\partial T^2}\right)_V=\frac{3}{2}N\kappa T\frac{dx}{dT}=\frac{9/2\,N\kappa(\kappa T/\epsilon_0)}{d(3\kappa T/\epsilon_0)/dx}$$

$$=C_e^0\bigg/\left\{1-\frac{5}{24}\frac{\epsilon_j}{\epsilon_0}-\frac{1}{2}\frac{\epsilon_j}{\epsilon_0}\ln\frac{x}{2}\right\}, \quad . \quad . \quad . \quad . \quad . \quad . \quad . \quad . \quad (2.8)$$

where $C_e^0=9/2\,N\kappa(\kappa T/\epsilon_0)$, the value obtained for specific heat in the absence of exchange, *i. e.* the Sommerfeld value. The factor 9 appears instead of the usual π^2 owing to the approximation (2.3).

For sodium $\epsilon_0/\kappa=3{\cdot}66\times10^4$ °K., $\epsilon_j/\kappa=4{\cdot}84\times10^4$ °K. so that (2.7) and (2.8) may be rewritten as

$$\left.\begin{aligned} C_e^0/C_e&=0{\cdot}72-1{\cdot}52\log_{10}y,\\ 4{\cdot}10\times10^{-5}T&=1{\cdot}38y-1{\cdot}52y\log_{10}y,\end{aligned}\right\}\quad . \; . \; . \; . \; . \qquad (2.9)$$

with $y=x/2=(2\alpha)^{-1}$. The solution of (2·9) has been obtained graphically and it is found that for $\log_{10}T$ between 0 and 3, and probably for even higher temperatures, as long as $T\ll\epsilon_0/\kappa$ the electronic heat of sodium is given by

$$C_e^0/C_e=8{\cdot}9-1{\cdot}7\log_{10}T. \quad . \; . \; . \; . \; . \; . \; . \; . \qquad (2.10)$$

Fig. 1.

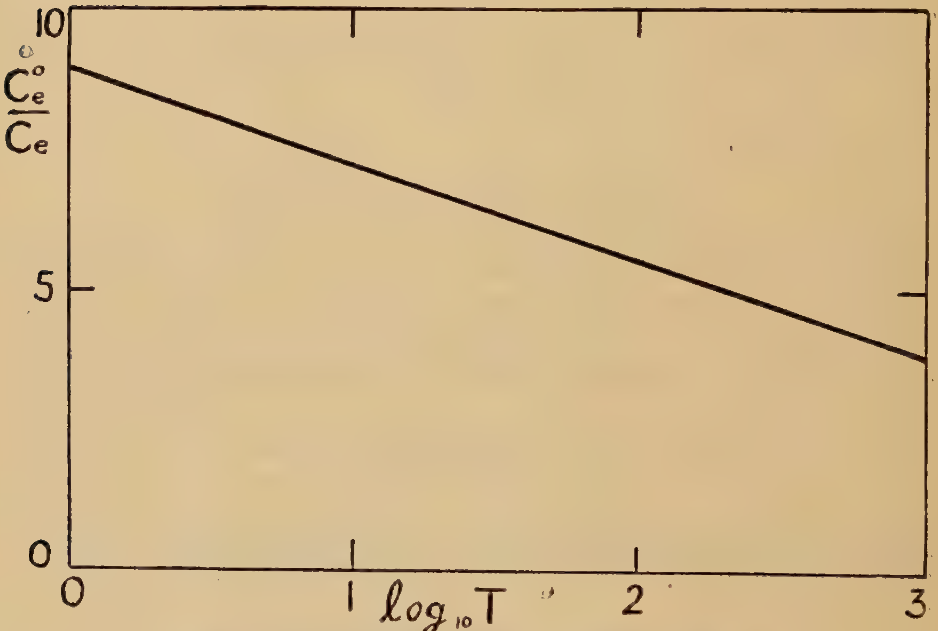

Decrease of electronic heat due to exchange, for sodium.
C_e, electronic heat with exchange ; $C_e^0=\gamma T$, Sommerfeld electronic heat.
Cf. relation (2·10).

This relation may be compared with that due to Bardeen, quoted by Wigner (1938) and stated to be " sufficiently accurate for temperatures between 1 and 100° K ". Bardeen obtains

$$C_e^0/C_e=1+\frac{4\pi me^2}{h^2k_0}\ln\frac{2e^2k_0}{\pi\kappa T}, \quad . \; . \; . \; . \; . \; . \qquad (2.11)$$

k_0 being the radius of the Fermi sphere. For sodium $k_0=0{\cdot}909\times10^8$ cm.$^{-1}$ so that (2.11) gives

$$C_e^0/C_e=8{\cdot}7-1{\cdot}5\log_{10}T.$$

It is difficult to see whether the close agreement between these two expressions is more than accidental, since no details as to the derivation of (2.11) are given. (It may be pointed out, however, that (2.11) is easily obtained if certain rough, and apparently unjustifiable assumptions are made.)

Fig. 1 gives a plot of (2.10), and fig. 2 of C_e/γ against T at very low temperatures, with $C_e^0=\gamma T$. The difference between the Sommerfeld value and that obtained by including exchange is seen to be very pronounced, not only at low temperatures where the ratio between them is very large (8·9 at 1° K. and 6·7 at 20° K.) and the C_e-T relation is not linear, but also at higher temperatures where the ratio is still large (3·8 at 1000° K.) although C_e is proportional to T over limited temperature ranges.

Fig. 2.

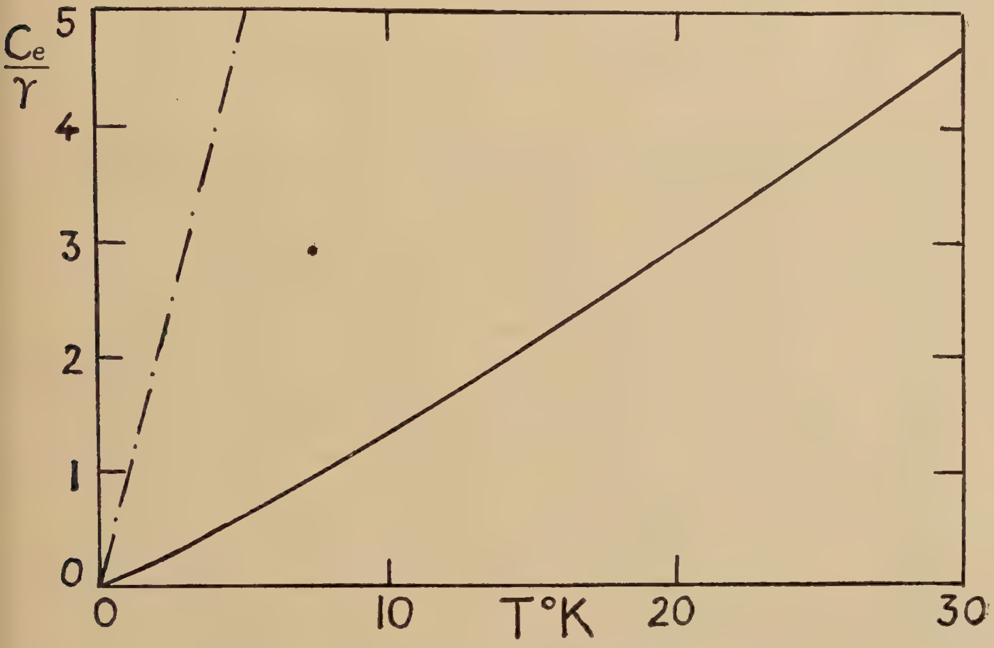

Variation of electronic heat with temperature, for sodium.
Full curve, with exchange ; broken curve, without exchange. γ, Sommerfeld factor.

Extensive measurements of low temperature specific heats of metals and alloys have been made. For sodium (Pickard and Simon 1948) an anomalous temperature variation of specific heat between 5 and 10° K. precludes the possibility of estimating the electronic contribution, but for a number of other metals for which the free electron approximation is applicable a linear temperature dependence, with a coefficient of the order of magnitude of the Sommerfeld value, has been established beyond doubt (*cf.* Jones and Mott 1937). For the transition metals where the electronic contribution to specific heat is much higher the same general conclusions have been drawn from some very precise measurements (*e. g.* Pickard and Simon 1948, palladium; Silvidi and Daunt 1950, tungsten); in some cases the linear temperature coefficient has been satisfactorily correlated with other physical properties of the metal. Whereas for the transition metals the effect of the exchange terms on the density of states and the electronic properties is at present incalculable, it is reasonable to suppose that theory would lead to similar anomalous results. It must be concluded, therefore, that the inclusion of the exchange terms in the way described provides an insufficient approximation.

§ 3. APPLICATION OF AN EMPIRICAL METHOD FOR ESTIMATING CORRELATION.

The anomalous results obtained in the preceding section arise as a consequence of the infinite slope at the Fermi surface of the curve relating energy and momentum (Brillouin 1934). Similar difficulties were encountered by Heisenberg (1947) in his theory of superconductivity. Heisenberg overcame this difficulty by considering electrons in a thin spherical shell at the Fermi surface to be excluded from normal electronic processes. More recently Landsberg (1949) found, in attempting a calculation of the width of the " tail " of the soft X-ray emission curve of sodium, in which a similarly divergent result was obtained, that even with reasonable values of the energy width of Heisenberg's shell the calculated tail width is still very much larger than that observed. He concluded that the discrepancy is due to the neglect of correlation forces, as in the present problem. Owing to the difficulties involved in an accurate treatment of correlation (Wigner 1934, 1938) it was suggested that the inter-electronic terms in the energy could be simulated by replacing the Coulomb potential in the exchange integral by a screened potential

$$V(r_{12})=e^2r_{12}^{-1}\exp(-\lambda r_{12}), \quad . \quad . \quad . \quad . \quad . \quad (3.1)$$

while the one-electron character of the total wave function is retained. The correlations introduced in this way are effective at large distances and are thus of a different nature from those considered by Wigner, which are effective at smaller distances only. The present method must be regarded as purely empirical, being introduced so as to attain agreement between the results of the theoretical treatment and a variety of experimental results. The use of (3.1) is still unsatisfactory in calculating cohesive energies of metals, since the screening term will affect the Coulomb as well as the exchange energy term in the total energy expression.

On calculating the tail width using (3.1) Landsberg finds that agreement with the observed value is attained if λ is taken to be about $1{\cdot}2\times10^8$ cm.$^{-1}$.

In this section the effect of using (3.1) on the calculated electronic heat is considered. At absolute zero the exchange energy becomes

$$\begin{aligned} J(k) &= \frac{1}{8\pi^8 V}\iiint \exp\{i(\boldsymbol{k}-\boldsymbol{k}')\,.\,(\boldsymbol{r}_1-\boldsymbol{r}_2)\}V(r_{12})\,d\tau_{12}\,d\tau_{k'} \\ &= \frac{e^2}{2\pi^2}\int_0^{k_0}\frac{d\tau_{k'}}{|\boldsymbol{k}-\boldsymbol{k}'|^2+\lambda^2} \\ &= \frac{e^2}{2\pi k}\int_0^{k_0} k'\ln\frac{(k+k')^2+\lambda^2}{(k-k')^2+\lambda^2}\,dk' \\ &= \frac{e^2k_0}{2\pi}\left\{2+\tfrac{1}{2}\left(\frac{1-x^2+l^2}{x}\right)\ln\frac{(1+x)^2+l^2}{(1-x)^2+l^2}-2l\tan^{-1}\frac{2l}{x^2+l^2-1}\right\}, \qquad (3.2) \end{aligned}$$

Fig. 3.

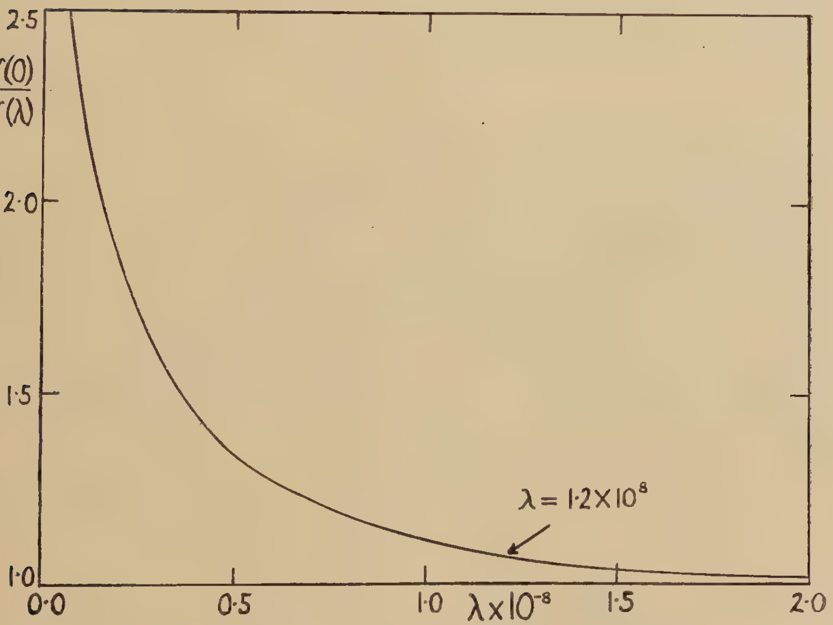

Change of electronic heat of sodium due to screening.

λ, screening constant in (3.1) ; γ (0), Sommerfeld linear temperature coefficient ; $\gamma(\lambda)$, coefficient for screened electrons. For $\lambda \neq 0$ it is assumed that $C_e=\gamma(\lambda)T$.

where k_0 is the radius of the Fermi sphere, $x=k/k_0$, $l=\lambda/k_0$. An adaptation of Koppe's procedure to evaluate J at finite temperatres would be difficult, but it is reasonable to suppose that once the infinity in the slope of $J(k)$ at the Fermi surface is removed the specific heat will have a normal temperature dependence at all temperatures except for a residual decrease of γ, depending on λ, below the Sommerfeld value. If this is assumed it is found that

$$\left.\begin{aligned} C_e^0/C_e &= 1+\frac{4\pi m e^2}{h^2 k_0}\, g(l), \\ \text{where}\qquad & \\ g(l) &= \frac{2+l^2}{4}\ln\left(1+4l^{-2}\right)-1. \end{aligned}\right\} \quad . \; . \; . \; . \; . \; . \quad (3.3)$$

Fig. 3 gives a plot of C_e^0/C_e against λ for sodium, and it is seen that C_e^0/C_e tends rapidly to 1 as λ increases and that for $\lambda = 1{\cdot}2\times 10^8$ cm.$^{-1}$ it is only about 8 per cent above unity. It may be shown that for this value of λ the density of states curve has very nearly normal form so that the above assumption is justified.

It appears, therefore, that using (3.1) in calculating specific heats the agreement with the simple theory may be regained, and that the value of λ required is of the same order as that deduced to bring about agreement with the observed soft X-ray emission spectrum.

REFERENCES.

BARDEEN, J., 1936, *Phys. Rev.*, **50**, 1098.
BRILLOUIN, L., 1934, *Helv. Phys. Acta*, **7** (Suppl. 2), 33.
HEISENBERG, W., 1947, *Z. Naturforsch.*, **2a**, 185.
JONES, H. and MOTT, N. F., 1937, *Proc. Roy. Soc.* A, **162**, 49.
KOPPE, H., 1947, *Z. Naturforsch.*, **2a**, 429.
LANDSBERG, P. T., 1949, *Proc. Phys. Soc.* A, **62**, 806.
PICKARD, G. J. and SIMON, F. E., 1948, *Proc. Phys. Soc.*, **61**, 1.
SEITZ, F., 1940, *Modern Theory of Solids* (New York : McGraw Hill).
SILVIDI, A. A. and DAUNT, J. G., 1950, *Phys. Rev.*, **77**, 125.
SOMMERFELD, A. and BETHE, H., 1933, *Handbuch der Physik* (2nd. ed.) **24**/**2**, 333.
WIGNER, E., 1934, *Phys. Rev.*, **46**, 1002 ; 1938, *Trans. Farad. Soc.*, **34**, 678.
WOHLFARTH, E. P., 1949, *Phil. Mag.*, **40**, 703.

L. *Note on the Inversion of the Laplace Transform.*

By B. GROSS *†.

[Received March 2, 1950.]

WHEN a function $h(\omega)$ is the Fourier transform of a function $H(\sigma)$, then $H(-\omega)$ will be the transform of $h(\sigma)$, the two functions forming a pair. A table of Fourier transforms therefore can be considered as having two entries. The Laplace transform, however, is different, in that the transform is not reciprocal. Thus, if $f(s)$ is the Laplace transform of $F(t)$,

$$f(s)=\int_0^{\infty} \exp(-st)F(t)\,dt=L\{F(t)\}, \quad . \quad . \quad . \quad . \quad . \quad (1)$$

the knowledge of $f(s)$ will not, in general, enable one to find the function $g(u)$, that is the inverse transform of $F(t)$, and therefore satisfies the relation :

$$F(t)=\int_0^{\infty} \exp(-ut)g(u)\,du=L\{g(u)\}. \quad . \quad . \quad . \quad . \quad . \quad (2)$$

For particular classes of functions, such a formula does however hold. With their aid it is frequently possible to invert the relation (2) and calculate $g(u)$, provided $f(s)$ is known. In spite of its particular nature this formula seems to us to be of considerable importance because it largely extends the scope of existing tables of Laplace transforms *restoring* to this transform up to a certain point, the " pair property " which has been found to be useful for the Fourier transform. The purpose of the present note is to call attention to this formula.

From (1) and (2) it follows that $f(s)$ is the iterated transform of $g(u)$, and therefore (Widder 1946),

$$f(s)=\int_0^{\infty}\frac{g(u)\,du}{u+s}. \quad . \quad . \quad . \quad . \quad . \quad . \quad . \quad . \quad (3)$$

This is Stieltjes equation, which is inverted by (Titchmarsh 1937)

$$g(s)=\frac{1}{\pi}\operatorname{Im} f[s\exp(-i\pi)]=-\frac{1}{\pi}\operatorname{Im} f[s\exp(+i\pi)]. \quad . \quad . \quad (4)$$

It has been supposed that all functions are real and s a real variable. The relation (4) obviously resolves the problem because it inverts (2), provided the transform of $F(t)$ is known. The condition of validity is that $g(z)=g[r\exp(i\theta)]$ is analytical for $-\pi<\theta<\pi$, and that

$$\int_0^{\infty} |g[r\exp(i\theta)]|^2\,dr$$

is bounded for $-\pi<\theta<\pi$ (Gross and Levi 1947).

---

* At present at the Electrical Research Association, on leave of absence from the National Institute of Technology, Rio de Janeiro, Brazil.

† Communicated by Dr. S. Whitehead.

The *result* may be summarized as follows :—

Laplace transform	Original function or inverse transform
$f(s)$	$F(t)$
$F(s)$	$\frac{1}{\pi}\operatorname{Im} f[t \exp(-i\pi)]$

As an *example*, consider the function

$$F(t)=\frac{1}{\sqrt{(\pi t)}}\exp(-k^2/4t),$$

$f(s)$ can be obtained from a table of transforms as

$$f(s)=\frac{1}{\sqrt{s}}\exp -k\sqrt{s}.$$

Since

$$\sqrt{[s\exp(-i\pi)]}=\sqrt{s}\exp(-i\pi/2)=-i\sqrt{s},$$

it follows that

$$f[s\exp(-i\pi)]=\frac{i}{\sqrt{s}}\exp(-ik\sqrt{s})=\frac{i}{\sqrt{s}}(\cos k\sqrt{s}-i\sin k\sqrt{s}).$$

and therefore

$$\frac{1}{\pi}\operatorname{Im} f[s\exp(-i\pi)]=\frac{\cos k\sqrt{s}}{\pi\sqrt{s}}.$$

Therefore

Laplace transform	Original function or inverse transform
$\frac{1}{\sqrt{s}}\exp(-k\sqrt{s})$	$\frac{1}{\sqrt{(\pi t)}}\exp(-k^2/4t)$
$\frac{1}{\sqrt{(\pi s)}}\exp(-k^2/4s)$	$\frac{\cos k\sqrt{t}}{\pi\sqrt{t}}.$

The author is greatly indebted to Dr. S. Whitehead for his helpful advice.

REFERENCES.

WIDDER, D. V., 1946, *The Laplace Transform* (Princeton: University Press), 339–341.

TITCHMARSH, E. C., 1937, *Introduction to the Theory of Fourier Integrals* (Oxford: Clarendon Press), 317–319.

GROSS, B. and LEVI, B., 1947, *Matematicae Notae*, **6**, 213.

LI. *The Fluorescence of Silver Halides at Low Temperatures.—* Part II. *Mixed Crystals of Silver Halides*[*].

By G. C. FARNELL, Ph.D., P. C. BURTON, B.Sc., and R. HALLAMA[†][‡].

[Received March 13, 1950.]

[Plates XIV.–XVII.]

ABSTRACT.

A description is given of the fluorescence emission spectra of mixed crystals of the silver halides. The results are interpreted from a knowledge of the emission and absorption spectra of the pure halides, and the extents of mixed crystal formation between them.

Some limited results for the temperature-variation of fluorescence efficiency are quoted, which are later shown to be quite compatible with theoretical predictions from a simple model put forward to explain the general result of pure crystal fluorescence.

§ 1. INTRODUCTION.

THE fluorescence spectra of pure silver halides at low temperatures have been described in a previous paper (Part I.). It was felt that an examination of the emission spectra of mixed crystals of the pure silver halides would also provide results of some interest. In particular the silver bromo-iodide system, which, for low iodide content, gave a strong green emission at 77° K., already mentioned briefly in Part I., seemed worthy of further investigation. The majority of results to be described in this Part are concerned with the emission spectra of mixed crystals, but some quantitative results on the variation of fluorescence intensity with temperature of silver bromo-iodide will be described and discussed.

§ 2. MIXED CRYSTAL PREPARATION.

Precipitated mixed crystals were made by pouring a mixed potassium halide solution into $AgNO_3$ solution, so that the differences of solubility of the different silver halides could not greatly affect the formation of mixed crystal. If the $AgNO_3$ solution is poured into the halide solution there is a tendency for the least soluble silver halide to precipitate first. A.R. quality reagents were employed, previous work having shown that the impurities present in them were not responsible for, nor had any influence on, the characteristic emissions of the halides at low temperatures.

---

[*] Communication No. 1315 H from the Kodak Research Laboratories.

[†] Now at the University of Helsinki.

[‡] Communicated by the Authors.

X-ray powder diffraction patterns were obtained for almost every specimen. It was deduced from these patterns that over ranges in which genuine mixed crystal formation was possible, the proportions of halides in the solutions represented with fair accuracy the actual composition of the mixed crystal. Thus the proportions quoted later are those of the halides in the precipitating halide solution, and may, when only one phase results, be taken as representing the composition of the mixed crystal.

Each of the three possible pairs of silver halides were precipitated together in the proportions of 5, 10, 20, . . . 90, 95 mol. per cent of one component in the other. In addition to these series, mixed crystals were also made of 5, 2, 1, 0·1, 0·01, 0·001 and 0·0001 mol. per cent of AgI in AgBr and AgCl.

Fig. 1.

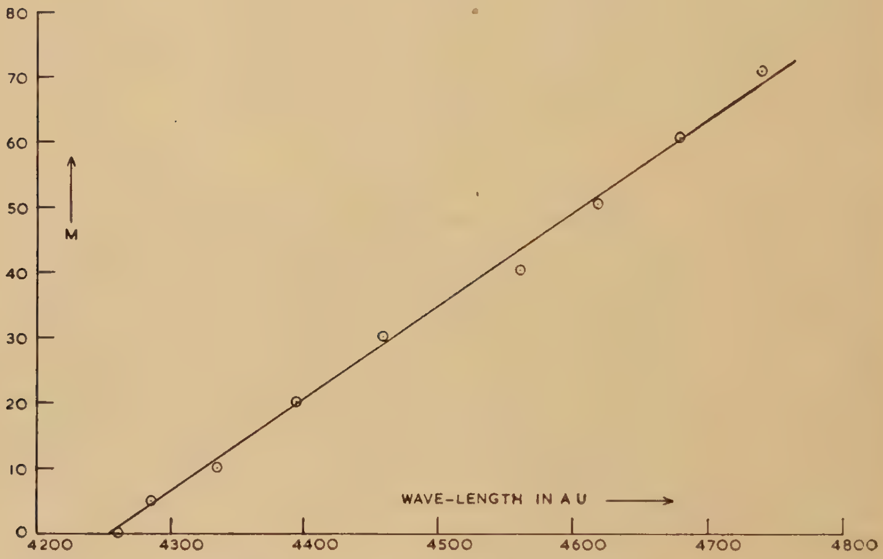

Shift of short wave-length end of emission band of bromo-chloride series with increase of AgBr content. M=mol. per cent AgBr.

§ 3. Bromo-Chlorides.

The bromo-chlorides are known to form a continuous series of mixed face-centred cubic crystals (Wilsey 1925). This result was confirmed by our own analysis. The emission spectra of the series are illustrated in Pl. XIV. As they were recorded at a specimen temperature of 77° K., only the red "silver" band of AgBr appears at high AgBr content: the characteristic green fluorescence of pure AgBr only just commences at 77° K. The regular shift of the short wave-length edge of the emission band towards longer wave-lengths with increasing AgBr content is illustrated graphically in fig. 1.

It is clear from spectral sensitivity measurements on bromo-chloride emulsions that the absorption edge moves over regularly from the AgCl position to the AgBr position on changing the bromo-chloride composition in that direction. It is therefore reasonable to suppose that the fluorescence emission spectra of a bromo-chloride series should show a regular change from that characteristic of AgCl to that characteristic of AgBr. The recordings illustrated in Pl. XIV. show this fairly clearly, even though they were made at a specimen temperature of 77° K. The characteristic emission of pure AgBr is known to lie in the range 5000 A. to 5500 A. at 77° K., and the spectra visible up to 70 mol. per cent AgBr tend towards this final position. Alternatively one can say that the spectra all appear to represent the emission of AgCl, but the short wavelength edge is progressively shifted to longer wavelengths by the self-absorption of the AgBr constituent (the absorption edge of AgBr lies at a somewhat longer wavelength than that of AgCl). It is important to remember, however, that the allowed energy band structure of the mixed halide is formed by interaction between silver and chloride and bromide ions, and that AgBr does not exist as a separate entity in the mixed crystal. For this reason the former explanation of the change in position of the spectra seems to be preferable.

§ 4. CHLORO-IODIDES.

X-ray powder diagrams showed that at the most there was only mixed crystal formation between AgCl and AgI to the extent of about 5 mol. per cent AgI in AgCl and vice versa. It is in fact well known that chlorides and iodides of identical cation only form small ranges of mixed crystals, owing to the large difference in size of the chloride and iodide ions (Grimm 1925). This lack of mixed crystal formation is evident from the appearance of the emission spectra shown in Pl. XV. Generally the emission spectrum of a particular specimen appears as the photographic sum of the emissions of the separate halides. An apparent exception, however, is the weakening of the AgCl emission for AgI contents of 0·001, and 0·01 and 0·1 mol. per cent AgI, particularly in the range 5400 A. to 5000 A. The spectra were all recorded under constant exposure conditions.

The narrow short wavelength band characteristic of pure AgI became visible at 10 mol. per cent AgI, and, like the main AgI band, showed no change of position with variation in precipitate composition. The X-ray powder diagrams showed that the structure of the AgI component was practically pure cubic (zincblende-type), very little of the hexagonal (wurtzite-type) phase being present.

§ 5. BROMO-IODIDES.

The results obtained with this series were rather more complex than those described in the preceding sections. Previous investigators (Wilsey 1925, Barth and Lunde 1926) have found that mixed crystals are formed at both ends of the range : the AgBr structure (face-centred cubic) accepts up to about 30 mol. per cent AgI, but the AgI structure (zincblende or wurtzite type) accepts only a few mol. per cent of AgBr. In the intermediate range both the AgBr-type and the AgI-type of mixed crystal are formed as separate phases. In our series of precipitated specimens the AgI-type of crystal began to appear at about 20 mol. per cent AgI, and could not be distinguished from pure AgI.

The emission spectra of our series at 77° K. are illustrated in Pl. XVI. Specimens of AgBr and AgBr containing 0·0001 and 0·001 mol. per cent AgI gave identical spectra, viz., the weak red band (5800 A. to 6450 A.) due to the presence of free silver, a phenomenon which has been previously described (Part I). At 0·01 mol. per cent AgI, however, a weak green band appeared (5050 A. to 5700 A.) whose intensity increased rapidly with increasing AgI content up to 4–5 mol. per cent AgI. The spectra illustrated were recorded with different exposure times and are thus deceptive as regards intensities. Beyond 5 mol. per cent AgI the intensity of the green band decreased and at the same time the band moved to slightly longer wavelengths (5130 A. to 6030 A.). The intensity decreased very suddenly beyond 30 mol. per cent AgI, but the band remained faintly visible up to 50 mol. per cent AgI. The main emission band of pure AgI became visible at 20 mol. per cent AgI and steadily increased in intensity up to 100 mol. per cent AgI. Meidinger (1939 b, 1940) has recorded essentially the same position for the intense green band when emitted by bromo-iodide gelatin emulsion layers of fairly low AgI content. He has also confirmed the fact that at around 88° K. maximum fluorescence efficiency is obtained with a specimen containing about 5 mol. per cent AgI. He actually measured the quantum efficiency of fluorescence of a gelatin suspension of AgBr+4 mol. per cent AgI at low temperatures, and obtained a value of about unity.

The emissions of AgBr+4 mol. per cent AgI at 77° K. and 20° K. are compared in Pl. XVII. Meidinger's result for the quantum efficiency was confirmed in so far as there was no difference in fluorescence efficiency at the two temperatures. It is reasonable to suppose that the temperature-dependent fluorescence of a pure solid will rise to a maximum efficiency of unity. It will be seen from Pl. XVII. that there is a very slight shift of the band towards longer wavelengths on reduction of the temperature. There was no observable shift of the band on raising the specimen temperature from 77° K. to 165° K.; however, the fluorescence was quenched at the latter temperature. Meidinger confirms the absence of a shift on raising the temperature from 88° K.

The green band could be excited by radiation of any wavelength up to the short wavelength edge of the emission band, the latter being known to also represent the long wavelength absorption edge of bromo-iodide.

The sudden fall of intensity of the green band beyond 30 mol. per cent AgI is presumably connected with the fact that almost pure AgI is precipitating out as a separate phase, but it is probably due more to a preferential absorption of the exciting radiation by the AgI than to a marked fall in the proportion of the bromide-type phase being formed. In the region of excitation silver iodide possesses a very much higher absorption coefficient than silver bromide. The second factor has probably some influence, however.

The fact that the green emission can be activated by such small percentages of AgI and that its position does not markedly shift over a wide range of AgI contents suggests that the emission is localized in the iodide ion. There is no tendency to approach the position of the emission band of pure AgBr, as in the case of bromo-chloride mixtures. The green bromo-iodide band probably has the same origin as the pure AgI band, but is displaced owing to the different environment of the iodide ion. In both types of the AgI crystal it has four silver ions as nearest neighbours, but in the bromide-type crystal it has six.

If the emssion is seated in the iodine ions of the mixed crystal it is essential that absorbed quanta should finally give rise to excited iodide ions. Silver iodide has a much higher absorption coefficient throughout the ultra-violet region than silver bromide, and thus a more than proportional amount of incident radiation will be absorbed by iodide ions. The remaining radiation not absorbed by them will be absorbed by bromide ions, and it must be assumed that the positive hole remaining after excitation travels a very short distance to a nearby iodide ion where it becomes trapped. Positive holes are not believed to be mobile over long distances in AgCl and AgBr at low temperatures (Mott and Gurney 1940) but it is quite possible that they can travel the few lattice spacings necessary for them to reach an iodide ion. Evidence in support of this contention of limited positive hole movement at low temperatures is provided by the observations on specimens of $AgCl+MnCl_2$ (described in Part I.), which showed a change in fluorescence colour from blue-green to red on reduction of the exciting intensity. It is impossible to explain the transfer of excitation from chloride ions to manganese ions without assuming a limited positive hole movement.

The fall in intensity of the green band at 77° K. for AgI contents higher than 5 mol. per cent may be due to a decrease in the localization of the iodide ion levels, *i. e.* the concentration of iodide ions reaches a level such that, with the bromide ions, there exists a more uniform energy band structure of the crystal. The probability of the excited electron returning to the ground state without fluorescence, as in AgBr at 77° K. or as a large number of electrons do in AgI, will be increased to a significant value.

§ 6. THE VARIATION OF FLUORESCENCE INTENSITY WITH TEMPERATURE.

The method employed was to focus the emission of a layer of silver halide, mounted on the outer surface of a black painted brass cylinder, on to a photovoltaic cell. The cylinder was allowed to warm up from 77° K. in the open air (protected from draughts) and the temperature of the specimen followed with a copper–constantan thermocouple. The temperature-variation of the cylinder (it required ten minutes to reach room temperature) was very reproducible. From a knowledge of the time which had elapsed since the withdrawal of the cylinder from the liquid nitrogen, the temperature could be predicted to within one or two degrees. The relative fluorescence intensity was measured in terms of a galvanometer deflexion, it having been ascertained that the measured deflexion was always proportional to the fluorescence intensity. The above simple method could not be employed for temperatures below 77° K. owing to the formation of solid air on the specimen.

Fig. 2.

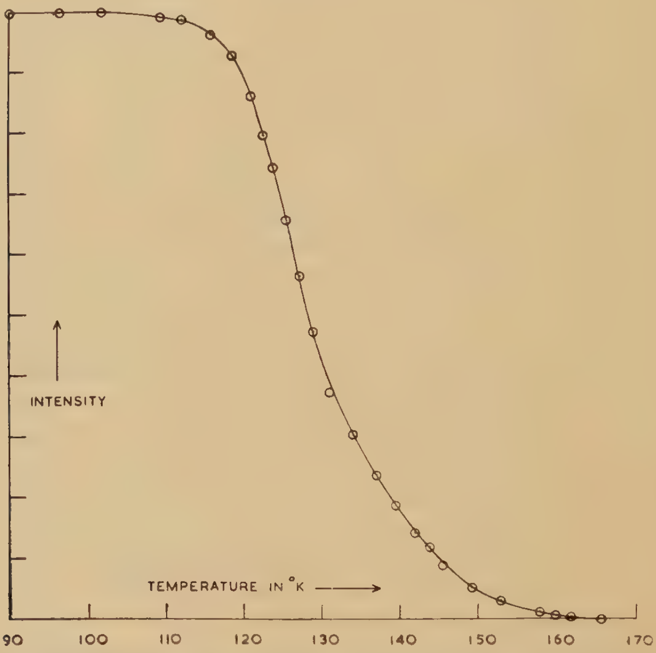

Variation of fluorescence intensity with temperature of AgBr+4 mol. per cent AgI. Intensity in arbitrary units.

As the sensitivity of the photovoltaic cell showed marked variation in the visible spectrum, and the emission band of AgCl shifts with temperature, it was only possible to obtain really useful results for a bromo-iodide specimen, and some limited results for AgI specimens for which the maximum fluorescence efficiency occurs at temperatures below 77° K. An attempt was made to examine the variation of fluorescence intensity of AgCl in narrow spectral regions with the aid of the photomultiplier arrangement described in Part I., but the intensities were too low to provide results of any accuracy.

The variation of fluorescence intensity of AgBr+4 mol. per cent AgI is illustrated in fig. 2. The curve was perfectly reproducible provided that a fresh specimen of precipitate was employed for each determination. The change of specimen was required as the electrons trapped at the low temperature always led to the formation of some "print-out" silver on warming up. This "print-out" silver activated a characteristic weak red emission, and also led to some screening of the silver halide. The curve was perfectly reproducible with the same specimen if the temperature was not allowed to rise above 130° K., which agrees with an observation by Meidinger (Meidinger, 1939a) that no photolytic silver is formed when a bromo-iodide emulsion is exposed at temperatures below 133° K. The flattening out of the curve to a constant high intensity for temperatures below 110° K., and the maintenance of this intensity level down to 20° K. (as already illustrated in Pl. XVII.) indicates that the maximum quantum efficiency of fluorescence obtainable by temperature reduction has been reached.

Fig. 3.

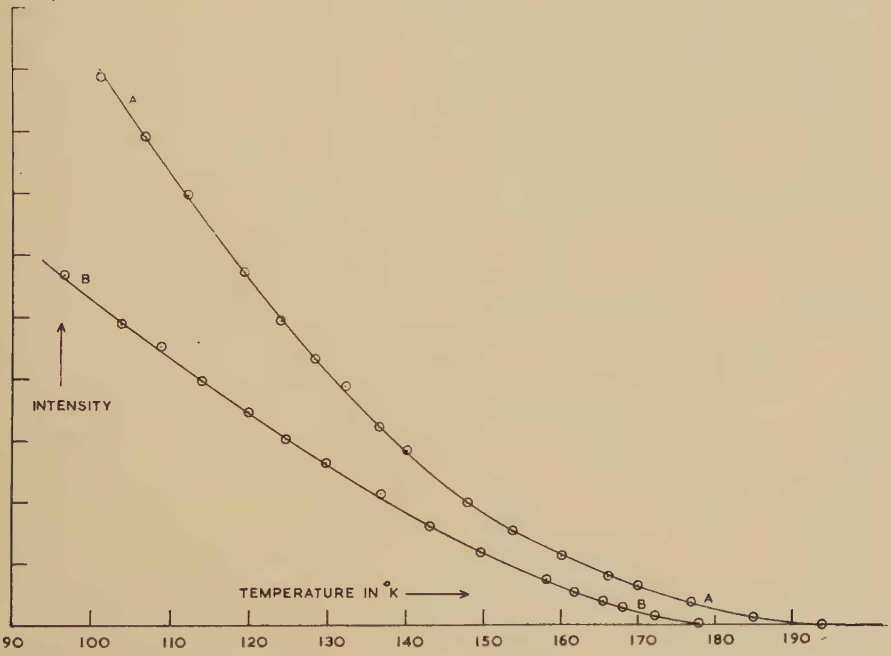

Variation of fluorescence intensity with temperature of two AgI specimens.
Curve A—a hexagonal specimen.
Curve B—a mixed specimen, containing rather more cubic than hexagonal AgI.
Intensities on same arbitrary unit scale for both specimens.

Fig. 3 illustrates the variation of fluorescence intensity with temperature of two AgI specimens, one predominantly hexagonal, the other mainly cubic. The measurements were made under precisely the same geometrical and optical conditions. It will be seen that over the temperature range investigated the hexagonal type possesses a higher fluorescence efficiency.

§ 7. Discussion of the Results.

Up till now the emission process has been pictured purely as the recombination of an electron with a positive hole, but in order to discuss the temperature-variation of fluorescence intensity a more detailed picture of the emitting centre is required. We make use of a model which has been employed by several investigators (von Hippel 1936, Mott 1938, Seitz 1939) in considering various problems, and which predicts that a pure solid will fluoresce at a sufficiently low temperature. The energy of the emitting centre depends on the configuration of the central and neighbouring atoms or ions, and although many coordinates are needed to specifiy this configuration, for the purposes of qualitative discussion we shall imagine that only one coordinate is required, as in the case of diatomic molecules. Fig. 4 shows the energy of the normal and excited states of the centre as a function of the configuration

Fig. 4.

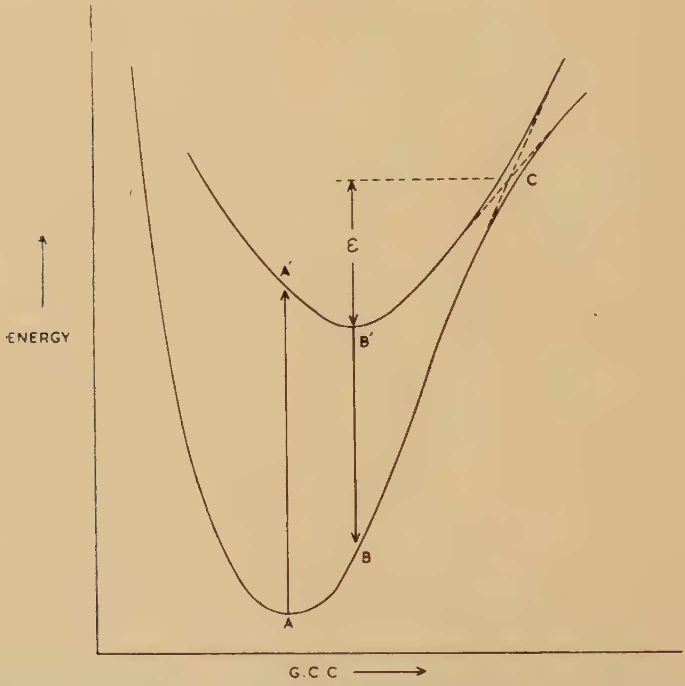

A model for the emitting centre in silver halides (after von Hippel, Mott and Seitz). G.C.C. is a generalized configurational coordinate which defines the positions of all ions at once.

coordinate. As the stable configuration of the lattice in the neighbourhood of the centre is different when the latter is in its normal and excited states, the minima of the two curves do not coincide. Moreover, as the excited state approximately corresponds to the transfer of an electron from a negative to a positive ion, the production of a given lattice displacement requires less energy in the region of excitation than it does when the lattice is in its normal state. This is represented by the degree of curvature of the upper curve being less than that of the lower.

Normal optical transitions between the ground state and excited state take place according to the Franck-Condon principle ; the re-arrangement of the ions surrounding the absorbing ion takes place after the electronic transition. The excess energy, corresponding to the difference between A′ and B′, is dissipated in the form of heat, *i. e.* it increases the vibrational energy of the lattice. It is to be noted that the transition indicated in fig. 4 corresponds to absorption in the tail of the band, an exciton, namely an electron bound in the field of a positive hole, being formed. Absorption of shorter wavelengths will raise electrons directly to the conduction band, but, provided that they are not trapped by some special singularity, they will ultimately return to excited states.

It is is advisable to remember at this point, however, that the energy level arrangement shown in fig. 4 is only applicable to a stationary exciton ; the movement of an exciton is too rapid to allow its surrounding ions to achieve equilibrium. A stationary exciton is probably formed in a pure silver halide after excitation by a positive hole becoming trapped at a positive ion vacancy (the latter being definitely known to be present), an electron being subsequently captured in the field of the positive hole. Thus it may not be strictly accurate to speak of the fluorescence of a pure solid, as some defect is required in order that the above mechanism be effective, but rather of a fluorescence which is not due to any specific impurity. All references to pure solid fluorescence in this work should therefore be read with this provision in mind. In the case of the bromo-iodide system positive holes are trapped at the sites of iodine ions to form stationary excitons after electron capture.

The excited system may return to the ground state in two ways, either by making a direct jump with the emission of fluorescence, or transferring to a high vibrational level of the ground state from which it may gradually return with the transfer of energy to the lattice. This latter process requires a little further explanation. In fig. 4 it will be seen that at an energy ϵ above the minimum of the excited state, the ground state and excited state curves closely approach each other. Theoretically, actual crossing is forbidden, but there is an appreciable chance of the excited state changing over, with the emission of one or two vibrational quanta, to a high vibrational level of the ground state. It will be seen immediately that this latter process is temperature-dependent ; if the excited system cannot receive energy ϵ from the lattice, a return to the ground state can only be achieved by emission of fluorescence. Thus at high temperatures there is competition between the dissipation process and the fluorescence process, whereas at low temperatures only the fluorescence process can occur.

The above ideas can be formulated mathematically. If F is the probability per second of the fluorescence process (which will be assumed to be independent of temperature), and D the corresponding quantity for the dissipation process, the quantum efficiency of fluorescence is given by

$$\eta=\mathrm{F}/(\mathrm{F}+\mathrm{D})=1/(1+\mathrm{D}/\mathrm{F}), \quad . \quad . \quad . \quad . \quad . \quad . \quad (1)$$

D being a function of temperature. D will contain the ordinary Boltzmann factor, $\nu \exp(-\epsilon/k\mathrm{T})$, where ν is the vibrational frequency of the system in its excited state, ϵ has the meaning illustrated in fig. 4, and T is the absolute temperature. A factor β must also be included in D to allow for the fact that the excited state does not necessarily transfer to the ground state every time it reaches the part C; β may possess any value up to unity. Thus (1) may be written

$$\eta=1/[1+\mathrm{K}\exp(-\epsilon/k\mathrm{T})], \quad . \quad . \quad . \quad . \quad . \quad . \quad . \quad (2)$$

where $\mathrm{K}=\nu\beta/\mathrm{F}$. For the purpose of comparison of experiment with theory it is to be noted that expression (2) can be transformed to

$$\ln(\eta^{-1}-1)=\ln\mathrm{K}-\epsilon/k\mathrm{T}. \quad . \quad . \quad . \quad . \quad . \quad . \quad . \quad (3)$$

Thus a plot of $\ln(\eta^{-1}-1)$ against $1/\mathrm{T}$ should yield a straight line the slope of which gives ϵ/k, and whose intercept with the $\ln(\eta^{-1}-1)$ axis gives ln K.

If this discussion is correct, the curve of fig. 2 represents essentially a plot of quantum efficiency against temperature; the flat low-temperature part fixes the level $\eta=1$, and we can replot the curve in accordance with expression (3). This is done in fig. 5. It will be seen that for values of η ranging from 1·0 to 0·5 [$\ln(\eta^{-1}-1)$ from $\bar{5}$·0 to 0] and temperatures from 110° K. to 130° K. ($1/\mathrm{T}°\mathrm{K}\times 10^4$ from 90 to 77) a straight line is obtained. Above 130° K., however, the plot corresponds to quantum efficiencies higher than those given by the theoretically predicted straight line. This deviation is to be expected, however, for below 130° K. no appreciable "printing out" occurs, but above this temperature silver commences to be formed. It has been mentioned several times previously that this silver behaves as an activator, and gives rise to a weak red fluorescence. Thus at temperatures above 130° K. the measured intensity is the sum of the green bromo-iodide emission and the red emission. Actually the deviation is of no real consequence as the theory outlined above does not apply when the crystal under consideration is undergoing a photochemical change. So far the experimental results can justifiably be claimed to be in agreement with theory.

The value of ϵ derived from the straight line plot is 0·35 eV., which appears reasonable. The situation with regard to the constant K is less satisfactory. The value derived from the intercept of the straight line plot with the $\ln(\eta^{-1}-1)$ axis is $10^{13\cdot 6}$, which is the experimental value of $\nu\beta/\mathrm{F}$. As no phosphorescence is observed with the bromo-iodides F must be at least 10^5 sec.$^{-1}$; the maximum value of β is unity; and ν will be $\sim 10^{12}$. Thus the maximum theoretical value of $\nu\beta/\mathrm{F}$ is $\sim 10^7$ giving a discrepancy between theoretical and experimental values of $\sim 10^7$.

Fig. 5.

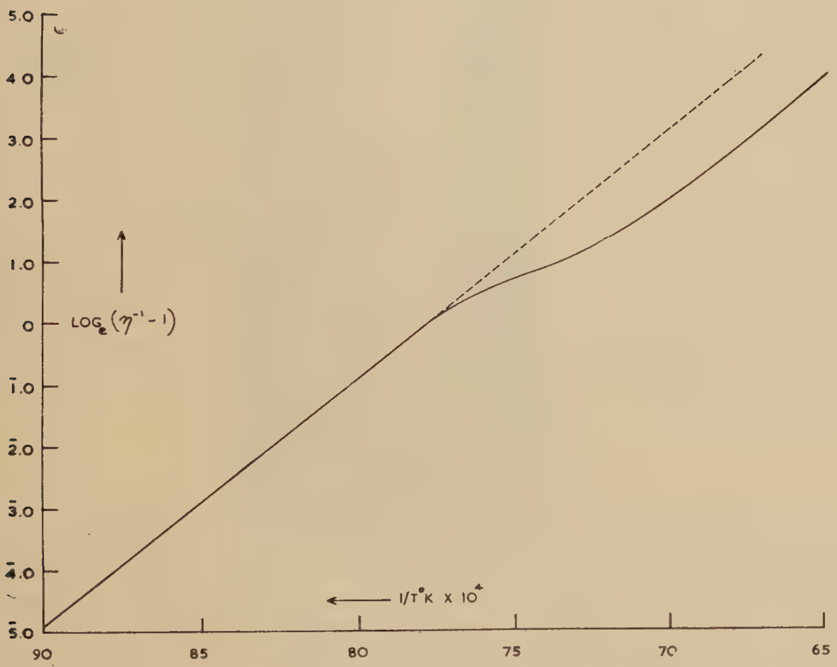

The plot of $l\eta\ (\eta^{-1}-1)$, where η=the quantum efficiency of fluorescence, against the reciprocal of the absolute temperature for AgBr+4 mol. per cent AgI. The dashed line represents the course of the plot if expression (2) had been obeyed at higher temperatures.

This discrepancy can be removed, however, by a slight increase in the rigour of the theory. It was assumed earlier that ϵ was independent of temperature, but this can hardly be true considering that the lattice constant and therefore the equilibrium configuration of the ions, is temperature dependent. We shall assume that

$$\epsilon=\epsilon_0+\alpha\mathrm{T}, \quad . \quad . \quad . \quad . \quad . \quad . \quad . \quad . \quad . \quad . \quad (4)$$

where ϵ_0 is the value of ϵ at absolute zero, and α is a small constant of dimensions energy/degree. Referring to expressions (2) and (3) it will be seen that the energy constant derived from the straight line plot is

ϵ_0 (0·35 eV.) and that K has now become equal to $(\nu\beta/F)\exp(-\alpha/k)$. Taking F now equal to 10^8 sec.$^{-1}$, $\beta=1{\cdot}0$, $\nu=10^{12{\cdot}6}$ sec.$^{-1}$, agreement between experiment and theory is achieved if $\alpha=-1{\cdot}8\times10^{-3}$ eV./degree. This is mere speculation, as the values of all other constants appearing in K are uncertain, but the fact that the quantum efficiency-temperature results follow a predicted course, as shown above, does suggest that the essentials of the theory are correct.

It should be mentioned, however, that the same formula for the temperature dependence of efficiency can be obtained on the assumption that ϵ represents the energy needed for the positive hole to escape from the fluorescence centre and travel to a quenching centre. On this basis one could understand why Meidinger, in his investigation of the fluorescence of photographic emulsions, found the quenching temperature of bromo-iodide to vary from one emulsion to another—a very fine-grain emulsion, for instance, showed no fluorescence even at 88° K. We have been unable to confirm this result.

To sum up, we may say that, in general agreement with previous investigators of pure-solid fluorescence (Kudriavzewa 1934, Kröger 1940), we find that the flourescence emission bands of pure and mixed silver halides lie just to the long-wavelength side of their respective absorption edges. Such results as are available on the variation of fluorescence efficiency with temperature are quite compatible with theoretical considerations, and support the simple model put forward to explain them.

ACKNOWLEDGMENTS.

Our thanks are due to Professor F. E. Simon, C.B.E., F.R.S., of the Clarendon Laboratory, Oxford, for his assistance in enabling us to carry out experiments at liquid hydrogen temperature. We are also indebted to Mr. A. H. Fox, a former member of these laboratories who recorded many of the X-ray powder diagrams of our specimens.

Research Laboratories,
Kodak Limited,
Wealdstone, Harrow, Middx.

REFERENCES.

BARTH, T. and LUNDE, G., 1926, *Zeit. phys. Chem.*, **122**, 293.
GRIMM, H. G., 1925, *Zeit. phys. Chem.*, **101**, 410.
VON HIPPEL, A., 1936, *Zeit. f. Phys.*, **101**, 680.
KRÖGER, F. A., 1940, *Physica*, **7**, 1.
KUDRIAVZEWA, W., 1934, *Zeit.f. Phys.*, **90**, 489.
MEIDINGER, W., 1939, *Phys. Zeit.*, **40**, 73 (*a*), 517 (*b*) ; 1940, *Phys. Zeit.*, **41**, 277.
MOTT, N. F., 1938, *Proc. Roy. Soc.* A, **167**, 384.
MOTT, N. F. and GURNEY, R. W., 1940, *Electronic Proccesses in Ionic Crystals* (Oxford : The University Press), p. 138.
SEITZ, F., 1939, *Trans. Faraday Soc.*, **35**, (1), 74.
WILSEY, R. B., 1925, *J. Franklin Inst.*, **200**, 739.

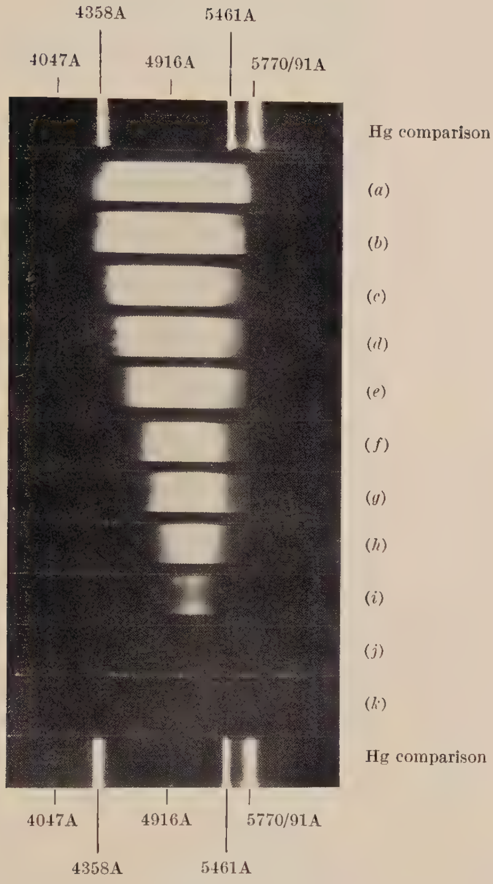

Emission spectra of mixed crystals of AgCl+AgBr at 77° K.

(*a*) Pure AgCl
(*b*) 95 mol. per cent AgCl, 5 mol. per cent AgBr
(*c*) 90 ,, 10 ,,
(*d*) 80 ,, 20 ,,
(*e*) 70 ,, 30 ,,
(*f*) 60 ,, 40 ,,
(*g*) 50 ,, 50 ,,
(*h*) 40 ,, 60 ,,
(*i*) 30 ,, 70 ,,
(*j*) 20 ,, 80 ,,
(*k*) Pure AgBr

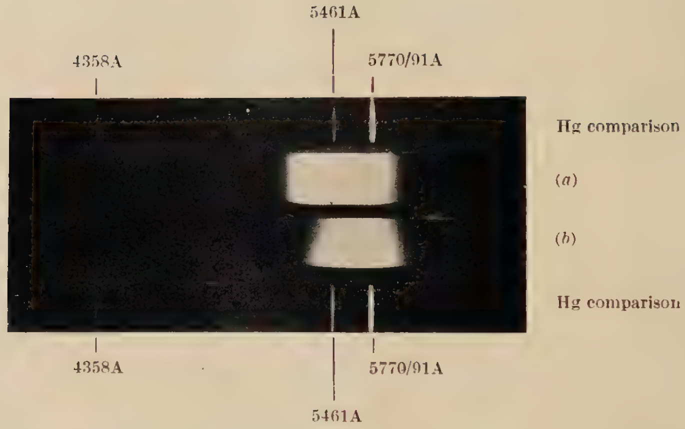

Comparison of the emission spectra of AgBr+4 mol. per cent AgI at 77° K. (*a*) and 20° K. (*b*). (Recorded with glass spectrograph of higher dispersion.)

LII. *A Determination of the Energy Distribution of Electrons in the Positive Columns of Gas Discharges.*

By C. HAIGH and T. SMITH*,
Physics Department, Leeds University †.

[Received March 20, 1950.]

SUMMARY.

The electron energies in the positive column of low pressure hot cathode glow discharges have been examined by the magnetic spectrum method.

From measurements of the energy distribution of electrons reaching a positive probe a method of finding the space potential is deduced. With this knowledge a comparison is made of the energy distribution of electrons, in the positive columns of air and argon discharges, determined by the present method and the conventional probe method. Wide discrepancies are observed.

The magnetic spectrum indicates a distribution of the Druyvesteyn form whilst that deduced from probes is Maxwellian. The changing form of the distribution reaching negative probes is proof of the failure at these pressures of the assumptions on which Langmuir probe theory is based. Calculations by Boyd on positive ion sheath formation may give some indication of the mechanisms producing the changing distribution.

§1. INTRODUCTION.

THE electrical conditions in a discharge are completely specified when the electron and ionic concentrations and energy distributions at every point are known. Of these parameters perhaps the most important is the electron energy distribution since it links many of the macroscopic features of a discharge with the nature of the particles involved. At the same time it is difficult to determine either by experiment or calculation.

The usual way, hitherto employed, of making a direct determination of this energy distribution is the probe method (Langmuir and Mott Smith, 1924), in which the variation of current, with the potential of the probe, is measured.

Langmuir showed that, under ideal conditions, if electrons having a Maxwellian energy distribution reach the probe, a plot of the logarithm of the electron current against the probe potential has a straight line section terminated by a sharp break at the space potential. Unfortunately, many factors, of which the reflection and secondary emission of electrons are the most important, mask the true shape of the characteristic and make the determination, of both the space potential and the energy distribution, difficult (Langmuir, 1924, Loeb 1939).

---

* Now Assistant Lecturer in Physics, Marischal College, Aberdeen.

† Communicated by Professor R. Whiddington, C.B.E., F.R.S.

If a non-linear characteristic is obtained under ideal conditions, it can be analysed by Druyvesteyn's method (1930) in which the energy distribution is obtained from a knowledge of the space potential and the second derivative at every point of the characteristic.

It was to develop a new method of making a direct determination of the electron energy distribution and thereby to test some of the information deduced from probe measurements that the present experiments were carried out. Electrons from the positive column of a discharge have been allowed to pass through a slit in a plane probe, placed parallel to the tube axis, and held at the space potential. The electrons were analysed by the magnetic spectrum method. In this way the energy distribution of the electrons crossing unit area of the discharge per second was obtained. The effect of various types of space charge on the energy distribution can also be investigated, by varying the probe potential, and therefore several assumptions of probe theory can be tested.

§2. DESCRIPTION OF APPARATUS.

The analysing system is essentially the same as that used in this laboratory for many years (Jones and Whiddington 1928). Its increased size gives a dispersion of 0·4 mm./volt and the different type of slit system produces a photographic trace of a homogeneous beam of electrons having a line width of 0·5 volts.

The slit system (fig. 1) consists of two slits, 0·005 mm. wide pierced in platinum foil at the end of two cylindrical tubes, A, B. The tube nearer to the discharge is 2·43 cm. long and 0·35 cm. in diameter whilst the second tube is 2·70 cm. long and 0·6 cm. diameter. These two tubes fit into two insulated brass cylinders, C, D, so that the slits are 4·7 cm. apart. The electrons are accelerated between the slits before entering the highly evacuated camera.

The system forms a weak electrostatic lens, when potentials are applied between the slits, but for a ratio of final to initial electron energies greater than 6 there is no appreciable aberration produced (Klemperer and Wright 1939). Thus with an accelerating potential of about 200 volts, all electrons having energies less than 30 volts would be brought to the same focus, and the fraction of the initial electrons which pass through the second slit would be independent of their initial velocity. Furthermore, any increase of the accelerating potential would not result in a displacement of the focus and so the fraction would also be independent of accelerating potential. Accordingly, the intensity of the electron beam emerging from the slits was measured whilst the accelerating potential was increased. When the accelerating potential exceeded 200 volts the intensity became constant, showing that the Klemperer and Wright criterion applied.

After selection by the slit system the electrons were analysed and recorded on a sensitized film (Brett and Whiddington 1925). The conversion of the photographic blackening, D, to electron intensity, I, was achieved by use of the reciprocity relation ($D=kIt$) over the toe region of the sensitometric curve (Haigh and Smith 1950).

Fig. 1.

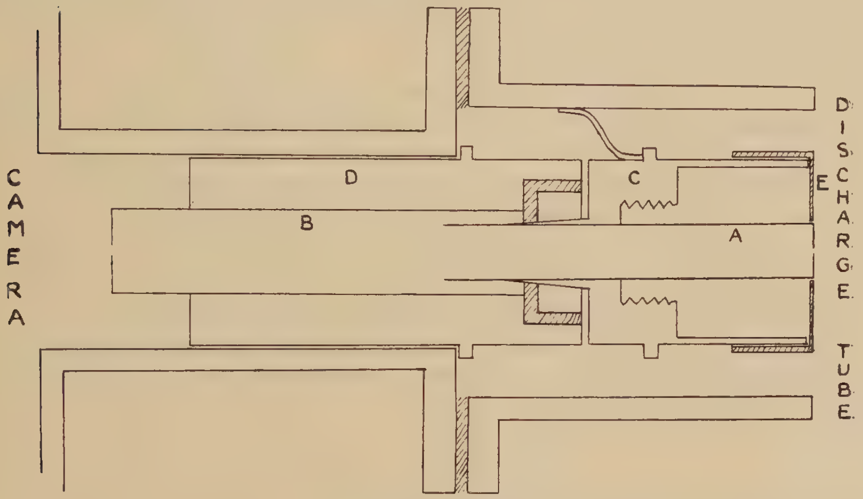

The slit system.

Fig. 2.

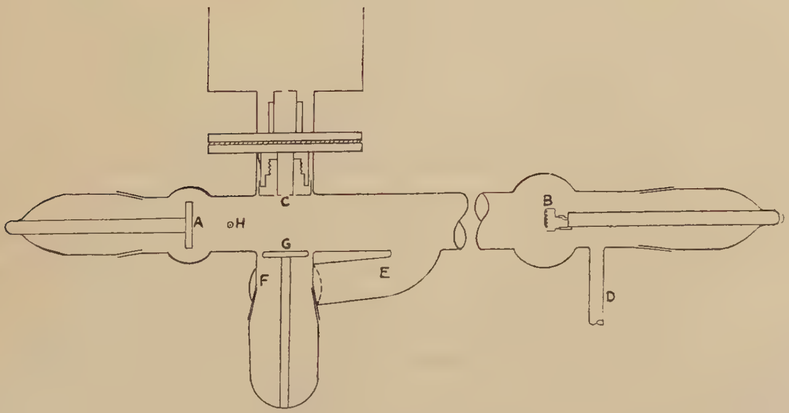

The discharge tube.

§ 3. RESULTS.

The discharges examined, so far, have been hot cathode glow discharges at pressures about 10^{-2} mm. Hg. The discharge tube (fig. 2) was constructed throughout of Pyrex tubing of 2 cm. external diameter.

The anode, A, and cathode, B, were fitted to the tube by means of ground joints, the separation between them being 57 cm. The slits, C, were inserted in the side of the tube at a point in the positive column 6·5 cm. from the anode. The gas inlet was through a tube, D, near the filament whilst evacuation was accomplished through a wide tube, E, 16 cm. from the slits. This ensured that the discharge was undisturbed in the region of the slits. The slits could be removed through an opening, F, in the side of the tube. This opening was closed by a glass stopper, G, when the discharge was in progress. A small wire probe, H, was inserted 3·1 cm. from the anode.

The tube potential was maintained by a stabilized power supply giving voltages up to 1000 volts over a range of tube currents of 10 to 100 m.amps. The tube current itself was controlled by variation of the filament heating current. Other potentials were maintained by banks of accumulators and controlled by means of suitable resistances. The circuit allowed variation and measurement of the potentials between the anode and first slit and between the first and second slit.

The ability to reproduce the discharge conditions was demonstrated by the constancy of the characteristic of the small wire probe on different occasions. It was found that careful control of the tube conditions yielded constant characteristics.

Probe Characteristics.

The slit system was of an irregular shape but by placing over the front a cap of copper, or mica, E, (fig. 1) the surface presented to the discharge could be used as a flat probe. The first investigations showed that, although the wire probe characteristic remained constant, those obtained with the slit suffered a gradual variation. If the slits had been cleaned the change in the characteristics was considerable during the first half hour. The change corresponded to a space potential variation of about 4 volts although the actual shape of the semi-log plot remained unchanged. The potential difference between the anode and the space always increased. Thereafter only a small drift in the characteristic was found. This may be readily accounted for by a progressive change in the state of the slit surface. It was necessary to clean the slits regularly and so the discharge was always allowed to run until a constant characteristic was obtained, before taking the energy distribution photographs.

These characteristics when analysed by the conventional methods indicate a Maxwellian energy distribution, as would be expected from the straight portion of the semi-log plot (fig. 3). It is to be noted that the straight line is quite definite, extending over a hundred fold range of probe current. A determination of the space potential from the current reaching a positive probe gives it at a point 6 volts positive to the break point. The determination, however, is rather uncertain (Langmuir and Mott Smith 1924). In the present investigations the space potential may be determined within one or two volts by a method independent of the probe characteristic.

Determination of the Space Potential.

When the first slit is held at a potential positive to the plasma the electron current is limited by a sheath of negative space charge across which there is a rapid change of potential. If the electrons pass through the space charge without collision they will reach the probe with the energy distribution characteristic of the positive column but having gained energy in crossing the sheath.

Fig. 3.

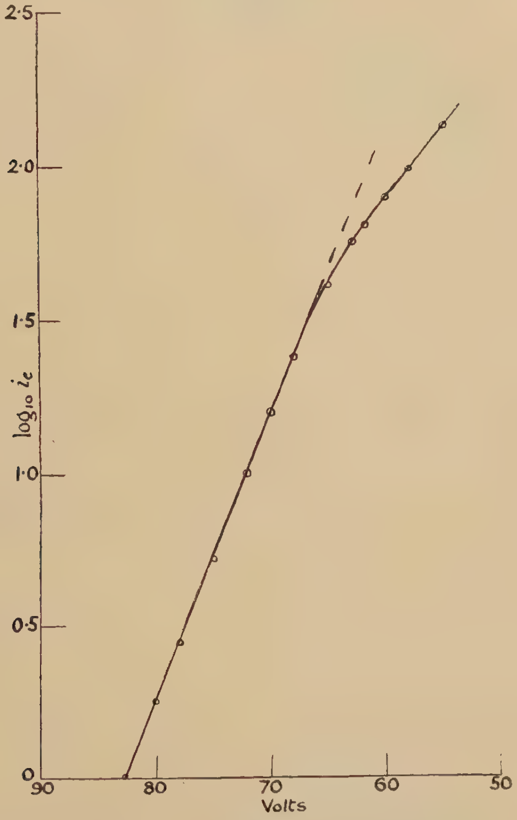

Semi-log plot obtained with a flat probe. Gas, argon ; tube voltage, 600 volts ; tube current, 40 m.amps. pressure, 0·025 mm. Hg.

A series of photographs was therefore taken at various potentials relative to the anode. Since the position on the film corresponding to zero energy in the discharge is known accurately, and since the distance on the film can be calibrated in volts, it is possible to measure the space charge interval corresponding to each voltage. A plot of probe potential against space charge interval enables a determination of the space potential to be made. The intensity curves of two photographs from one of the many series which have been obtained are shown in fig. 4. Similar photographs have been obtained with both air and argon discharges.

It can be seen that, when the distributions obtained with the first slit at two different potentials are extrapolated to the abscissa their slowest electrons have an energy corresponding to 2 volts and 10 volts respectively, the potentials of the slit were therefore 2 volts and 10 volts above the space potential, and so the space potential can be found. The low energy electrons which make the extrapolation necessary are made up of secondary electrons emitted from the slit edges, and of electrons which have lost energy by collision in the sheath (Smith, Tait and Whiddington 1949). Little error is introduced by the extrapolation since the form of the distribution in this region is taken from the distribution reaching a negative probe. Here no extrapolation is needed and the uncertainty introduced by the slightly different distribution does not amount to more than 1 volt. This method indicates that the space potential in both air and argon discharges, at these pressures, may be regarded as being about 4 volts positive to the break point.

Fig. 4.

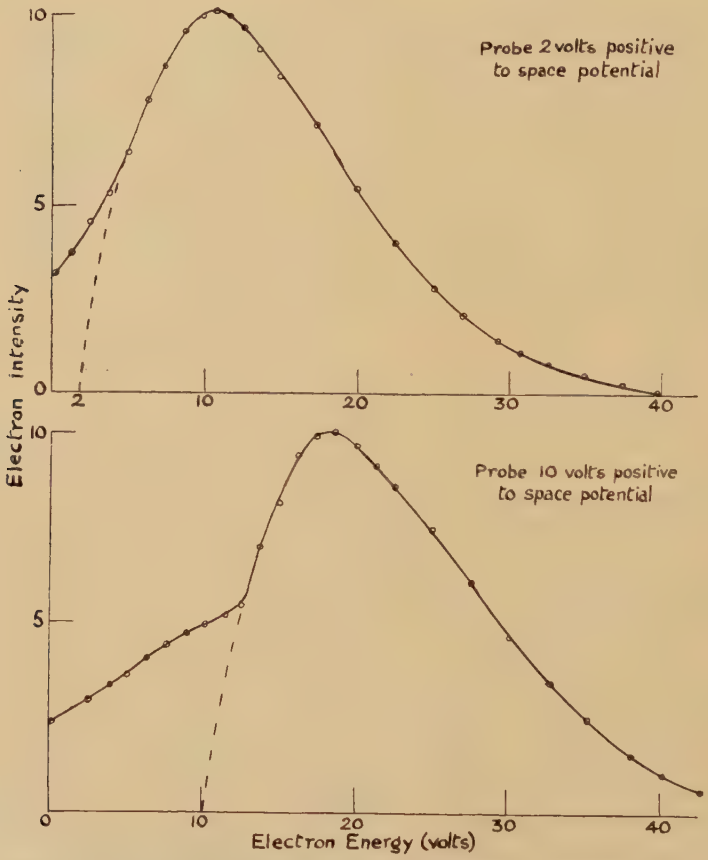

Energy distribution reaching positive probes. Gas, air ; pressure, 0·018 mm.Hg ; tube voltage, 600 volts ; tube current, 40 m.amps.

The Energy Distribution.

Having determined the space potential, the energy distribution photographs were obtained with the first slit held at that voltage, when the electrons striking it have the undisturbed energy distribution of the plasma.

Points from three separate determinations of the energy distribution in an argon discharge (pressure, 0·025 mm. Hg; tube current, 40 m.amps.; tube voltage, 600 volts) are given in fig. 5. It can be seen that there is close agreement between the different determinations.

Fig. 5.

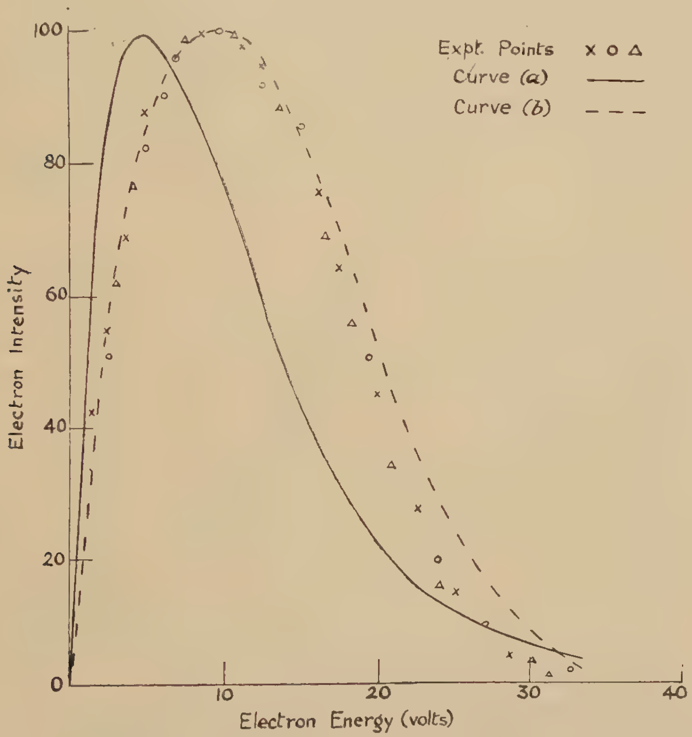

Electron energy distribution in argon (pressure, 0·025 mm. Hg; tube current, 40 m.amps.; tube voltage, 600 volts).

Experimental points; × ○ △

(*a*) Maxwellian flux distribution E=7 5 volts.

(*b*) Druyvesteyn flux distribution E=11·0 volts.

For this discharge, an analysis of the probe characteristic obtained with the first slit, gives the energy distribution of the electrons as Maxwellian with an average energy of 7·5 volts. For a Maxwellian distribution the number of electrons crossing unit area per second having energies in the range V to V+dV is given by

$$N=AV \exp(-1{\cdot}5\, V/E)\, dV. \qquad (1)$$

The flux distribution corresponding to E=7·5 volts is given in fig. 5 (Curve *a*). There is considerable discrepancy between the flux distribution expected from the probe readings, and that actually found, and it is found that no Maxwellian distribution can be fitted to the experimental curve.

The motion of an electron in an electric field is not governed by the simple laws from which the Maxwellian distribution of energies is deduced. The existence of free paths varying with energy and energy losses which are a function of the electron energy have to be considered. Owing to the continual gain and loss of energy in the field, electrons are not in thermal equilibrium with the gas molecules or atoms. Thus in discharge plasma the energy distribution cannot be of the Maxwellian form unless other mechanisms produce further energy exchange. The most important mechanism of this type is electron interaction, but for the electron concentrations obtained in this type of discharge its effect is negligible.

Fig. 6.

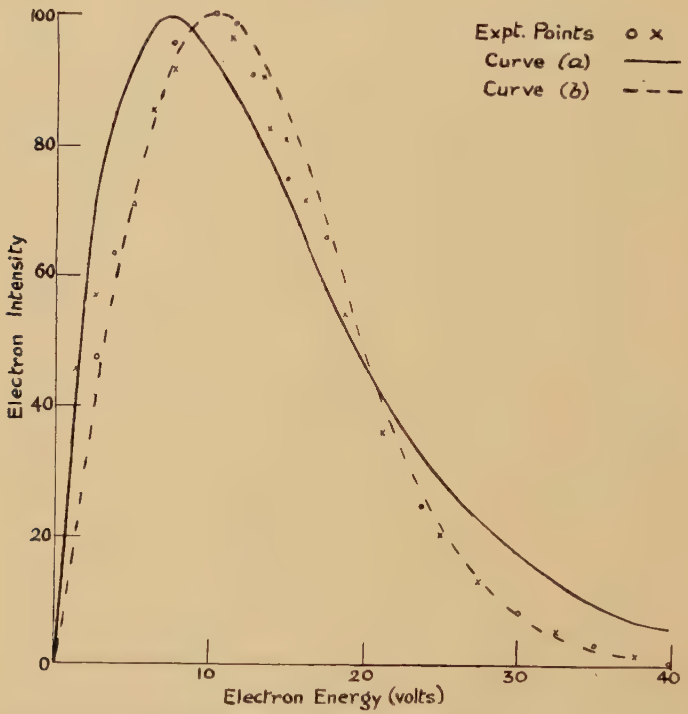

Electron energy distribution in air, (pressure, 0·018 mm. Hg; tube current, 40 m.amps.: tube voltage, 600 volts).

Experimental points; ○ ×

(*a*) Maxwellian flux distribution E=10·8 volts.

(*b*) Druyvesteyn flux distribution E=11·0 volts.

The full derivation of the distribution function has only been completed for the case of He (Smit 1936) but a simplified solution has been given by Dryvesteyn (1930).

The flux distribution corresponding to a Druyvesteyn energy distribution of average energy E is given by

$$N=AV\exp(-0\cdot55\ V^2/E^2)\,dV \quad . \quad . \quad . \quad . \quad . \quad . \quad . \quad (2)$$

and it was found that a curve of this form could be fitted approximately to the photometer curve if E=11·0 volts (fig. 5). Even so it is evident that there is a dearth of electrons at energies higher than the mean.

Similar results have been obtained with air discharges. For a discharge (pressure, 0·018 mm. Hg ; tube current, 40 m.amps. ; tube voltage, 600 volts) the measured flux distribution is given in fig. 6 together with that deduced from probe measurements. Again a considerable difference is obtained between the two distributions and again the distribution obtained by the present method can be represented approximately by a Druyvesteyn flux disuribution.

4. DISCUSSION OF RESULTS.

Linear semi-log plots have been obtained frequently from probe measurements under widely differing discharge conditions where the existence of a Maxwellian energy distribution has been doubtful. The factors leading to error have been examined (Loeb 1939), but particular attention may be drawn to the effect of the reflection and secondary emission of electrons from the probe surface. It is interesting to note that in argon discharges the shape of the characteristic in the region of large negative potentials was seriously affected by these factors (Uyterhoeven 1929) yet the electron energy distribution deduced from the semi-log plot was still Maxwellian (Uyterhoeven and Harrington 1930). In the present method errors due to these causes are eliminated, for, although electrons are reflected and secondary electrons are produced, they are only recorded when the slit is at a potential positive to the plasma. Similarly, because in the present method the energy distribution is determined when the slit is at the space potential all the factors which introduce error into probe determinations, due to their effect on the space charge, are obviated.

Confirmation of the form of the energy distribution obtained is given by recent calculations of Deas and Emeleus (1949) from the values of the Townsend coefficient, α, with field strength, X, at various pressures, p. Their results show that in the case of argon discharges the experimental variation of α/p with X/p necessitates the assumption of an energy distribution function with a paucity of electrons having energies much in excess of the mean.

Finally, some subsidiary observations bearing on the validity of the probe method of finding energy distributions may be noted. In the derivation of the theory it is assumed that no exchange of electron energy occurs within the sheath. Under these conditions the number of electrons N in an energy range V to V+dV, reaching a probe against a negative potential V_0 is given by

$$N=A(V-V_0)f(V)dV. \quad . \quad . \quad . \quad . \quad . \quad . \quad . \quad . \quad (3)$$

Where the volume distribution function outside the space charge sheath is $f(V)$ (Eakin and McCrea 1940).

Fig. 7.

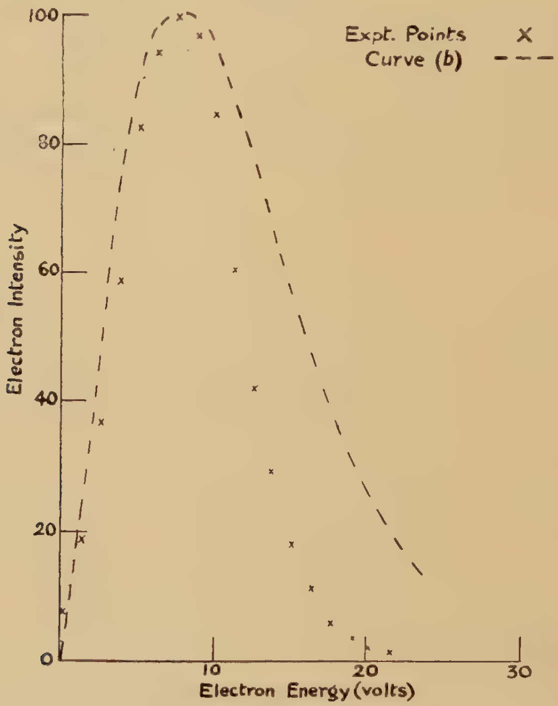

Energy distribution reaching negative probe.

(*a*) Probe 8 volts negative to space potential.
(*b*) Distribution according to equation (3).

Accordingly the energy distribution was obtained with the first slit held at voltages negative to the space potential. The distribution obtained in the case of the argon discharge, with the slits held 8 volts negative to the space potential, is shown in fig. 7 together with the distribution calculated from equation (3), when $f(V)$ is assumed to be Druyvesteyn of average energy 11·0 volts.

The increased discrepancy between the experimental and calculated distributions indicates the inadequacy under these conditions of one of the assumptions of probe theory.

Recently Boyd (1950) has used a small screened probe in order to separate the components of the probe current and determine the energy distribution of both the electrons and positive ions. He claims that with the conventional probe, if the positive ion current does not become saturated, the field from the probe modifies the energy distribution and concentration in the probe neighbourhood until, if the probe voltage is sufficient, a positive ion sheath forms. He obtains an electron energy distribution with few electrons having more than 15 volts energy.

ACKNOWLEDGMENTS.

We wish to acknowledge our debt to Professor Whiddington for his continual interest and advice during the course of the investigations and also we would like to take this opportunity of expressing our thanks to all those who have helped in any way. Financial assistance has been afforded to both authors by the D.S.I.R.

REFERENCES

BOYD, 1950, *Nature*, **165,** 228.
BRETT and WHIDDINGTON, 1925, *Proc. Leeds Phil. Lit. Soc.*, **1,** 1.
DEAS and EMELEUS, 1949, *Phil. Mag.*, **40,** 461.
DRUYVESTEYN, 1930, *Physica*, **10,** 69.
EAKIN and MCCREA, 1940, *Proc. Roy. Irish Acad.*, **46** A, 91.
HAIGH and SMITH, 1950, *Proc. Leeds Phil. Lit. Soc.*, in the press.
JONES and WHIDDINGTON, 1923, *Phil. Mag.*, **6,** 889.
KLEMPERER and WRIGHT, 1939, *Proc. Phys. Soc.*, **51,** 296.
LANGMUIR and MOTT SMITH ,1924, *Gen. Elec. Rev.*, **27,** 762.
LOEB, 1939, *Fundamental Processes of Electrical Discharge in Gases* (New York).
SMIT, 1936, *Physica*, **3,** 543.
SMITH, TAIT and WHIDDINGTON, 1949, *Proc. Leeds Phil. Lit. Soc.*, **5,** Part III., 207.
UYTERHOEVEN, 1929, *Proc. Nat. Acad. Sci.*, **15,** 32.
UYTERHOEVEN and HARRINGTON, 1930, *Phys. Rev.*, **36,** 709.
WHIDDINGTON and TAYLOR, 1932, *Proc. Roy. Soc.* A, **136,** 651.

LIII. *The Cohesive Energy of Metallic Magnesium.*

By S. Raimes, B.Sc., A.R.C.S., D.I.C.,
Department of Mathematics, Imperial College, London*.

[Received February 7, 1950.]

Summary.

The method of Wigner and Seitz is applied to metallic magnesium, using an ion-core field of the Hartree type. Two alternative self-consistent fields in the metal are considered, and the wave functions and energies are found not to differ significantly in the two cases. The total energy of the metal is obtained as the sum of four terms: the eigenvalue of the Schrödinger equation for the lowest state, and the Fermi, exchange, and correlation energies. The free-electron approximation is used to evaluate the latter two terms, but, in the case of the Fermi energy, both the free-electron value and a modification of this using the effective electronic mass at the zone centre are considered: the effective mass being calculated by a method due to Bardeen. The energy of the valence electrons in a free atom is obtained by a self-consistent field calculation, and, in addition, an estimate is made of the correlation energy of these electrons. It is pointed out that the method employed in the latter case appears to be inapplicable to beryllium, so that the true correlation energy may differ significantly from the estimated value. However, the calculated values of the lattice constant, cohesive energy, and compressibility are found to be in fair agreement with experiment, and a discussion of the effects of the various approximations is given.

§1. Introduction.

The cellular method introduced by Wigner and Seitz (1933, 1934) has been used with considerable success in the calculation of the cohesive energies of the monovalent metals. So far, however, little has been done in this direction for metals of higher valency. Apart from certain work of an essentially approximate nature, the only detailed investigation of the cohesion of a polyvalent metal has been that of Herring and Hill (1940) in the case of beryllium. The present paper describes an attempt to calculate, by means of the cellular method, the lattice constant, compressibility, and cohesive energy of the divalent metal magnesium. The procedure adopted is not the same as that of Herring and Hill, but is a more direct extension of that used by Wigner and Seitz for sodium. The effective electronic mass at the centre of the Brillouin zone is, however, determined by a method due to Bardeen (1938).

---

* Communicated by Professor H. Jones.

There have been two previous attempts to calculate the cohesive energy of magnesium, among other divalent metals; namely, that of Fröhlich (1936), and that of Hellmann and Kassatotschkin (1936). Both treatments involve the cellular method to some extent, but also include additional approximations; and in neither case are wave functions obtained such as those given in this paper. Fröhlich makes use of his approximate analytical method (1936, 1937) of calculating the energies of the alkali metals; an empirical screening factor being introduced into the potential field to account in some degree for the presence of a second valence electron. Although this method applies extremely well to the alkali metals, its extension to the divalent metals must be regarded only as a rough approximation. It is to be noted, however, that the calculation of the Fermi energy, in the latter case, yields a value considerably less than that for perfectly free electrons: this will be further discussed in §5.

Hellmann and Kassatotschkin use what they term the "combined approximation method." The basis of this lies in the use of an artificial ion-core field so constructed that the empirical energies of the valence electrons in a free atom are obtained when the ground state of a valence electron is taken to be a $1s$ state, and the first and second excited states are taken to be $2p$ and $2s$ states respectively. There is a certain arbitrariness in the construction of this field, since two parameters are fitted to three atomic term values, and so, apart from the ground-term, which is made to agree exactly, the correspondence between the theoretical and experimental energies of the atom is not exact: it is postulated, however, that the resulting error in the energy of the metal will be small. The whole reason for this procedure is that the wave functions of the valence electrons in the metal now have no spherical nodes in the neighbourhood of each nucleus, so that an approximation to the energy may be obtained by assuming that they are just plane waves. The results are in fair agreement with experiment, but the effects of the various approximations are rather difficult to assess.

The present work is essentially an investigation of the direct applicability to divalent metals of the method of Wigner and Seitz, and the ion-core field used is of the Hartree type.

§2. THE WAVE FUNCTIONS.

Metallic magnesium has a close-packed hexagonal structure, and a polyhedron drawn around any atom of the lattice, so that the faces bisect perpendicularly the lines joining this atom to its nearest and next nearest neighbours, has the form shown* in fig. 1. This atomic cell has not the high degree of symmetry possessed by those of the cubic lattices, but, for the purpose of calculating the wave function of the lowest electronic state, it is still a reasonable approximation to replace the cell by a sphere of equal volume.

---

[*] *Cf.* Seitz (1940) p. 331, fig. 4: this figure is believed to be incorrect.

W. J. Yost (1940) has calculated the wave functions of the K and L shells in a free, doubly-ionized, magnesium atom according to the approximations of both Hartree and Fock. The spherically symmetrical ion-core field used in the present work was calculated from the Fock functions, on the assumption that the ion-core remains unchanged in the solid state. Exchange interaction between the valence and core electrons will be neglected both in the metal and in the free neutral atom, so that the error should be small as far as the cohesive energy is concerned.

Fig. 1.

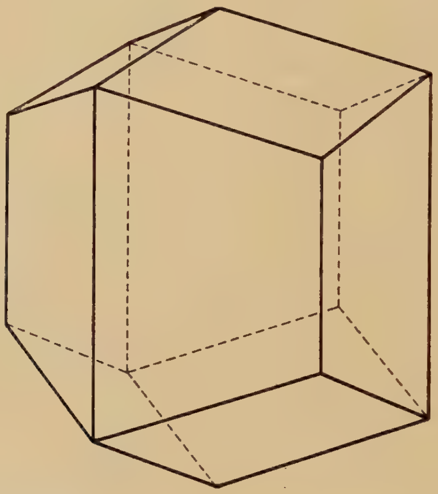

Atomic polyhedron for a close-packed hexagonal lattice.

It will be shown that the wave function $\psi_0(r)$ of the lowest state of a valence electron in the metal is approximately constant throughout most of the volume: hence, as in the case of the monovalent metals, we shall assume that the wave function of an excited electronic state is

$$\psi_j(\mathbf{r})=\psi_0(\mathbf{r})\exp i\mathbf{k}_j\cdot\mathbf{r}, \quad \ldots\ldots\ldots \quad (1)$$

where $\mathbf{k}_j$ is the wave vector. If there are N atoms in the crystal, therefore, the charge density at $\mathbf{r}$ due to electrons with one type of spin only is *

$$\sum_j|\psi_j(\mathbf{r})|^2=N|\psi_0(\mathbf{r})|^2. \quad \ldots\ldots\ldots\ldots \quad (2)$$

---

* In this paper the following units are used:

$$\text{Unit of energy (Rydberg unit)}=\frac{2\pi^2me^4}{h^2},$$

$$\text{Unit of length (Bohr unit)}=\frac{h^2}{4\pi^2me^2}.$$

In the case of divalent metals there are two alternative self-consistent fields which are plausible on physical grounds, and we shall refer to these as field A and field B :

Field A. It may easily be shown, by regarding the electrons as approximately free, that those with parallel spins rarely approach one another within a distance smaller than r_s, the radius of an atomic sphere. It is therefore reasonable to assume that the presence of an electron with, say, positive spin effectively excludes from an atomic sphere all other electrons with positive spin. Hence we may take the potential field $V_A(r)$ in which this electron moves as the sum of the ion-core field $v_c(r)$ and that due to the charge distribution, within the sphere, of all electrons with negative spin ; *i. e.* using (2),

$$V_A(r)=v_c(r)+2N\int_\sigma \frac{|\psi_0(\mathbf{r}')|^2}{|\mathbf{r}-\mathbf{r}'|}d\tau', \quad . \quad . \quad . \quad . \quad . \quad (3)$$

the integration being over the atomic sphere σ. (The factor 2 appears owing to our choice of units.) This field is similar to that used by Manning and Krutter (1937) in their work on calcium, except that these authors use, instead of $\psi_0(\mathbf{r})$, that portion of an atomic wave function, suitably normalized, which would be enclosed by an atomic sphere. Owing to the form of the wave functions ψ_j, as given in equation (1), the field A becomes that of the valence electrons in the Hartree calculation for the free atom when the atomic sphere becomes infinitely large.

Field B. If correlations between the electronic positions are ignored altogether the potential field $V_B(r)$ within an atomic sphere is the sum of the ion-core field and that due to the charge distribution, in the sphere, of all the electrons : *i. e.*

$$V_B(r)=v_c(r)+4N\int_\sigma \frac{|\psi_0(\mathbf{r}')|^2}{|\mathbf{r}-\mathbf{r}'|}d\tau'. \quad . \quad . \quad . \quad . \quad . \quad (4)$$

This is the ordinary Hartree field of a valence electron in the metal.

The above definitions have been given, for convenience in the following discussion, with respect to a single atomic cell, or sphere, but the extension to the crystal as a whole is obvious, since the cells are assumed to be electrostatically neutral and the situation within each cell is the same.

It may be remarked that neither of these fields is correct ; they are both approximations to the Fock field in the metal, but it was decided that field A gives a more plausible representation of the physical picture, and this field was used in the bulk of the work.

Wave functions ψ_0 corresponding to the atomic radii 3·28 and 4·56 Bohr units are given in Table I., as calculated with the two alternative fields. These particular radii were chosen because they include between them the most important part of the range, as can be seen from fig. 3. It is at once apparent that the corresponding functions are very similar, so that we might expect the resulting energy of the crystal to be about the same in the two cases ; and, in fact, this is borne out by calculation.

It will be seen later that the total energy per electron is the sum of the eigenvalue ϵ_0 of the Schrödinger equation for the lowest state and certain other terms. Now, taking the case of $r_s=3{\cdot}28$ only, we find the eigenvalue for field A to be $-{\cdot}66$, and that for field B to be ·05 Rydberg units. However, in the second case, the total energy contains an extra term representing the Coulomb interaction of the electrons, and this is found to have the value $-{\cdot}72$ Rydberg units. The other energy terms remain the same in the two cases, so the net result is that the total energy for field B is ·01 Rydberg units lower than that for field A. This difference, it will appear, is certainly less than the errors expected from other sources.

Table I.

r (Bohr) units)	ψ_0 for $r_s=3{\cdot}28$ Field A	Field B	ψ_0 for $r_s=4{\cdot}56$ Field A	Field B
0·00	5·316	5·236	3·748	3·444
0·08	1·826	1·800	1·287	1·183
0·16	0·270	0·267	0·189	0·174
0·24	−0·401	−0·394	−0·284	−0·261
0·40	−0·690	−0·681	−0·485	−0·447
0·56	−0·548	−0·545	−0·383	−0·354
0·72	−0·348	−0·350	−0·240	−0·224
0·88	−0·173	−0·179	−0·114	−0·109
1·04	−0·036	−0·046	−0·017	−0·021
1·36	0·142	0·131	0·110	0·096
1·68	0·237	0·225	0·173	0·155
2·00	0·282	0·275	0·200	0·183
2·32	0·302	0·298	0·206	0·912
2·64	0·307	0·309	0·202	0·193
2·96	0·308	0·313	0·193	0·189
3·28	0·307	0·313	0·184	0·183
3·60			0·175	0·178
3·92			0·168	0·175
4·24			0·164	0·172
4·56			0·163	0·172

Although the calculations for field B have not been carried to the same degree of self-consistency as those for field A, we may conclude that the final results are not significantly different in the two cases. A similar conclusion was reached by Wigner and Seitz in the case of sodium, using a perturbation method.

We shall confine all further discussion to field A, the procedure for field B differing only in detail.

That portion of ψ_0 lying within a given atomic sphere is obtained by integrating the Schrödinger equation

$$\frac{d^2\psi_0}{dr^2}+\frac{2}{r}\frac{d\psi_0}{dr}+[\epsilon_0-V_A(r)]\psi_0=0, \quad . \quad . \quad . \quad . \quad . \quad . \quad . \qquad (5)$$

subject to the boundary condition

$$\left(\frac{d\psi_0}{dr}\right)_{r=r_s}=0. \quad . \quad . \quad . \quad . \quad . \quad . \quad . \quad . \quad . \quad (6)$$

With the form of $V_A(r)$ given by (3), ψ_0 must satisfy the normalizing condition

$$4\pi N\int_0^{r_s} r^2\,|\,\psi_0(r)\,|^2 dr=1. \quad . \quad . \quad . \quad . \quad . \quad . \quad . \quad . \quad (7)$$

In addition ψ_0 must possess two spherical nodes within the atomic sphere.

Fig. 2.

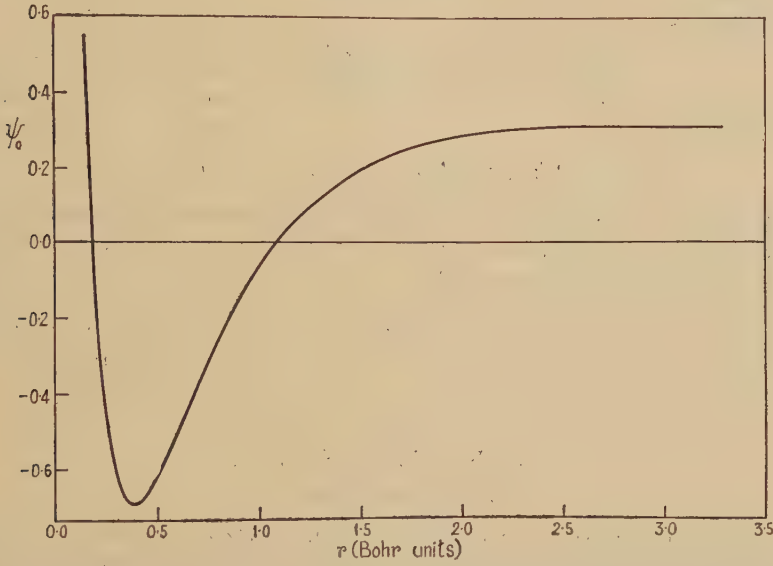

Wave function of the lowest electronic state, for atomic radius 3·28 Bohr units.

Since V_A depends upon ψ_0, a method of successive approximation had to be used in solving equation (5). Furthermore, ϵ_0 had to be chosen so as to satisfy condition (6), with the value of r_s fixed beforehand, and this could be done only by trial and error. Consequently the work involved was much more laborious than in the corresponding calculation for sodium. In the latter case a single integration provided two points on the ϵ_0-versus-r_s curve, while here several integrations, and several recalculations of V_A, were necessary to obtain a single point on the curve. For this reason the solution for a given atomic radius was terminated after two or three recalculations of V_A. This provided a value of ϵ_0 to three significant figures, the third being, however, rather unreliable. Solutions of this accuracy were obtained at six points covering the most important part of the range of r_s, and the resulting curve is shown in fig. 3.

The general form of the wave functions ψ_0 is shown in fig. 2, which represents that for $r_s=3{\cdot}28$ Bohr units, the observed value being 3·35 Bohr units. It is apparent that our previous assumption of the approximate constancy of ψ_0 is justified. The number of intervals actually used in the calculations was about four times the number shown in Table I. All the wave functions given are normalized according to the equation

$$\int_0^{r_s} r^2\psi_0^2 dr=1. \quad . \quad . \quad . \quad . \quad . \quad . \quad . \quad . \quad . \quad (8)$$

Although we have been concerned with a single atomic sphere, ψ_0 must, of course, extend periodically throughout the crystal. The Schrödinger equation for an electronic state ψ_j, referred to the metal as a whole, is

$$\nabla^2\psi_j+[\epsilon_j-\mathrm{V}_{\mathrm{A}}(\mathbf{r})]\psi_j=0, \quad . \quad . \quad . \quad . \quad . \quad . \quad . \quad . \quad (9)$$

where $\mathrm{V}_{\mathrm{A}}(\mathbf{r})$ reduces to (3) within any cell. Substituting (1) in (9), we obtain

$$\nabla^2\psi_0+2i\mathbf{k}_j\,.\,\mathbf{grad}\,\psi_0+(\epsilon_j-\mathbf{k}_j^2-\mathrm{V}_{\mathrm{A}})\psi_0=0. \quad . \quad . \quad . \quad . \quad . \quad (10)$$

Owing to the approximate constancy of ψ_0 the second term may be neglected to a first approximation, and, within an atomic sphere, equation (10) reduces to (5). Then

$$\epsilon_j=\epsilon_0+\mathbf{k}_j^2. \quad . \quad . \quad . \quad . \quad . \quad . \quad . \quad . \quad . \quad . \quad . \quad (11)$$

This will be used in the following section, but a fuller discussion will be given in §4.

§3. THE TOTAL ENERGY.

(i) *The solid metal.*

In order to construct a total Hamiltonian for the metal the following simplifying assumptions, which are implicit in the previous work, will be made: (*a*) The atomic nucleii are at rest. (*b*) The inner closed shells of electrons remain the same in the metal as they are in the free atom, and their effect may be described by a spherically symmetrical potential term. (*c*) The ion-cores do not overlap appreciably, and Van der Waals terms may be neglected.

The divalent metallic system then consists essentially of 2N valence electrons moving in a lattice of N doubly-charged positive ions, and the corresponding Hamiltonian operator is

$$\mathrm{H}=-\sum_{i=1}^{2\mathrm{N}}\nabla_i^2+\sum_{i=1}^{2\mathrm{N}}\sum_{a=1}^{\mathrm{N}}\mathrm{U}_a(\mathbf{r}_i)+\sum_{i\neq j}^{2\mathrm{N}}\sum\frac{1}{\mathbf{r}_{ij}}+\sum_{a\neq b}^{\mathrm{N}}\sum\frac{4}{\mathbf{r}_{ab}} \quad . \quad . \quad . \quad (12)$$

Here $-\nabla_i^2$ is the kinetic energy operator of the *i*th electron; $\mathrm{U}_a(\mathbf{r}_i)$ is the potential energy of the *i*th electron due to the *a*th ion; $2/r_{ij}$ is the Coulomb interaction energy between the *i*th and *j*th electrons, where r_{ij} is the distance between them; and, similarly, $8/r_{ab}$ is the Coulomb interaction energy between the *a*th and *b*th ions.

In the one-electron approximation, when there are N electrons with each type of spin, we may take the total wave function to be of the form :

$$\Psi=\frac{1}{\mathrm{N}\,!}\begin{vmatrix}\psi_1(\mathbf{r}_1)\ldots\psi_{\mathrm{N}}(\mathbf{r}_1)\\ \vdots \qquad\quad \vdots\\ \psi_1(\mathbf{r}_{\mathrm{N}})\ldots\psi_{\mathrm{N}}(\mathbf{r}_{\mathrm{N}})\end{vmatrix}\cdot\begin{vmatrix}\psi_1(\mathbf{s}_1)\ldots\psi_{\mathrm{N}}(\mathbf{s}_1)\\ \vdots \qquad\quad \vdots\\ \psi_1(\mathbf{s}_{\mathrm{N}})\ldots\psi_{\mathrm{N}}(\mathbf{s}_{\mathrm{N}})\end{vmatrix} \quad . \;.\;. \quad (13)$$

where the $\mathbf{r}_i$ and $\mathbf{s}_i$ are the position vectors of electrons with positive and negative spin respectively, and

$$\int_{(v)}\psi_i^*\psi_j\,d\tau=\delta_{ij},$$

the integration being over the volume v of the crystal.

The total energy of the crystal in this approximation is

$$\mathrm{E}=\int\ldots(2\mathrm{N})\ldots\int_{(v)}\Psi^*\mathrm{H}\Psi\,d\tau(\mathbf{r}_1,\ldots\mathbf{r}_{\mathrm{N}}\,;\,\mathbf{s}_1,\ldots\mathbf{s}_{\mathrm{N}}). \quad . \quad (14)$$

In evaluating this expression use is made of equation (9) and the atomic sphere approximation ; the latter in so far as the charge distribution within an atomic cell is assumed to be spherically symmetrical, so that, as far as points outside are concerned, the charge can be regarded as concentrated at the centre of the cell. Finally, after some calculation, (14) reduces to

$$\mathrm{E}=2\sum_{i=1}^{\mathrm{N}}\epsilon_i-2\sum_{i,j}^{\mathrm{N}}\iint_{(v)}\frac{1}{r_{12}}\psi_i^*(\mathbf{r}_1)\psi_j^*(\mathbf{r}_2)\psi_i(\mathbf{r}_2)\psi_j(\mathbf{r}_1)d\tau(\mathbf{r}_1,\mathbf{r}_2). \qquad (15)$$

It is noteworthy that this contains no specific term for the Coulomb interaction energy, the second term being the exchange energy. This is due entirely to our use of field A ; when field B is used an additional Coulomb term does appear, as mentioned in §2.

We may express (15) in the form

$$\mathrm{E}=2\mathrm{N}(\epsilon_0+\epsilon_{\mathrm{F}}+\epsilon_{\mathrm{X}}), \quad . \;.\;.\;.\;.\;.\;.\;.\; \quad (16)$$

where ϵ_{F} is the Fermi energy and ϵ_{X} the exchange energy, each referred to a single electron. If we assume that the ψ_j are approximately plane waves ϵ_{F} and ϵ_{X} can be evaluated by well-known methods. In the case of ϵ_{F} use is made of equation (11). We find

$$\epsilon_{\mathrm{F}}=\frac{3{\cdot}51}{r_s^{\,2}} \quad \text{and} \quad \epsilon_{\mathrm{X}}=-\frac{1{\cdot}154}{r_s} \quad \text{Rydberg units.}$$

Correlations between the positions of electrons have not been entirely neglected in the foregoing work, since the exchange energy is due to those of electrons with parallel spins. So far, however, antiparallel spin correlations have not been taken into account. No method has yet been devised for doing this in the case of real metals, but Wigner

(1934; *cf.* Seitz, 1940, p. 343) has dealt with the problem for perfectly free electrons. He uses a modified wave function of the form (9) in which the position vectors $\mathbf{s}_i$ of the negative spin electrons appear as parameters in the ψ_i of the first determinant, and the energy is then minimized. The final result is an additional energy ϵ_C per electron, called the "correlation energy," and, taking into account the increased electron density of a divalent metal, this is given by

$$\epsilon_C = -\frac{\cdot 576}{\cdot 79 r_s + 5\cdot 1} \text{ Rydberg units.}$$

Fig. 3.

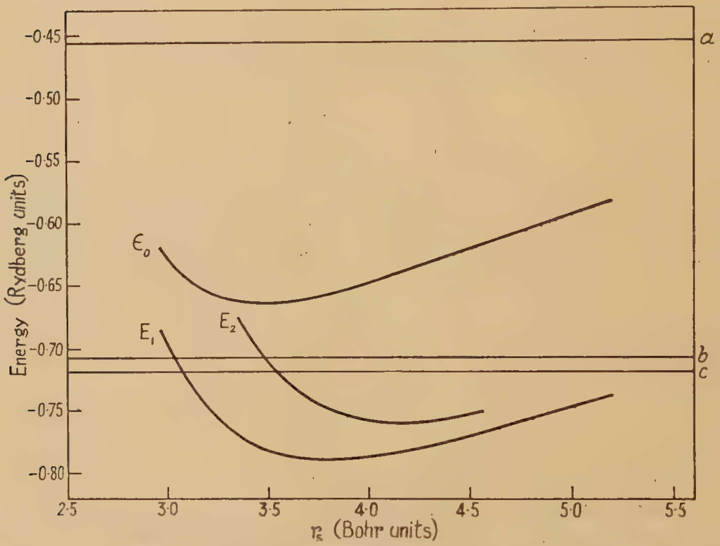

Eigenvalue and energy curves for the metal. E_1 includes the free-electron Fermi energy. E_2 includes the Fermi energy modified according to the effective electronic mass at the zone centre. The lines *a*, *b* represent the eigenvalue and energy in a free atom as calculated by the Hartree method, and line *c* represents the total energy in a free atom, including correlation energy.

Wigner estimates that this result is accurate to within 20 per cent. Since we have already used the free-electron approximation in evaluating two of our energy terms, there is little objection to our incorporating the above expression for ϵ_C, which in any case is small, in the total energy.

Finally, then, with the approximations so far made, the total energy per electron of the crystal is

$$\begin{aligned} E_1 &= \epsilon_0 + \epsilon_F + \epsilon_X + \epsilon_C, \\ &= \epsilon_0 + \frac{3\cdot 51}{r_s^2} - \frac{1\cdot 154}{r_s} - \frac{\cdot 576}{\cdot 79 r_s + 5\cdot 1} \text{ Rydberg units} \end{aligned} \qquad (17)$$

E_1 is shown graphically in fig. 3, and the values of the three physical constants corresponding to this curve are given, in more conventional units, in the second line of Table III. The lattice constant, ρ, is the atomic radius at which the minimum of E_1 occurs. The compressibility, κ, referred to a single atom, is given by

$$\frac{1}{\kappa}=\frac{1}{6\pi\rho}\left(\frac{d^2E_1}{dr_s{}^2}\right)_{r_s=\rho}.$$

The cohesive energy, S, per electron is the difference between the minimum of E_1 and the mean energy of a valence electron in the free atom (line *c* in fig. 3), and the method of calculating the latter must now be discussed. All the quantities considered here are referred to the absolute zero of temperature.

(ii) *The free atom.*

The Hartree calculation. It would be quite wrong to use the experimental value for the energy of the valence electrons in the free atom, since this would emphasize the flaws in the ion-core field which has been used in the metal. Furthermore, valence-core exchange and correlation effects have been neglected in the metal, and serious error would occur if they were included in the free atom. In fact, use of the experimental energy in the free atom would lead to a negative cohesive energy. In view of this, the wave functions and energies of the atomic valence electrons were calculated by Hartree's method, using the ion-core field derived from Yost's inner shell functions, as in the metal. The equation used was just equation (5), and the procedure exactly the same as in the calculation of ψ_0, except that r_s is now infinite. The eigenvalue was found to be $-\cdot 456$ Rydberg units (line *a* in fig. 3), and the ϵ_0 curve must approach this value with increasing r_s. Now, in the Hartree method, the total energy of the electrons is found by subtracting their mutual potential energy from the sum of the eigenvalues. When this has been done it is found that the mean energy of a valence electron in the free atom is $-\cdot 708$ Rydberg units (line *b* in fig. 3). In this, as in the energy calculations for the metal, the third figure is unreliable.

The correlation energy. A difficulty now arises which is not encountered in the case of monovalent metals. In the above calculation, since the two valence electrons are assumed to have opposite spins, there is no exchange energy. There will, however, be an energy term due to correlations between the electronic positions, which does not appear in the Hartree approximation. This must be taken into account, since an analogous term has been included in the energy of the metal. In this case it is not advisable to disregard both terms, since it seems likely that the correlation energy in the metal will be much greater than that in the free atom. As there is at present no method of calculating the correlation energy directly, an attempt to estimate this was made in the following manner:

The two valence electrons in magnesium spend most of their time in a region where the potential field of the ion-core is almost the same as that of the helium nucleus. It seems reasonable to assume, therefore, that the correlation energy of the valence electrons in a magnesium atom will bear approximately the same ratio to their observed energy as in the case of helium. The energy of a helium atom obtained by the Hartree method (Bethe, 1933) is $-5{\cdot}734$ Rydberg units, while the observed value is $-5{\cdot}810$. The difference of $\cdot 076$ Rydberg units is due to the correlation interaction of the electrons. Thus the correlation energy in a helium atom amounts to $\cdot 013$ of the observed energy. Now the observed mean energy of a valence electron in a magnesium atom is $-{\cdot}834$ Rydberg units, so that we may expect the correlation energy per electron to be approximately $-{\cdot}834 \times {\cdot}013 = -{\cdot}011$ Rydberg units, and this, when added to the energy obtained by the Hartree method, gives a total of $-{\cdot}719$ Rydberg units per electron (line *c* in fig. 3). It was this value which was used in computing the cohesive energy.

An alternative method which suggests itself is one similar to the preceding, but based upon the Coulomb interaction energies of the electrons rather than upon their total energies. The two methods in this case, however, lead to almost identical results. Thus, the ratio of the correlation energy to the Coulomb energy of the electrons in helium, is $-{\cdot}037$, and the Coulomb energy per valence electron in a magnesium atom is found to be $\cdot 252$ Rydberg units, so that the expected correlation energy is now about $-{\cdot}252 \times {\cdot}037 = -{\cdot}009$ Rydberg units per electron. Although this value is practically the same as the previous one, the method of deriving it is probably better, since it depends more directly upon the electronic charge distributions, and hence might be expected to apply to the electrons in other shells, for which the ion-core field does not approximate to that of helium.

Although it seems unlikely that either of these methods of estimating the correlation energy should give results of quite the wrong size, it must be admitted that neither seems to apply to the case of beryllium. The energies of neutral Be and Be^{++} have been obtained by D. R. Hartree and W. Hartree (1935), using the methods of both Hartree and Fock, and the correlation energies obtained by comparison with experiment have been discussed by Seitz (1940, p. 248). The correlation energy of the 2*s* electrons appears to be four times as large as that estimated by the above methods. We cannot at present account for this discrepancy, but there are two reasons for suggesting that the smaller value may be nearer the truth. First, the method based on the Coulomb energies gives almost exactly the *total* correlation energy of Be, although the results for the separate electronic shells are not in accord with those of Seitz : it appears that, if the correlation energy of the 1*s* electrons were just over twice that given by Seitz there would be complete agreement. Secondly, in their work on metallic beryllium, Herring and Hill (1940) have used the experimental value of the energy of the valence electrons in the free atom, and their calculated cohesive energy is much too small. If the energy given by the Fock method had been used, together with the smaller correlation energy estimated as above, the calculated cohesive energy would have corresponded more closely with the observed.

Unless this discrepancy with regard to beryllium can be completely resolved, however, we must not ignore the possibility of a correlation energy in the free atom much larger than that used in the present work, and a calculated cohesive energy correspondingly smaller.

§4. THE EFFECTIVE MASS AT THE ZONE CENTRE.

In the previous section the Fermi energy ϵ_F has been calculated on the assumption that the valence electrons are perfectly free. We shall now attempt to correct this, at least as far as states near the centre of the Brillouin zone are concerned, using a method developed by Bardeen (1938) for the alkali metals.

According to the Bloch theory, an electronic state ψ_j is not given strictly by equation (1), but is of the form

$$\psi_j(\mathbf{r})=u_j(\mathbf{r})\exp(i\mathbf{k}_j\,.\,\mathbf{r}), \qquad \ldots \ldots \quad (18)$$

where u_j has the periodicity of the lattice and satisfies the Schrödinger equation

$$\nabla^2 u_j+2i\mathbf{k}_j\,.\,\mathbf{grad}\,u_j+(\epsilon_j-\mathbf{k}_j^2-\mathrm{V_A})u_j=0. \qquad \ldots \quad (19)$$

To be perfectly accurate, $\mathrm{V_A}$ is no longer given by (3), but must be calculated using the wave functions (18). This refinement, however, will be neglected in the following work, since the correction arising therefrom should be insignificant, as the results of using fields A and B seem to indicate. A similar assumption was implicit in the work on sodium.

When, previously, u_j was taken to be simply ψ_0, the second term in equation (19) could be neglected to a good approximation, and this gave rise to the free-electron Fermi energy. In general, this cannot be done; but, for small $\mathbf{k}_j$, the term $2i\mathbf{k}_j\,.\,\mathbf{grad}\,u_j$ may be treated as a perturbation. In this case, following Bardeen, we shall assume that

$$u_j(r)=\psi_0(r)+i\mathbf{k}_j\,.\,\mathbf{r}\phi(r),$$

where

$$\phi(r)=\frac{\mathrm{P}(r)}{r^2}-\psi_0(r), \qquad \phi(r_s)=0,$$

and the equation for $\mathrm{P}(r)$ is

$$\frac{d^2\mathrm{P}}{dr^2}+\left(\epsilon_0-\mathrm{V_A}-\frac{2}{r^2}\right)\mathrm{P}=0. \qquad \ldots \ldots \quad (20)$$

Then, to the second order in $\mathbf{k}_j$, we find

$$\epsilon_j=\epsilon_0+\alpha\mathbf{k}_j^2, \quad \quad (21)$$

with

$$\alpha=\gamma\left[\frac{r}{\mathrm{P}}\frac{d\mathrm{P}}{dr}-1\right]_{r=r_s},$$

and

$$\gamma=\frac{4\pi}{3}r_s^3[\psi_0(r_s)]^2.$$

The quantity α is the ratio, m/m^*, of the mass of an electron to its effective mass near the centre of the zone. If it is assumed that all the electrons have this same effective mass, the resulting Fermi energy ϵ'_{F} is just α times the free-electron Fermi energy ϵ_{F}.

TABLE II.

r_s (Bohr units)	γ	α	ϵ'_{F} (Rydberg units)
3·28	1·112	1·321	0·431
3·92	0·969	1·143	0·261
4·56	0·838	1·100	0·186

TABLE III.

	Lattice constant ρ (Å)	Cohesive energy S (K cal./mole)	Compressibility $10^6\,\kappa$. (cm.^{2}/kg.)
Experimental	1·77	38	3·0*
Calculated (E_1)	2·00	43	3·2
Calculated (E_2)	2·20	25	3·4

Equation (20) was solved, and α calculated, for three atomic radii covering the important part of the range; intermediate values being obtained by quadratic interpolation. The directly computed values of α and the resulting Fermi energy ϵ'_{F} are given in Table II. The new total energy E_2 per electron, in which all the terms except the Fermi energy are the same as in E_1, is shown in fig. 3, and the calculated physical constants are given in the last line of Table III.

The values of α corresponding to the observed lattice constant, the minimum of E_1, and the minimum of E_2, are 1·29, 1·17, and 1·11 respectively. In the case of beryllium, Herring and Hill (1940) found

---

* This is the value at room temperature: at absolute zero the compressibility will be slightly smaller than this.

α to be ·62 for the observed lattice constant. This large difference is not unexpected, however, since the corresponding values for sodium and lithium (Bardeen, 1938) are 1·07 and ·65 respectively.

§ 5. Discussion of Results.

The calculated values of ρ, S, κ are all in fair agreement with the experimental values, but those based on the free-electron Fermi energy are uniformly better than the others. In order to assess the significance of these results correctly the effects of several approximations must be taken into account.

First, the exchange and correlation energies of the metallic electrons have been calculated using the free-electron approximation. One consequence of this is that the curves for E_1 and E_2 in fig. 3 will not, as they should, approach asymptotically the line c, representing the energy in the free atom, but the line a, representing the eigenvalue in the free atom. This is not a serious difficulty, however, since we are only concerned with a small range of values of r_s in the immediate neighbourhood of the minima of E_1 and E_2, and, in this range, the wave functions are so flat that the free-electron approximation cannot be far wrong. The possible error of 20 per cent in Wigner's formula for the correlation energy in the metal contributes an uncertainty of about ·01 Rydberg units per electron (6 K cal./mole) to the value of the cohesive energy, and it is believed that the error due to using the free-electron exchange energy will not add greatly to this. The estimate of the correlation energy in the free atom has already been discussed in § 3(ii). It should be noted that an error of 1 per cent in the total energy of the metal produces an error of more than 10 per cent in the cohesive energy, and this must be taken into account when comparing the calculated with the experimental values of the latter.

Secondly, exchange and correlation interactions between the core and valence electrons have been neglected in this treatment. Gorin (1936), for potassium, and Fuchs (1935), for copper, have found such interactions to be important, but, since the ion-core of magnesium is smaller in relation to the size of the atomic sphere than for either of these metals, it is reasonable to assume that the effect will be much less in this case. The value of the cohesive energy, at least, should not be greatly affected, since the error in the energy of the metal will largely be cancelled by a similar error in the energy of the free atom.

Finally, the effect of the zone boundaries has not been taken into account. In magnesium, unlike the alkali metals, the first zone is almost full and there is a small overlap of electrons into the second zone. Within the scope of the present work we are only concerned with the effect of this upon the Fermi energy. In this respect, if Bardeen's method of calculating the effective mass at the zone centre is correct, as the results for sodium and lithium seem to indicate, it appears from Table III that the energy gaps at the zone boundaries must distort the distribution of states curve from the parabolic form in such a way that the resulting Fermi energy is not much different from that for free electrons. The calculation of the Fermi energy by Fröhlich (1936) yields a value considerably less than that for free electrons, but, owing to the approximations involved in the work, this result cannot be regarded as conclusive. Skinner (1940) finds the observed width of the soft X-ray emission band of magnesium to be 6·2±·3 eV. compared with the free-electron band width of 7·3 eV., but, until the distribution of states is known more accurately, only qualitative conclusions can be drawn regarding the Fermi energy. However, in view of this evidence, and the results of the present work, it is reasonable to conclude that the Fermi energy of magnesium is not greatly in excess of that calculated on the free-electron approximation. A Fermi energy even smaller than the latter would improve the calculated value of the lattice constant, but would tend to make the value of the cohesive energy too large.

I am glad of this opportunity to express my gratitude to Professor H. Jones for many valuable discussions.

References.

Bardeen, J., 1938, *J. Chem. Phys.*, **6**, 367.
Bethe, H., 1933, *Handbuch der Physik*, **24**/**1**, 368.
Fröhlich, H., 1936, *Elektronentheorie der Metalle* (Berlin: Julius Springer); 1937, *Proc. Roy. Soc.* A, **158**, 97.
Fuchs, K., 1935, *Proc. Roy. Soc.* A, **151**, 585.
Gorin, E., 1936, *Physik. Z. Sowj.*, **9**, 328.
Hartree, D. R., and Hartree, W., 1935, *Proc. Roy. Soc.* A, **150**, 9.
Hellmann, H., and Kassatotschkin, W., 1936, *Acta Physicochimica U.R.S.S.*, **5**, 23.
Herring, C. C., and Hill, A. G., 1940, *Phys. Rev.*, **58**, 132.
Manning, M. F., and Krutter, H. M., 1937, *Phys. Rev.*, **51**, 761.
Seitz, F., 1940, *Modern Theory of Solids* (New York: McGraw-Hill).
Skinner, H. W. B., 1940, *Phil. Trans. Roy. Soc. A*, **239**, 95.
Wigner, E., 1934, *Phys. Rev.*, **46**, 1002.
Wigner, E., and Seitz, F., 1933, *Phys. Rev.*, **43**, 804; 1934, *Ibid.*, **46**, 509.
Yost, W. J., 1940, *Phys. Rev.*, **58**, 557.

LIV. *Nuclear Reactions Produced by Slow Negative π-Mesons.*

By M. G. K. MENON, H. MUIRHEAD, and O. ROCHAT,
The H. H. Wills Physical Laboratory, University of Bristol *,

[Received April 26, 1950]

[Plates XVIII. & XIX.]

CONTENTS

PAGE
INTRODUCTION 584
§ 1. Statement of the problem 584
§ 2. Scope of the present experiments 585
PART I.—*General characteristics of the disintegrations and separation of the stars due to light and heavy elements* 586
§ 3. Definition of σ-stars; classification of ejected particles 586
§ 4. Identification of stars from light and heavy nuclei by the use of " sandwich " plates—Method (*a*) 588
§ 5. Separation of stars by observations on ejected α-particles and protons—Method (*b*) 590
§ 6. Separation of stars by observations on Auger electrons—Method (*c*) 592
§ 7. Unobserved disintegrations produced by π^--particles 593
§ 8. Recoil fragments 594
§ 9. The emission of energetic charged particles from σ-stars 595
PART II.—*Interaction of slow π^--mesons with heavy nuclei* 598
§ 10. General features 598
§ 11. Frequency distribution of the numbers of charged particles emitted in the disintegration of heavy nuclei 598
§ 12. The α:p ratio 601
§ 13. The energy distribution of the particles produced in the evaporation process 601
§ 14. Energy spectrum above 30 MeV 602
§ 15. Discussion 604
PART III.—*Interactions of slow π^--mesons with light nuclei* 607
§ 16. General features of the disintegrations 607
§ 17. Capture by ^{14}N 610
§ 18. Capture by ^{12}C 612
§ 19. Comparison of the disintegrations of light and heavy nuclei 616
CONCLUSIONS 616
ACKNOWLEDGMENTS 618
REFERENCES 618

ABSTRACT.

Reactions produced by the nuclear capture of slow negative π-mesons have been studied by the photographic method. The disintegrations of the light and heavy elements of the emulsion have been distinguished by methods which are described in detail. Because of the large number of " stars " observed—more than 2500—it has been possible to make a statistical approach to the study of the disintegrations.

---

* Communicated by Professor C. F. Powell, F.R.S.

The general features of the "stars" produced by the disintegration of heavy nuclei are in satisfactory agreement with the predictions of the evaporation theory. In addition, the emission of fast, singly-charged particles has been observed, most of which must be attributed to an alternative process to that of evaporation. Preliminary results have been obtained for the frequency of emission and the energy "spectrum" of these particles. The conclusion is reached that in the initial process of capture—the so-called "primary" process—the energy corresponding to the rest-mass of the π^--meson is shared among a larger number of nucleons than has commonly been assumed hitherto.

Observations on "stars" produced by the disintegration of light nuclei indicate that there is a wide variety in the characteristics of the disintegrations which appear to be strongly dependent on the manner in which the primary distribution of energy takes place. A detailed analysis has been made of some of the disintegrations due to $^{12}_{6}$C and $^{14}_{7}$N nuclei, by applying the conservation laws of mass energy and momentum. In the majority of cases, the primary interaction results in the production of one or two fast neutrons and an excited residual nucleus which then disintegrates. In a few cases, however, the primary interaction involves the nucleus as a whole, resulting in its total disruption and the ejection of fast α-particles.

INTRODUCTION.

§ 1. STATEMENT OF THE PROBLEM.

AMONG the first mesons observed in photographic plates exposed to the cosmic radiation were those which, at the end of their range in the emulsion, produced nuclear disintegrations. These particles were described, phenomenologically, as σ-mesons, and subsequent work has shown that they are all, or almost all, π^--particles. A disintegration of this type is due to the capture of a meson by a nucleus; and to the distribution, among the nucleons, of the energy liberated by the disappearance of the rest-mass of the π-particle.

Whilst this view of the origin of the disintegrations produced by σ mesons appears to be beyond question, the detailed characteristics of the physical process by which the rest-energy of the meson is communicated to the nucleons have remained obscure. It appears reasonable to consider the disintegration as being produced, at least in the case of heavy nuclei, in two stages:—the "primary process", in which the π^--particle interacts with a limited number of nucleons, is followed by a general excitation of the nucleus as a result of the collisions of the fast nucleons formed in the primary process. This excitation leads to an "evaporation" of charged particles and neutrons, and the formation of the "star".

The primary interaction accompanying the nuclear capture of mesons has been studied theoretically by Bruno (1948), Marshak (1949) and other writers. The simplest example of the process would be the capture of a π^--particle by a proton, the latter being transformed into a neutron.

In order to provide for the conservation of mass-energy and momentum, such an interaction must, however, be accompanied either by the emission of a photon—the so-called radiative capture (Marshak, *loc cit.*)—or of a neutretto ; and any such neutral radiation would absorb most of the rest-energy of the meson.*

The above features of the postulated interactions of π^--particles with individual free protons, makes it necessary to assume that in the capture of mesons by heavier nuclei, more than one nucleon is involved in the primary act of absorption. For if the process of radiative capture occurred, involving a single proton, most of the rest-energy would commonly escape from the nucelus as γ-radiation or as a neutretto ; and little would be available for producing the subsequent disintegration of the nucleus. Contrary to this conclusion, it is frequently observed that the energy represented by the disintegrations produced by σ-mesons is a large fraction of the rest-energy of the meson.

These difficulties can be avoided if the primary process of capture involves two or more nucleons, for the conservation laws can then be satisfied without the assumed emission of photons or neutrettos. It has therefore been suggested (Perkins 1948, Heidmann and Leprince-Ringuet 1948) that the primary act of absorption invloves a neutron–proton pair in the nucleus ; and that, as a result, two fast neutrons of energy $\sim$70 MeV. are produced. Alternatively, it has been suggested that even more nucleons may be involved. Such a view has been adopted by Ruddlesdon and Clark (1949) in a theoretical treatment of the capture of π^--particles by helium nuclei, ${}_2^4\mathrm{He}$.

§ 2. Scope of the Present Experiments.

2553 examples of σ-disintegrations recorded in photographic emulsions have now been examined in this laboratory, a number sufficiently great to allow a statistical analysis to be made. It has thus been possible to begin a detailed study of the nature of the processes associated with the nuclear capture of the mesons, and the subsequent nuclear explosion which commonly leads to the formation of a " star ".

One serious obstacle in making such an investigation arises from the complex nature of the emulsion, which usually makes it difficult to identify the type of nucleus involved in any particular disintegration. The first step, described in Part I. has therefore been to separate the observed stars into two groups :—those originating from the interactions of π^--mesons with the light nuclei, carbon, nitrogen and oxygen on the one hand, and those from heavy nuclei, mostly silver and bromine, on the other.

---

* *Note added in proof.*—In recent experiments at Berkeley, it has been observed that high energy γ-radiation is produced as a result of the capture of π^--mesons in liquid hydrogen. The results can be interpreted in terms of a competition between two types of transmutation corresponding to the emission of either a γ-ray of energy about 140 MeV., or the emission of a π^0-particle which subsequently decays into two γ-rays. (Panofsky 1950, Marshak and Whitman 1950.)

Heidmann and Leprince-Ringuet (1948) and Perkins (1949), have previously separated the σ-stars in a similar manner, but the statistical weight of the experimental material at their disposal was small.

The separation of the stars due to light and heavy elements has been carried out by three methods which yield results in satisfactory agreement with one another. The "prong distributions"—the relative frequencies with which the disintegrations are accompanied by the emission of different numbers of charged particles—can thus be determined separately for the two classes of stars. Examples in which the capture of the π-meson does not result in a visible "star", or in which it produces only a recoil particle of very short range, are also discussed.

In disintegrations produced by the capture of π-mesons by heavy elements, described in Part II., the "primary" process is followed by nuclear excitation which leads to the evaporation of nucleons and the formation of the star. Observations on the characteristics of these stars permit estimates to be made of the total energy involved in the evaporation, and conclusions to be drawn regarding the primary process (Perkins 1949.)

A second important source of information about the primary interaction is provided by observations on the ejection of singly-charged particles of energy greater than 30 MeV. The frequency of occurrence of these particles has been calculated by Tamor (1950), and preliminary results from experiments made with artificially produced π^--mesons have been reported by Adelman and Jones (1949), and by Cheston and Goldfarb (1950). No attempt was made by these authors, however, to consider separately the disintegrations of light and heavy nuclei.

In the case of the disintegrations of light elements, described in Part III., it is sometimes possible, as a consequence of the simpler nature of the systems involved, to make a more detailed analysis by an application of the conservation laws, and thence to draw conclusions about the nature of the primary interactions.

PART I.

General Characteristics of the Disintegrations and Separation of the Stars Due to Light and Heavy Elements.

§ 3. DEFINITION OF σ-STARS; CLASSIFICATION OF EJECTED PARTICLES.

In the present experiments, 1337 disintegrations due to artificially generated mesons, and 1216 due to cosmic-ray mesons have been scrutinized. The evidence is now very strong that the negative mesons produced artificially, and the σ-mesons of the cosmic radiation are of the same type. Firstly, the masses of the two types are equal within the limits of the experimental errors; secondly, Franzinetti (1949) has shown that, in the cosmic radiation, the number of σ-mesons which are not π^--particles is very small or zero; and thirdly, the prong distributions of the stars produced by the two types are indistinguishable. This and other evidence makes it almost certain that the naturally occurring σ-mesons are identical with the π^--particles produced artificially at Berkeley, and in what follows this will be assumed to be the case.

For the purposes of the present paper, we assume that a meson has produced a star—a nuclear disintegration— if the tracks of one or more charged particles—other than those of electrons or μ-mesons—appear to originate from the end of the trajectory of the meson in the emulsion. For each star, a preliminary classification of the ejected particles as protons, α-particles or heavy fragments has been made; and the lengths of the tracks have been measured. The identification of the particles has been based on an inspection of the grain-density and scattering characteristics of the tracks; and also, in the case of the heavy fragments due to recoil nuclei or "fission" particles, from the lengths of the tracks. With this rough method of identification most of the singly charged particles ($^1_1$H, $^2_1$H, $^3_1$H) will be classified as protons, whilst the group ascribed to α-particles will also include some heavier fragments. The term of "heavy fragment" is reserved for, (1) heavily ionizing particles producing tracks less than 5μ in length; (2) particles producing longer tracks if their ionization appears to be much greater than that produced by an α-particle; and (3) $^8_3$Li nuclei which produce the characteristic "hammer" tracks.

TABLE I.

Element	Composition of normal emulsion		Composition of gelatin	
	In gms. per cc.	Atomic composition	Percentage composition	Atomic composition
Silver	1·85	30·9	—	—
Bromine	1·34	30·3	—	—
Iodine	0·052	0·7	—	—
Sulphur	0·010	0·8	—	—
Carbon	0·27	49·0	43·8	49·7
Hydrogen	0·056	100·0	7·4	100·0
Oxygen	0·27	26·7	33·7	28·7
Nitrogen	0·067	10·5	15·2	14·7

§ 4. THE IDENTIFICATION OF STARS FROM LIGHT AND HEAVY NUCLEI BY THE USE OF "SANDWICH" PLATES—METHOD (*a*).

In these experiments, we have used gelatine "sandwich" emulsions exposed to π^--mesons produced in the Berkeley cyclotron. The emulsions were composed of layers of pure gelatine, 5μ thick, sandwiched between layers, 30μ thick, of Ilford C2 emulsion loaded with boron; the composition of the gelatine employed in given in Table I. (col. 4). It can be seen that the atomic composition of the gelatine in the sandwich is similar to that in the normal nuclear emulsions (cols. 3 and 5, Table I.).

TABLE II.

Number of charged particles ejected per star	Phenomenological classification of the star	Number of stars (observed)	Number of stars (after correction for loss)
1	1p	5	4
	1α	5	5
	1f	3	6
2	2p	1	1
	2α	3	3
	1α, 1p	5	4
	1p, 1f	1	2
	2f	1	1
3	3α	1	1
	2α, 1p	10	10
	1α, 2p	4	4
	1α, 1p, 1f	1	2
4	2α, 2p	1	1

Of the 600 stars observed in these plates, 41 were produced in the gelatine, and therefore must certainly be attributed to the disintegration of light elements. Photo-micrographs of three typical examples of these events are reproduced in Pl. XVIII. (*a*), (*b*), (*c*). Table II. gives details of the 41 stars originating in the gelatine; the letters "p", "α", "f", refer to protons, α-particles and heavy fragments respectivley.

We have also observed 38 mesons which appeared to stop in the gelatine and did not give rise to any visible disintegration.* Some of the particles emitted from the disintegrations will not be observed either through failing to emerge from the gelatine, or as a result of entering the emulsion at a considerable distance from the parent star, so that the association of the track with the meson is uncertain. Taking account of these effects and of the smaller stopping power of the gelatine, simple geometrical considerations suggest that the probability of "loss" is less than 0·1, for α-particles and protons of energy greater than 3 MeV. and 1 MeV. respectively. For the shorter tracks due to heavy fragments, the probability of loss is greater and approximate calculations give a value of 0·5. The appropriate corrections are included in the fourth column of Table II.

---

* We cannot exclude the possibility that some of these mesons may have stopped in the emulsion, just before entering, or immediately after leaving the gelatine layer.

The experimental distribution in prong number for σ-stars, in Ilford C2 emulsion and gelatine respectively, is given in Table III. Using this experimental material, the separation of the "stars" produced in light and heavy elements of the normal emulsion has been carried out in the following manner :

TABLE III.

No. of prongs	1137 stars by π^--mesons from cyclotron (percentage)	665 stars by π^--mesons from cosmic radiation (percentage)	Total no. of stars in the emulsion (percentage)	44 stars produced in gelatine (percentage)
1	33·7±1·7	34·7±2·3	33·9±1·4	34±9
2	33·1±1·7	28·1±2·0	31·3±1·3	25±8
3	22·1±1·4	21·4±1·8	21·8±1·1	38±9
4	9·3±1·0	13·5±1·4	10·9±0·8	2±2
5	1·7±0·4	2·5±0·6	1·9±0·3	—
6	—	0·3±0·2	0·1±0·1	—

It has been assumed that the "three-prong" stars which appear in the normal emulsion, and which are of the same type as those observed in the gelatine (Table II.), are the products of the interaction of the π^--mesons with light nuclei. In the gelatine, the proportion of such stars with three prongs is 17/44=0·38. On the other hand, in the emulsion, 71 three-prong stars of the same type were found in a sample of 460 stars. The proportion is therefore $71/460x$, where x represents the fraction of the 460 stars which must be attributed to light nuclei. Assuming that the two frequencies are equal, it is found that $x=0{\cdot}40\pm0{\cdot}12$.

Using this value, one can deduce, from the observed prong distributions in normal emulsion and gelatine, the corresponding distribution for the stars produced in heavy nuclei only. The results, normalized to 100 σ-stars in the emulsion, are given in Table IV.

§ 5. Separation of Stars by Observations on Ejected α-Particles and Protons—Method (*b*).

An alternative method of estimating whether a star is due to a light or heavy element, employed by Heidmann and Leprince-Ringuet (1948), is based on the assumption that an α-particle with an energy less than that corresponding to the potential barrier of bromine can only have emerged from a light nucleus. At first sight, it might appear that some caution should be observed in applying the method, for the production of short-lived radioactive heavy nuclei might permit the ejection of α-particles of lower energy. Further, some of the tracks, assumed to be produced by α-particles, may actually represent nuclear fragments of greater charge and mass.

Table IV.

No. of prongs	Method (*a*)		Method (*b*)		Method (*c*)		Mean values		
	L	H	L	H		H	L	H	L+H
1	13±4	21	10±1·5	24±4		35±5	11	27	37
2	10±3	20	15±2	18±3		18±3	13	18	31
3	15±4	7	15±2	5·5±1·5		1±1	15	4	20
4	2±1	10	8±1·5	3·5±1·0		—	6	4	10
5	—	2	1·5±0·8	0		—	1	1	2
6	—	—	—	0·5±0·5		—	—	—	—
Totals	40	60	49	51		(54)	46	54	100

Percentages of σ-stars of different types produced in light elements (L) and heavy elements (H) as determined by different methods. The absolute values for method (*c*) have been deduced from the observations, assuming that 54 per cent of the σ-stars originate in heavy nuclei. 21 per cent of the σ-stars have associated electrons.

Strong support for the "potential-barrier" method is given, however, by the observed distribution in energy of the α-particles emerging from those σ-stars in which a single α-particle track is the only visible product of the disintegration. Such an energy distribution, deduced from observations on 146 tracks, is shown in fig. 1, suitable geometrical corrections having been made to allow for the "loss" of tracks of great range.

The results shown in fig. 1 suggest that the single tracks identified as due to α-particles, fall into two groups. We shall show in a later section that many of the tracks which have been attributed to low energy α-particles, must in fact be due to the recoil of a light nucleus. The α-particles in the high energy group, which can be identified with much more confidence, must be attributed to the disintegration of heavy nuclei; for the emergence of a high energy α-particle from a light element would normally be accompanied by a detectable recoil of the residual nucleus.

It can be seen from fig. 1 that the point of separation of the two groups of α-particles is situated at ∼9 MeV. Perkins (1949) by a similar method obtained a value of ∼10 MeV.

On the basis of the above result, it has been assumed that a partial separation of the "stars" can be made by considering the range of the α-particle tracks, irrespective of the "prong-number" of the star. The division has been made in the following manner :—

If one or more α-tracks in a star have ranges corresponding to a kinetic energy of less than 9 MeV., the star has been attributed to a light nucleus. Further, in the cases where no α-particles are emitted, the occurrence of a proton of energy less than 4 MeV. has been taken to indicate disintegration of a light nucleus ; the possibility of proton decay of heavy nuclei can hardly lead to serious errors. Among 500 stars which were examined, it was found that 214 could be attributed to the disintegration of light nuclei, and 162 to heavy nuclei. Among the others, 32 were composed of short range fragments only. In 92 cases all the particles left the emulsion after traversing a distance smaller than 50μ (for an α-particle) or 120μ (for protons). These distances correspond to the limits of energy considered in our above criterion.

Fig. 1.

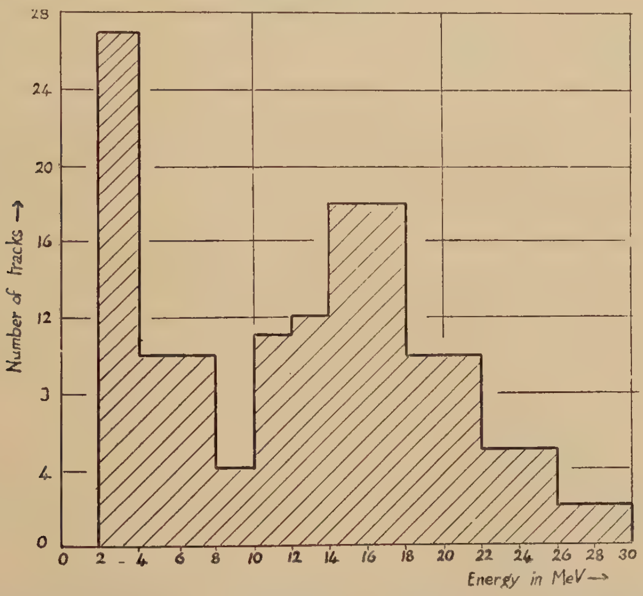

Histogram showing the distribution in energy of α-particles from 147 single-prong stars.

It is reasonable to suppose that most of the 32 disintegrations in which heavy fragments only were emitted, are due to the break up of light nuclei. Thus it will be shown in a later section that the maximum energy that can be imparted to a heavy recoil fragment coming from a disintegrating silver or bromine nucleus is 6 MeV. The average energy of such a fragment will be much smaller—only ~0·7 MeV. Such fragments will, in the majority of cases, be unable to produce an observable track. The 92 stars in which the lengths of the tracks in the emulsion were too short for the above criterion to be applied have all been attributed to heavy nuclei, since the prong distribution for these 92 cases was very similar to that for the 162 cases which could be definitely classified.

The fraction of σ-stars attributed to light nuclei by this method is 0·49, a result in satisfactory agreement with the data based on the stars in gelatine. The corresponding prong distribution for light and heavy elements normalized to 100 stars in the emulsion is included in Table IV.

§ 6. SEPARATION OF STARS BY OBSERVATIONS ON AUGER ELECTRONS—METHOD (*c*).

A third method for distinguishing the stars produced in light and heavy elements is based on the observation of tracks of slow electrons emerging from some of the σ-stars. A typical example is shown in Pl. XIX. (*a*). Although all these electrons are not necessarily produced in the same type of process, the evidence is very strong that they are all associated with the capture of π^--particles by heavy nuclei.

Most of the electrons probably arise in the process of atomic capture of the negative mesons. The energy released in the transition of the meson from one level to another can be transferred to an atomic electron—a form of Auger effect. The recent work of the Brussels group (Cosyns *et al.* 1949) has shown that this process occurs in the capture of μ^--mesons, and that slow electrons are rarely associated with the mesons which suffer direct β-decay. The last point strongly suggests that, in nuclear emulsions, the Auger electrons only appear during the capture of μ^--mesons by silver and bromine nuclei, for it is well known that with such heavy elements, the meson commonly interacts with the nucleus before suffering β-decay. The observations of the Brussels group on the energy spectrum of the slow electrons provides further support for this conclusion; and it is also confirmed by the work of Franzinetti (1950), who finds that no slow electrons accompany the decay of μ^--particles.

The slow electrons under consideration might also be attributed to the internal conversion of γ-rays, emitted after the capture of negative mesons by nuclei. In this case, however, the emission of a slow electron from the point where the nuclear disintegration occurred would only take place if a residual radiaoctive nucleus remained after the disintegration. There is good evidence, however, for the view that, following the interaction of a π^--meson with a light nucleus, the whole nucleus commonly disintegrates, and that no residual nucleus remains. A third possible origin of the slow electrons could be the emission of a β-decay particle as the final stage of the " cooling " of a nucleus excited by the capture of a π^--meson. Here again, however, the process is restricted to heavy nuclei.

It is reasonable to suppose that the process of atomic capture of π^- and μ^--mesons will differ only as a result of the difference in mass of the two particles, which will be manifest in a slightly greater energy of any emitted slow electrons in the case of the heavier π^--particles. 400 σ-stars, formed by π^--mesons of the cosmic radiation in Ilford G5 and Kodak NT4 emulsions were therefore examined for the presence of slow electrons. The slow-electron back-ground in an "electron-sensitive" emulsion is commonly high. Through a random coincidence, the tracks of unassociated slow electrons will therefore sometimes appear to diverge from the point where a meson stops in the emulsion. A correction for this effect was made by examining the point of the decay of 133 π-mesons for the presence of similar unrelated electrons. Three apparently associated electron tracks were found. The plates used were the same as those employed for the examination of σ-stars, and the slow electrons may have been due either to random coincidences, or to δ-rays produced by μ-mesons near their point of origin. The last feature would correspond very roughly to the chance production of a δ-ray by one of the products of disintegration of a σ-star.

The relative frequencies with which stars due to heavy nuclei, as identified by the above method, have different numbers of prongs, are shown in Table IV. The method does not give absolute values because the probability of the Auger transitions is not known, but the numbers given in Table IV. have been calculated on the assumption that 54 per cent of the σ-stars are due to heavy nuclei.

The final conclusions regarding the prong distributions from light and heavy elements are included in Table IV. They were obtained by a combination of the values given by the three methods (*a*), (*b*) and (*c*). The errors indicated throughout are the standard deviations. On the basis of the results obtained with methods (*a*) and (*b*), 54 ± 5 per cent of the stars observed have been attributed to heavy nuclei, and 46 ± 5 per cent to light nuclei.

Of the 57 single-prong stars accompanied by Auger electrons, 11 were identified as 1α, and 32 as 1p stars. In the remaining 14, the length of path in the emulsion of the secondary particle was not sufficiently great for an identification to be made. The value of the α/p ratio for heavy nuclei corresponding to these figures is 0·3, a result which may be attributed to the different heights of the potential barriers for protons and α-particles.

It is to be expected that the α/p ratio for light nuclei should be greater than that for heavy nuclei. In accordance with this expectation, the ratio of the number of α-particles and heavy fragments to that of protons was found to be $1{\cdot}55 \pm 0{\cdot}2$ for the stars in gelatine; and for the 246 stars identified by the potential barrier method as due to the disintegration of light nuclei, the α/p ratio was found to be $273/271 = 1$.

§ 7. UNOBSERVED DISINTEGRATIONS PRODUCED BY π^--PARTICLES.

Many of the π^--mesons, on being brought to rest in the emulsion, do not produce observable disintegrations (Occhialini and Powell 1948).

Thus Adelman and Jones (1949) have observed that 27±2 per cent of the π^--mesons do not produce a visible star. Our results from similar data give a value of 28±2 per cent.

We have observed that many of these " star-less " π^--mesons, at the end of their range, produce a " blob "—a rudimentary track of very restricted range, apparently due to a heavily ionizing particle. Adelman has informed us in a private communication that he has made similar observations. A typical example is shown in Pl. XVIII. (*d*). Whilst it is premature to attempt a final explanation of these events, the observations of Franzinetti (1950) strongly suggest that they are associated with the capture of negative mesons by silver and bromine nuclei. In an examination of 100 examples of such starless mesons, in plates exposed in the Berkeley cyclotron, 40 have been found to have blobs associated with them. We regard this figure as representing a lower limit to the proportion of " starless " mesons captured in heavy nuclei.

It is possible to make an estimate of that fraction of the starless mesons which corresponds to cases in which the π^--particles have been captured by hydrogen :—Our results show that out of 100 σ-stars observed in the emulsion, 54±5 occur in silver and bromine, and 46±5 in light nuclei. The number of starless mesons corresponding to 100 mesons producing stars is 39. If we assume, (1), that the capture of a meson by the nuclei of C, N, O always results in a visible " star " (see later section regarding cases in which only a recoil is produced) ; and, (2), that the probability of capture by different kinds of nuclei is proportional to the atomic charge (Fermi and Teller, 1947), then the 45 stars produced in C, N, O nuclei will be accompanied by 8 cases in which the meson is captured by a hydrogen atom. This result suggests that 80 per cent of the π^--mesons which stop in the emulsion without producing an observable disintegration correspond to cases of capture by heavy nuclei in which neutrons alone are " evaporated ".

§ (8). RECOIL FRAGMENTS.

The tracks of heavily ionizing particles of short range have been observed in 27±2 per cent of the disintegrations with which one or more prongs are associated. It is important to decide whether these are due to heavy nuclei, recoiling in order to provide for the conservation of momentum in the disintegrations.

The kinetic energy of such a heavy fragment will result from a process in which energy of such a heavy fragment will result from a process in which $n+1$ particles (including the recoil fragment itself) share a total energy E in such a way that the total momentum is zero. If A is the total mass of the nucleus, M the mass of the recoil fragment, and E the total available energy, then the maximum energy of the recoil nucleus, E_r(max), is E(A−M)/A. E is equal to $\mu c^2 - \sum_{i=1}^{i=n} B_i$ where μc^2 represents the energy equivalent to the rest-mass of the meson, and B_i the binding energy of the emitted particles. If it is assumed, for simplicity, that only individual nucleons are emitted, then we may write $\sum_{i=1}^{i=n} B_i = 8n$ MeV. for nuclei of intermediate mass (n being the number of nucleons emitted). We therefore obtain $E_r(\max)=(140-8n)n/A$.

The maximum value of the above expression for $E_r(\max)$ occurs for $n=9$ and gives a value of 6 MeV. for $A=100$. This corresponds to a very improbable case in which the nine evaporated particles are emitted in the same direction. The average energy of a recoil fragment from a heavy nucleus will be one-ninth of the maximum. These considerations make it unlikely that any track longer than 3μ is due to the recoil of a heavy nucleus, and justify the previous assumption that the stars containing only heavy fragments are due to the disintegration of light nuclei.

Harding (1949) has shown that among the stars produced in plates exposed to the cosmic radiation by fast neutrons, it is possible to identify short thick tracks due to the recoil of heavy nuclei. In such cases, however, an important part of the energy of the recoil fragment is due to the motion of the centre of mass (c.m) of the interacting particles, whereas in the nuclear capture of π^--mesons the centre of mass is at rest.

§ 9. THE EMISSION OF ENERGETIC CHARGED PARTICLES FROM σ-STARS.

The charged particles emitted as a result of the nuclear capture of π^--particles may be divided into two categories : (*a*), low energy nucleons or fragments which result from the evaporation processes in heavy nuclei or from the disintegration of light nuclei ; and ,(*b*), fast particles arising directly from the primary process (Tamor 1950). The production of thick "electron-sensitive" plates has made it possible to study these fast particles. We have examined a total of 361 σ-stars recorded in Ilford G5 emulsion 400μ thick, exposed to the cosmic radiation at an altitude of 70,000 feet, and determined the number of tracks with a grain density less than 150 grains/100μ.

In the particular conditions of development of the emulsions, these tracks are due to particles with the following characteristics :—protons with energy greater than 30 MeV.; deuterons with energy greater than 60 MeV. ; and tritons with energy greater than 90 MeV. Only tracks of which the horizontal projection was greater than 200μ were accepted for measurement, in order, (1), to maintain statistical accuracy in the determination of the grain density ; and, (2), to distinguish the fast particles giving rise to the single prong of some σ-stars from examples of $\pi \rightarrow \mu$ decay. A simple geometrical analysis allows the total number of particles in the stated energy interval, associated with the stars examined, to be determined from the observed numbers of tracks of range greater than 200μ, and the results are shown in Table V. The correctness of this procedure has been checked by determining approximate values of the grain-density in all the tracks, irrespective of their length, and the results thus obtained are included in the Table V. It will be seen that there is satisfactory agreement between the results obtained by the two methods.

The separation of the results given in Table V. into those corresponding to light and heavy nuclei, respectively, has been carried out by the potential barrier method described previously, and from evidence based on the observation of slow electrons associated with the star. The results indicate that 4·9±1·5 per cent of the stars observed in light nuclei and 21·4±2·5 per cent of the stars observed in heavy nuclei have associated fast particles of charge $|e|$; and that 11·9±1·4 per cent of all the disintegrations are accompanied by the emission of fast protons or heavier hydrogen nuclei with energy greater than 30 MeV. This figure does not take into account the " starless " mesons which form 28±2 per cent of the

TABLE V.

Stars examined		Observed no. of particles (G.D.<150 gr./100 μ ; range in emulsion >200 μ)	Calculated no. of particles after geometrical correction	Observed no. of fast particles, including those with range in the emulsion <200 μ
In heavy nuclei :	159	21	34	33
In light nuclei :	202	6	10	10
Total :	361	27	44	43

TABLE VI.

Range in μ	Particle	Energy of particle in MeV.*	No. of prongs	Probable nucleus
>1150	p	38±5	1	Ag or Br
4070	p	33±1	1	Ag or Br
>1500	p	37±4	1	Ag or Br
>1200	p	60±8	1	Ag or Br
>2550	p	56±4	4	Oxygen
>1000	p	32±5	2	Ag or Br
>3760	p	53±4	4	Oxygen
>1700	p	51±5	1	Ag or Br
>3500	p	82±6	1	Ag or Br
>1200	p	31±5	1	Ag or Br
>5900	p	62±4	1	Ag or Br
5250	d	50±2	1	Ag or Br

* In this table the errors indicated are " probable errors ".

total number of mesons captured in the emulsion. If these are included, the results therefore indicate that 9·5±1·4 per cent of all the mesons captured by atoms result in the emission of fast singly-charged particles.

Cheston and Goldfarb (1950) have reported that 8±2 per cent of the particles emitted from σ-disintegrations are protons with energies between 30 and 70 MeV. The present observations, in which all the particles arising fron 361 stars have been scrutinized, lead to the conclusion that 5·7±1·4 per cent of the ejected particles are protons with energy greater than 30 MeV.

In some cases, the length of the trajectory of a fast particle in the emulsion is greater than 1000μ. It is then possible to determine both the grain-density and Coulomb scattering of the track, and thus to measure the mass and energy of the corresponding particle. The results are given in Table VI.

Tamor (1950) has calculated the probability of the emission of these fast particles, and his theoretical results are shown in Table VII. In making the calculations, he considers two alternative mechanisms for the capture process. In the first, it is assumed that the primary interaction of the π^--meson takes place with a neutron–proton pair. Two fast neutrons are thus produced which travel in opposite directions, each with an energy of 70 MeV. The second model assumes that the primary interaction is with an α-particle group, which disintegrates with the emission of a 90 MeV. neutron and a 30 MeV. triton. These " primary " neutrons are assumed to create fast charged " secondary " particles in collisions with other nucleons of the nucleus. In all these calculations, charge exchange is assumed to occur in half the neutron–proton collisions.

Table VII.

	Model	Nitrogen	Silver
No. of fast protons (E>30 MeV.) per 100 mesons absorbed	I—neutron-neutron	48	24
	II—neutron-triton	12	13

Whilst the present experimental data is not of sufficient statistical weight to allow any final conclusions to be drawn, it is possible to indicate general tendencies, and to make a comparison with Tamor's theoretical predictions.

The observed frequency of occurrence of fast protons associated with σ-stars (9·5 per cent) agrees very well with the results based on Tamor's model (II.). This may be a coincidence, however, for there is a large disparity between the observed and calculated ratios of the frequency of occurrence of fast particles emitted in the disintegration of light and heavy nuclei, respectively. On the other hand, the neutron–neutron

Model (I.) suggests a much greater proportion of fast protons than is observed ; in particular, the proportion of 48 per cent obtained from this model, in the case of light nuclei, appears to be much too great. Although the statistical weight of the present observations is small, they strongly suggest that the ratio of the number of fast particles, arising from the disintegration of light nuclei, to the corresponding figure from heavy nuclei, is considerably less than 1, whereas Tamor's calculations, based on Models I. and II. give values of 2 and 1, respectively. Further comments on these questions are made in a later section.

PART II.

Interaction of Slow π^--Mesons with Heavy Nuclei.

§ 10. GENERAL FEATURES.

The problem of the interaction of slow π^--mesons with heavy nuclei (Ag and Br) has received more extensive theoretical treatment than the corresponding problem with light nuclei (Perkins 1948, Fujimoto and colleagues 1949). In these theoretical calculatons, it has generally been assumed that the primary process leads to the excitation of the nucleus, which subsequently " evaporates ". By assuming particular mechanisms for this process, it is possible to calculate the initial excitation energy, a quantity upon which the following features of the subsequent nuclear disintegration depend :—

(*a*) the prong distribution for the stars and the average number of ejected charged particles per star ;

(*b*) the α/p ratio ; and

(*c*) the distribution in energy of the emitted particles of charge $|e|$. Fujimoto and Yamaguchi (1949), and Le Couteur (1950), have treated these problems in considerable detail. Further, investigations on :—

(*d*) the distribution in energy of the fastest particles of charge $|e|$— already briefly discussed in the preceding section, enable tentative conclusions to be drawn regarding the mechanism of the " primary " excitation.

§ 11. FREQUENCY DISTRIBUTION OF THE NUMBERS OF CHARGED PARTICLES EMITTED IN THE DISINTEGRATION OF HEAVY NUCLEI.

In determining the " prong " distribution for the disintegrations of heavy nuclei, the relative frequencies with which the disintegrations result in the ejection of different numbers of charged particles, account must be taken of that fraction of the " starless " mesons which correspond to capture by Ag and Br. Two methods of estimating this quantity have been described in a previous section. The results obtained show that 54 ± 5 per cent of the visible disintegrations in the emulsion occur in heavy nuclei ; and that every 54 of these events are accompanied by 31 cases* in which the meson is captured by a Ag or Br nucleus without producing a star. This estimate has been employed in determining the distribution shown below, which corresponds to 100 mesons captured by Ag or Br nuclei :—

0–prong	36	(37)
1–prong	33±2	(54)
2–prong	22±1	(6)
3–prong	5±1	(2)
4–prong	5±2	(1)

Fig. 2.

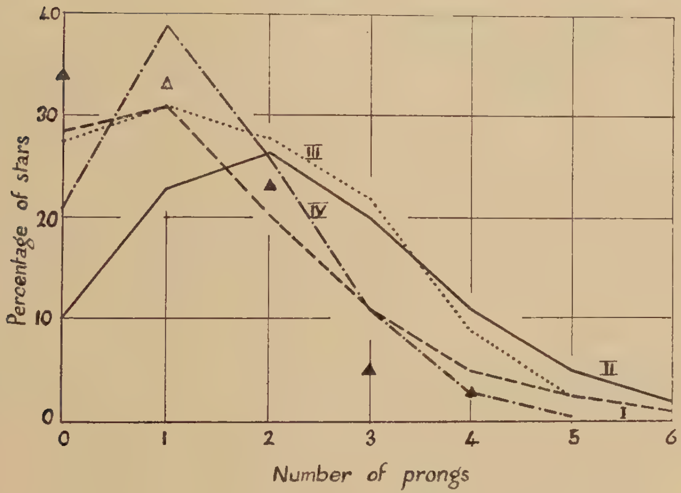

Theoretical prong distributions for heavy nuclei.

Curve I. — — — — Fujimoto and colleagues.
Curve II. ———— Fujimoto and colleagues.
Curve III. .... Clementel and Puppi.
Curve IV. –·–·–·–·–· Authors.

The experimental values are shown thus : ▲

The bracketed values are percentages deduced by Perkins from an analysis of 128 stars. The average number of prongs per disintegration is 1·1±·15 (0·78). It may be pointed out that the value for the frequency of occurrence of starless mesons, captured by heavy nuclei, is less accurate than the relative proportions of stars with 1, 2 and 3 prongs.

---

* Thus 28 per cent of the π^--mesons fail to produce a recognizable disintegration ; *i. e.* there are 39 starless mesons for every 100 σ-stars of which 54 are due to heavy nuclei. But of the 39 starless mesons, 8 are estimated to be due to interactions with hydrogen nuclei.

The present results appear to indicate a higher value of the excitation energy than that estimated by Perkins.

Fig. 2 shows the prong distributions predicted from theoretical considerations, the methods employed being indicated below.

Curve I.	Fujimoto and colleagues (1949).	Average initial excitation : 91 MeV. Average number of prongs : 1·4. Poisson's fluctuation law. Fermi-gas model.
Curve II.	Fujimoto and colleagues (1949).	Excitation energy : 140 MeV. Average number of prongs : 2·2. Poisson's fluctuation law. Fermi-gas model.
Curve III.	Clementel and Puppi (1949).	Excitation energy : 140 MeV. Average number of prongs : 1·2. Poisson's fluctuation law. Liquid-drop model (restricted to volume waves).
Curve IV.	Authors.	Excitation energy : 100 MeV. Average number of prongs : 1·2. Binomial distribution law. Fermi-gas model.

We have calculated curve IV. using a slight modification of Fujimoto's curve I., and a binomial distribution law. The average number of nucleons ejected being 7, the probability of observing ν protons is

$$P(\nu)=\binom{7}{\nu} \cdot (a)^{\nu} \cdot (1-a)^{7-\nu},$$

where "a" is the probability for an ejected nucleon to be a proton. We have considered the fact that we are dealing here with a Poisson rather than a Bernouillian series, since the probability of emitting a proton changes during the evaporation. The probabilities have been determined using seven successively smaller values of the excitation energy, but this refinement has little effect on the calculated distribution.

Curve III., based on the liquid drop model, gives good agreement between the observed and calculated values of the average number of prongs, but it predicts a distribution in the energy of the emitted particles which is widely different from that observed. We therefore regard the model as unsatisfactory for the description of these processes.

In all the calculations referred to above, one important factor has been neglected :—viz., the reduction of the charge of the nucleus by one unit as a result of the absorption of the meson. This produces both a change in the binding energy and an excess of neutrons in the excited nucleus. It should therefore have the effect of increasing the relative yield of neutrons at the beginning of the evaporation. For this reason, all the theoretical calculations probably tend to underestimate the proportion of " starless " mesons.*

§12. THE α/p RATIO.

The ratio of the number of particles with charge $|2e|$, emitted from heavy nuclei, to that with charge $|e|$, has been determined in the following manner :—

The total number of "protons" and "α-particles" has been deduced from observations on the 1-prong stars among a group of 780 recorded in C2 emulsion, making suitable geometrical corrections for "loss". The histogram showing the energy distribution of single α's (fig. 1) has been " cut off " below 9 MeV., since the particles of lower energy are believed to arise from light nuclei. The penetrability of the potential barrier has little effect on the results, for excitation energies in the range under consideration, and few of the short range α-particles can have been due to heavy nuclei.

Using this method, 58 single α-particles and 193 protons were found among the 1-prong stars. The corresponding value of the α/p ratio is $0{\cdot}3\pm0{\cdot}04$, identical with Perkins' estimate of 0·3. These values also agree well with Le Couteur's theory for an excitation energy of 100 MeV. A previous estimate, in which the stars from heavy nuclei were identified by the observation of slow electrons, as described in an earlier section, (§6). also gave a value of 0·3.

§13. THE ENERGY DISTRIBUTION OF THE PARTICLES PRODUCED IN THE EVAPORATION PROCESS.

The distribution in energy of particles of charge $|e|$, emitted from the 1- and 2-prong stars attributed to heavy nuclei, has been determined assuming that all the particles are protons. For this purpose, the range was measured of all of these particles which were brought to rest in the emulsion. The resulting distribution in range was then corrected for " loss ", and transformed to a distribution in energy. The result thus obtained, based on measurements on 309 tracks found in a group of 1430 stars recorded in Ilford C2 and G5 emulsions, is shown in fig. 3.

---

* The " heavy " nuclei considered here are those of silver and bromine. For the nuclei of lead, the average number of prongs resulting from the capture of a π-meson should be even smaller than that for silver, since the potential barrier for lead is about 10 MeV. A similar conclusion applies to the disintegrations produced by fast mesons ; namely, that the average number of the secondary particles produced in lead will be smaller than that observed in the emulsion. These considerations may have a bearing on the measurements of the mean-free-path between collisions of the particles produced in penetrating showers and observed in cloud chambers crossed by lead plates. A large fraction of the disintegrations, produced in the lead plates of the thickness commonly employed, will be undetected. This will tend to lead to an overestimate of the value of the mean-free-path.

The average energy per particle—of all the particles of energy less than 30 MeV.—is 9·6 MeV. Perkins had previously obtained a value of 7·6 MeV. Using the Weisskopf evaporation theory, and the relation between excitation energy and density of states given by the Fermi gas model, the calculated distribution in energy is obtained as a relation of the form

$$\mathrm{P(E)}\,d\mathrm{E}=(\mathrm{E}-4)\exp\left[-\cdot316(\mathrm{E}+8)/\sqrt{(\mathrm{U})}\right], \quad . \quad . \quad . \quad . \quad (1)$$

where U is the excitation energy of the nucleus. With a suitable value of the parameter, U, an expression of this form is found to give a satisfactory fit with the experimental results. The value of U, thus obtained, is 109±20 MeV., the errors being those associated with statistical fluctuations only. The above treatment is very approximate, and lack of precise knowledge of the magnitude of the potential barrier may introduce systematic errors up to 30 per cent ; but it gives an estimate of the order of magnitude of the excitation energy.

Fig. 3.

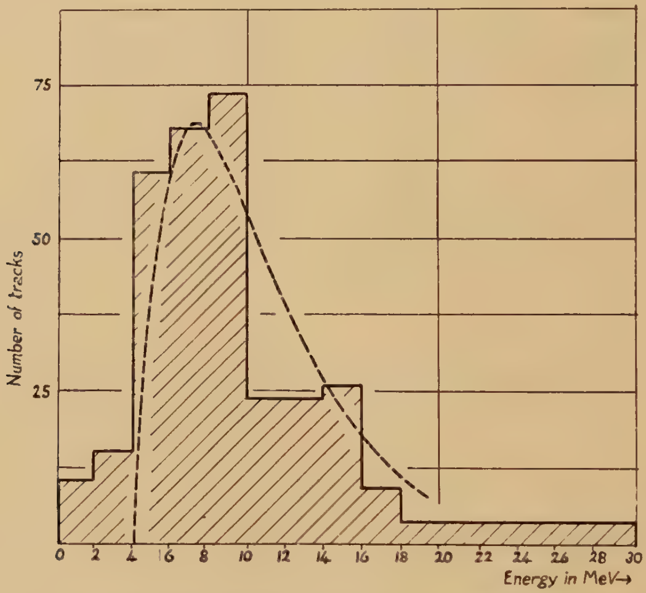

Histogram showing energy distribution of protons (E<30 MeV.) in 1- and 2-prong σ-stars. Dotted curve is the theoretical distribution.

§ 14. ENERGY SPECTRUM ABOVE 30 MeV.

Measurements on "fast protons" from σ-stars have been described in an earlier section—§ 9. Here we shall consider the energy spectrum of those emitted from heavy nuclei.

Fig. 4 shows the distribution in energy of all the particles of charge $|e|$ observed in an examination of 146 one-prong stars originating from heavy nuclei. The presence of a considerable proportion of protons of energy greater than 30 MeV. cannot be accounted for as due to a "tail" in a Maxwellian distribution, and they must be attributed to an alternative process other than that of evaporation. The distribution in the values of the energy of the fast protons ejected from heavy nuclei is shown in Table VIII. A possible explanation of the production of these energetic protons is that they are projected from nuclei in collisions with neutrons of energy ~70–90 MeV., the latter arising in the primary process.

Fig. 4.

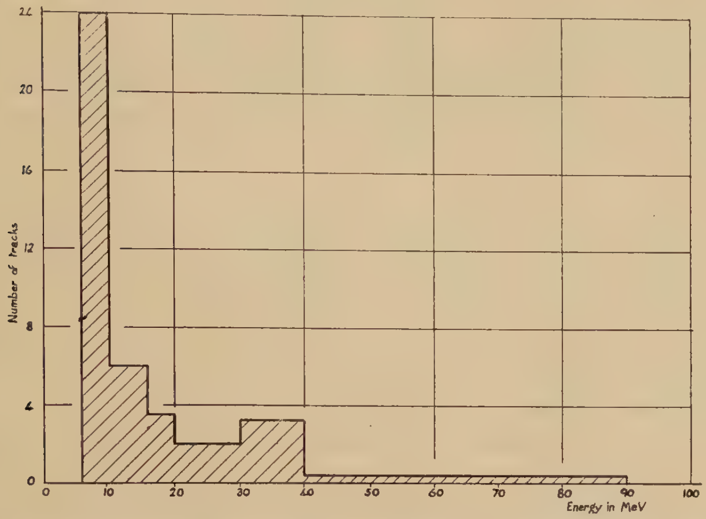

Energy distribution of all protons ($0<E<90$ MeV.) from 146 single-prong σ-stars in Ilford G5 emulsion. Allowance has been made for α-particles of range $>230\,\mu$ by considering the scattering characteristics along the tracks. It can be seen from fig. 1 that in any case this proportion is negligible.

TABLE VIII.

Energy range in MeV.	30–40	40–50	50–60	60–70	70–80	80–90
Number of fast protons	14	—	3	2	—	2

Approximate estimates have been made of the ratio of the number of fast protons with energies in the interval $30<E<50$, to the number with energy greater than 50 MeV. that would be expected to occur if the protons are indeed due to the impact of fast neutrons, with energy ~70 MeV., created in the primary process. The estimates have been based on calculations of the distribution in energy of secondary nucleons produced by the passage through nuclear matter of neutrons of about this energy, made by Goldberger (1948) and Heisenberg (1937). Both these calculations, and the experimental results of Tracy and Powell (1949) on the bombardment of carbon by 90 MeV. neutrons, give values significantly smaller than 1 for the above ratio, whereas the observed ratio is about 2. It appears therefore that most of the fast protons cannot be regarded as "knock-on" particles, produced by collision with such energetic "primary" neutrons.

§15. DISCUSSION.

It will be convenient to summarize here the evidence obtained from the present study of the disintegrations of heavy nuclei and its bearing on the nature of the "primary" interaction responsible for the absorption of the meson.

The energy spectrum, prong distribution and α/p ratio of the stars produced in heavy nuclei, all support the view that the average excitation energy is of the order of 100 MeV. That it is, in general, less than the rest-energy of the π-meson, is clearly shown by the disagreement between the experimental results and the theoretical predictions—both for the prong distribution and the average number of prongs—based upon a value of 140 MeV. for the excitation energy. (Curves II. and III., fig. 2.) The present observations, therefore, give support to an earlier conclusion reached by Perkins and several other workers. It follows that, on the average, about a quarter of the rest-energy of the meson is lost to the nucleus by the emission of fast particles before the general excitation, and the associated process of evaporation has been established.

The observed value of the excitation energy, $\sim$100 MeV., is not widely different from that calculated on the assumption that the primary interaction takes place with a neutron–proton pair. Thus, assuming that the mean free path for collision of nucleons in nuclear matter is 4×10^{-15} . E cm. where E is the energy of the particle in MeV., Perkins (1949) has obtained a value of 80 MeV. for the average value of the excitation energy. It has been shown by Tamor (1950), however, that this type of interaction should result in a much greater proportion of fast protons, of energy greater than 30 MeV., than is actually observed :—24 per cent from heavy nuclei and 48 per cent from light nuclei—see §9 and Table VII. It therefore seems certain that in the majority of the disintegrations of heavy nuclei the primary interaction is not confined to a pair of nucleons.

Any postulated mechanism of the primary interaction in which the rest-energy of the meson is regarded as being shared by one or two nucleons, the subsequent excitation resulting from secondary collisions, has to meet the following fundamental difficulty. The experimental results establish two salient facts : firstly, that the excitation energy is equal to a large fraction of the rest-energy of the meson ; and, second, that the proportion of energetic protons is small. From the point of view of an assumed primary interaction involving one or two nucleons, these two facts are contradictory ; for in order to keep the proportion of energetic secondary particles small it is necessary to assume a large mean free path for the primary nucleons in nuclear matter. They thus only infrequently make collisions in escaping from the nucleus, and will rarely produce projected protons. This assumption of a small probability of interaction has the second consequence, however, that the nucelus, being relatively transparent to the fast nucleons, will be given only a small average energy of excitation ; a conclusion which is in contradiction with the experimental results.

It also appears to be difficult to reconcile the present observations with the results of recent calculations by Tamor in which it is assumed that the primary interaction involves an α-particle " cluster " and leads to the production of a triton and a neutron. These calculations lead to the conclusion that 43 per cent of the nuclei should be excited with an energy of less than 40 MeV., in which case almost all this fraction would fail to produce a visible " star ". Because of the increased probability of the emission of neutrons at the beginning of the " evaporation ", the expected proportion may be put even higher—even 50 per cent or more. We have seen, however, that the experimental results give a figure of 36 per cent for the proportion of "starless" mesons in heavy nuclei; and the calculated " prong distribution ", using an excitation energy of 100 MeV., leads to a value of 21 per cent. Further, the neutron–triton model predicts a ratio of approximately 1 for the relative numbers of fast protons from light and heavy nuclei. On the other hand, experimental observations recorded in § 9 give a value of 1:4 for this ratio.

The following alternative hypothesis appears to be in better accord with the experimental results :—Let us assume that, in the primary interaction, the rest-energy of the π^--meson is shared among three or four nucleons, charged and uncharged. The fast protons observed may then be attributed, at least in part, to protons which have taken part in this primary act. The initial distribution may take place, for example, in an α-particle group, and lead to its complete disruption. After the interaction, most of these four nucleons, of which one will be a proton, will be captured within the nucleus, for they are of relatively low energies, and the Ag and Br nuclei will be opaque to them. In particular circumstances, however, it will be possible for one of these nucleons to escape ; viz., if the following three conditions are satisfied after the interaction :—

(1) the momentum of the nucleon is directed outward ;
(2) the nucleon is sufficiently near the surface of the nucleus ; and
(3) the kinetic energy of the nucleon inside the nucleus is much greater than the maximum Fermi energy plus the binding energy of the nucleon.

Condition (3) may be written as

$$E_i > E_F + 8 + 30 (\text{in MeV.}), \quad \ldots \ldots \quad (2)$$

where E_i is the energy of internal motion and E_F the maximum Fermi energy, and the binding energy is taken as 8 MeV.; (30 MeV. is the minimum energy of the fast protons considered).

The Heisenberg relation then gives us (Rosenfeld 1948) that only those protons produced in a spherical shell of thickness $1{\cdot}6r_0$ and satisfying the above conditions will be observed as fast protons, r_0 being the "nucleon radius" $=1{\cdot}47\times10^{-13}$ cm. Thus we obtain for the number of fast protons with energy greater than 30 MeV.,

$$n(E_0>30)=n(E_i>E_F+8+30)\times\tfrac{1}{2}\times\frac{\text{volume of spherical shell}}{\text{volume of nuclear sphere}}, \quad . \quad (3)$$

E_0 being the energy of the proton observed outside the nucleus.

As a first approximation, the spectrum of E_i-E_F may be considered to be similar to that which would result from the sharing of the total energy of the π-meson between 4 nucleons of a free helion. The results of this interaction have been studied theoretically by the Liverpool group (Ruddelsdon and Clark 1949). Introducing into the right hand side of the equation (3) the proportion of particles in their calculated spectrum with energy greater than 38 MeV., it is found that 13 per cent of the π^--mesons absorbed in silver nuclei should be accompanied by the emission of fast protons of energy greater than 30 MeV. It will be possible to test the validity of the assumptions employed in obtaining this result when more experimental material becomes available, but the preliminary result appears to be in satisfactory agreement with the value for heavy nuclei obtained experimentally :—viz., 21 per cent.

An approximate value of the average energy of excitation may also be calculated on the basis of this model. The fraction of the energy carried away by the fast protons is about a quarter of the rest-energy of the meson, and the relative abundance of the fast protons is approximately 0·1 per star. The three neutrons have an equal probability of emission with the same energy, and therefore the amount of energy which is not used in "heating" the nucleus is equal to $0{\cdot}1\times4\times\frac{1}{4}\mu c^2$ where μc^2=rest mass energy of the meson.

This gives an average excitation energy of ∼120 MeV. after accounting for the binding energy of the fast nucleons emitted.

To a first approximation, the energy spectrum of the fast nucleons emitted, would be expected from this model to be similar to that resulting from the sharing of the rest-energy of the meson between 4 particles in the primary interaction, and to display a maximum at an energy between 30 and 40 MeV. A preliminary estimate of the ratio of the number of fast protons with energy greater than 50 MeV. to the number between 30 and 50 MeV., as deduced from the spectrum calculated by the Liverpool group, gives a value in good agreement with out experimental observations.

PART III.

Interaction of Slow π⁻-Mesons with Light Nuclei.

§16. GENERAL FEATURES OF THE DISINTEGRATIONS.

The capture of π^--mesons by light nuclei commonly leads to more complete disintegration than in the case of heavy nuclei. It therefore seemed probable that a detailed study of the characteristics of the corresponding stars would give important information complementary to that obtained from the observations described above.

In the conditions of our experiments, the stars representing the disintegration of light elements can only arise from the three types of nuclei $^{12}_{6}C$, $^{14}_{7}N$ and $^{16}_{8}O$. It is therefore possible to make a tentative identification of the disintegration of particular nuclei by an application of the principle of the conservation of charge. Although many 1- and 2-pronged stars occur in which the fragments are of charge three or more, and of which the parent nucleus is unknown, a sufficient number of stars with three or more prongs have been found to render this process useful. Among the latter, the following three types are most frequently observed:—

A, stars with 2 prongs of charge $|2e|$ and 1 prong of charge $|e|$ identified as due to the disintegration of $^{12}_{6}C$;

B, stars with 3 prongs of charge $|2e|$, identified as due to the disintegration of $^{14}_{7}N$; and,

C, stars with 3 prongs of charge $|2e|$ and 1 prong of charge $|e|$ identified as due to the disintegration of $^{16}_{8}O$.

The recognition of stars of these types is facilitated by the fact that in Ilford C2 emulsions, with normal processing conditions, it is usually possible to distinguish between singly and doubly charged particles by inspection if the track is longer than 10μ. It must, however, be borne in mind that the star types A, B and C are not the only modes of disintegration of the nuclei $^{12}_{6}C$, $^{14}_{7}N$ and $^{16}_{8}O$. Thus, 22 ± 7 per cent of the stars observed in the gelatine sandwiches (Table II.) are of the type A, yet on the basis of Fermi and Teller's formula, approximatley 43 per cent of the stars in the gelatine should be attributed to $^{12}_{6}C$ nuclei.

Using Fermi and Teller's theory, and taking account of the capture of π^--mesons by hydrogen nuclei, the proportion of the stars due to the various nuclei in the gelatine has been calculated. Since our results indicate that 45 ± 5 per cent of all the stars in the emulsion are formed in light nuclei, the fraction of all the stars which come from $^{12}_{6}C$, $^{14}_{7}N$ and $^{16}_{8}O$ nuclei may be determined. The results are shown in the second column of Table IX., whilst the fourth column shows the frequency of occurrence of stars of type A, B and C as observed in 780 σ-stars in C2 emulsions.

The analysis of the stars is complicated by the emission of neutrons which cannot be observed, but reactions A, B, C may be represented, tentatively, by the equations :—

$$\text{A,}\quad {}^{12}_{6}\text{C}+\pi^{-}\longrightarrow 2\,{}^{4}_{2}\text{He}+1\,{}^{1}_{1}\text{H}+3\,{}^{1}_{0}\text{n}\,;$$

$$\text{B,}\quad {}^{14}_{7}\text{N}+\pi^{-}\longrightarrow 3\,{}^{4}_{2}\text{He}+2\,{}^{1}_{0}\text{n}\,;$$

$$\text{C,}\quad {}^{16}_{8}\text{O}+\pi^{-}\longrightarrow 3\,{}^{4}_{2}\text{He}+1\,{}^{1}_{1}\text{H}+3\,{}^{1}_{0}\text{n}.$$

Among the various mechanisms which have been proposed to account for the disintegrations produced by the nuclear capture of a meson, the simplest is that the total available energy is symmetrically distributed amongst the products of the disintegration ; such a model was, we have seen, proposed tentatively, by the Liverpool group, for the case of the ${}^{4}_{2}$He nucleus. The total energy is regarded as distributed among n particles in such a way that each has the same probability of receiving a certain fraction of the maximum possible energy ; a probability which is only proportional to the corresponding volume in configuration space. The magnitude of the energies involved is sufficiently great to allow the effect of binding forces to be neglected, except in considering the total balance of energy.

Table IX.

Calculated percentage * of the stars which originate in		Observed percentage * of the stars of type	
${}^{12}_{6}$C	20±2	A	7·6±1
${}^{14}_{7}$N	5·2±5	B	3·7±7
${}^{16}_{8}$O	20±2	C	4·2±7

* Percentages are expressed in terms of the total number of stars in the emulsion.

The above assumption leads to a distribution function of the form

$$\mathrm{P(E)}\,d\mathrm{E}=\mathrm{E}_{\max}^{\frac{5-3n}{2}}\;\frac{\Gamma\left(\frac{3n-3}{2}\right)}{\Gamma\left(\frac{3n-6}{2}\right)}\cdot\frac{2}{\sqrt{\pi}}\cdot\mathrm{E}^{1/2}(\mathrm{E}_{\max}-\mathrm{E})^{\frac{3n}{2}-4}\,d\mathrm{E},\qquad .\quad (4)$$

where n is the number of particles sharing the rest-energy of the meson ; and $\mathrm{E}_{\max}$, the maximum energy of the particle considered, equals $\mathrm{E}_0(\mathrm{A}-\mathrm{M})/\mathrm{A}$. In this expression, E_0 is the total available energy, A the mass of the nucelus, and M that of the particle considered.

Fig. 5 gives the distribution in energy of 102 α-particles form the stars of reaction A, 65 from stars of reaction B, and 100 from stars of reaction C. The dotted lines in the figure represent the distribution function (4)

Fig. 5.

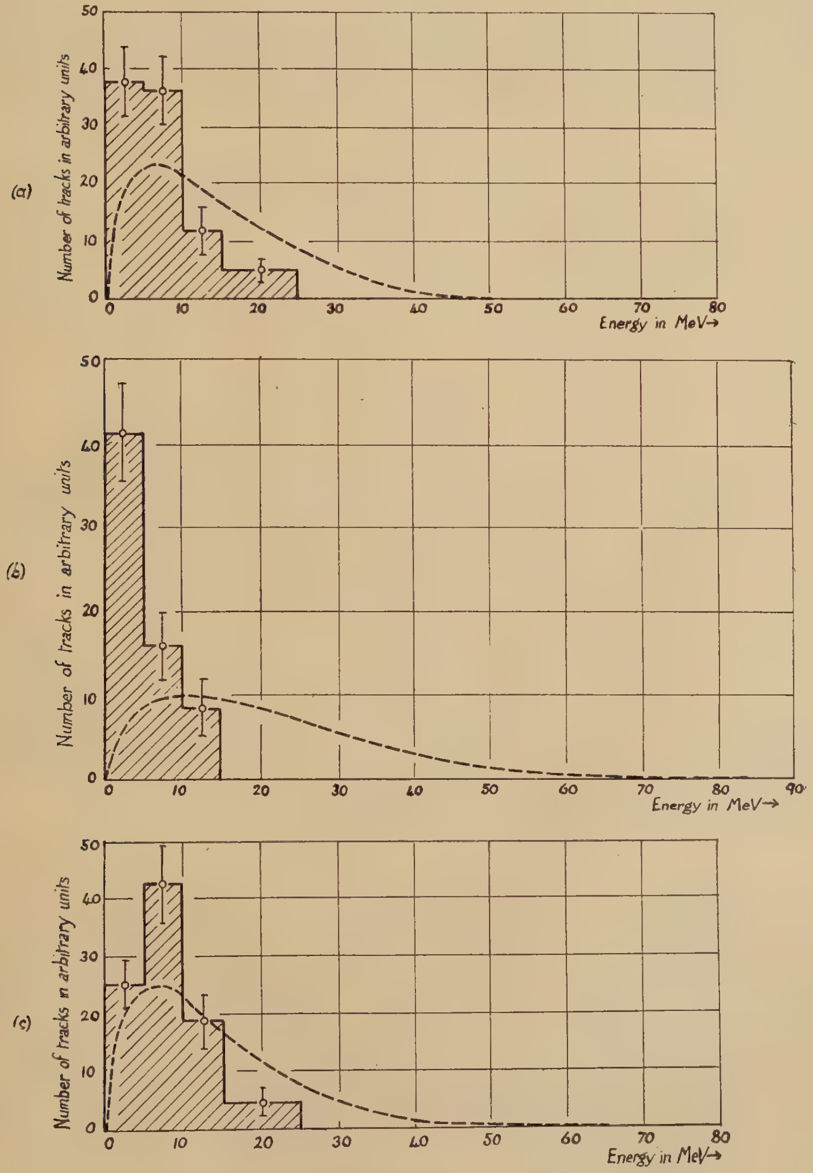

Distribution in energy of α-particles.

(*a*) 102 α-particles from disintegration of $^{12}_{6}C$.

(*b*) 65 α-particles from disintegration of $^{14}_{7}N$.

(*c*) 100 α-particles from disintegrations of $^{16}_{8}O$.

Dotted curves give corresponding theoretical distributions using function (4) (see text).

calculated for $n=6$ in case A, $n=5$ in case B and $n=7$ in case C, values which correspond to the number of secondary particles in each of the reactions A, B and C if they are correctly represented by equations given above.

The disagreement between experimental and theoretical distributions in fig. 5 indicates that there is a large disparity in the distribution of the rest-energy of the meson among the ejected particles. The same conclusion is reached by considering their average energy which is given by equation

$$\int_0^{E_{\max}} E\,.\,P(E)\,dE=\bar{E}=[1/(n-1)]E_{\max}. \quad . \quad . \quad . \quad . \qquad (5)$$

Table X. shows the calculated and observed values of the energy of these particles, and it will be seen that the theoretical values of the energy of the neutrons are much lower than those deduced from the experimental results.

TABLE X.

Reaction	$\bar{E}_\alpha$ observed (MeV.)	$\bar{E}_\alpha$ calculated (MeV.)	$\bar{E}_p$ observed (MeV.)	$\bar{E}_p$ calculated (MeV.)	$\bar{E}_n$ * observed (MeV.)	$\bar{E}_n$ † calculated (MeV.)
A	5·8	13·6	8·6	18·7	~82/3	56/3
B	5·0	21	—	—	~105/2	56/3
C	7·5	11·8	~8	14·8	64/3	44·4/3

* Difference between the total available energy and the average total energy in the charged particles divided by the number of neutrons.

† The average calculated energy of one neutron.

§ 17. CAPTURE BY $^{14}_{7}$N.

The second row of Table X. shows that in the disintegration of $^{14}_{7}$N, most of the energy is imparted to two neutrons, and that the three α-particles receive a total kinetic energy of only approximately 15 MeV. In this case, an attempt has been made to make a closer analysis of the reaction by considering the momentum balance, although the nature of the charged particles, assumed to be α-particles, is not always certain.

If the three α-particles represent the visible products of the disintegration of $^{14}_{7}$N, the resultant of their momenta gives some information about the energies and directions of ejection of the two neutrons. The The momenta have been determined for those cases in which all three α-particles remain in the emulsion. In such cases, it is possible to determine upper and lower limits for the energy of the two neutrons, limits which correspond to the maximum and minimum possible values of the angle between their directions of ejection. The results are shown in Table XI.

Let us choose to consider, first, those limiting cases in which there is the greatest disparity between the energy of the two neutrons. Most of the rest-energy of the π-meson must then be assumed to have been imparted to one neutron, whilst the other may be considered as resulting from the disintegration of the residual nucleus. The characteristics of the observed disintegrations are such, however, that this slow neutron must be assumed to have been emitted in a direction making a small angle to the vector representing the sum of the momenta of the three α-particles. This result implies either that the neutron has a very small velocity of ejection compared to the velocity of the recoiling nucelus, or that it has a preferential direction of emission with respect to the line of motion of the nucleus. Both features are inconsistent with the view that the neutron arises in the spontaneous break up of a moving excited nucleus.

TABLE XI.

Total energies of the α-particles in MeV.	Maximum and minimum values for the angle of separation between the two neutrons	Limits of energy of each of the two neutrons	
		First	Second
15·4	$154° < \theta < 180°$	$51{\cdot}2 < E_1 < 74{\cdot}8$	$27{\cdot}6 < E_2 < 51{\cdot}2$
16·5	$130° < \theta < 180°$	$50{\cdot}8 < E_1 < 89{\cdot}3$	$12{\cdot}3 < E_2 < 50{\cdot}8$
17·3	$130° < \theta < 180°$	$52{\cdot}4 < E_1 < 92{\cdot}9$	$11{\cdot}9 < E_2 < 52{\cdot}4$
14·3	$132° < \theta < 180°$	$51{\cdot}9 < E_1 < 90{\cdot}3$	$13{\cdot}5 < E_2 < 51{\cdot}9$
20·7	$155° < \theta < 180°$	$48{\cdot}6 < E_1 < 69{\cdot}2$	$28 < E_2 < 48{\cdot}6$
10·6	$94° < \theta < 180°$	$53{\cdot}7 < E_1 < 107$	$0{\cdot}7 < E_2 < 53{\cdot}7$
9·0	$142° < \theta < 180°$	$54{\cdot}5 < E_1 < 91$	$17{\cdot}8 < E_2 < 54{\cdot}5$
7·3	$167° < \theta < 180°$	$55{\cdot}3 < E_1 < 65{\cdot}7$	$45{\cdot}9 < E_2 < 55$

In the second extreme case the two neutrons are approximately equal in energy. We must then visualize the production of two fast neutrons moving in nearly opposite directions and carrying most of the rest energy of the π^--particle. The remaining part of the disintegration may then be described in terms of an excited ${}^{12}_{6}C$ nucleus disintegrating whilst in motion. With this assumption, the excitation energies of the carbon nucleus can be calculated, and the values obtained lie between 16 and 25 MeV. These values are in good agreement with the results of Hanni, Telegdi and Zunti (1948), who have shown that the formation of three α-particles is the most common mode of disintegration of ${}^{12}_{6}C$ nuclei, excited to energies in the region of 20 MeV.

§18. CAPTURE BY ${}^{12}_{6}C$.

Because of the α-particle structure of the ${}^{12}_{6}C$ nucleus, the possibility exists that, following the capture of a meson, the primary distribution of energy may take place among nucleons of one of the α-particles, leaving the rest of the nucleus unaffected. If the result of this interaction is a triton and a neutron (Tamor 1950), stars corresponding to the reaction

$$ {}^{12}_{6}C+\pi^{-}\rightarrow {}^{4}_{2}H+{}^{4}_{2}He+{}^{3}_{1}H+{}^{1}_{0}n \quad . \; . \; . \; . \; . \; . \quad (6) $$

could occur, either through the escape of the "primary" triton with energy 30 MeV. or as a result of the escape of the "primary" neutron of 90 MeV. and the formation of a residual ${}^{11}_{5}B^{*}$ nucleus excited to about 30 MeV. The latter nucleus is known to disintegrate into two α-particles and a triton at high excitation energies (Lattes and Occhialini 1947, Goward, Titterton and Wilkins 1950). For such values of the excitation energy, the concept of a compound nucleus is, of course, very crude, and the mode of decay probably depends on the mechanism of excitation. Although the study of the disintegrations of heavy nuclei, discussed in a previous section, indicates that an interaction giving rise to a triton and a neutron occurs only infrequently, a disintegration of carbon giving two α-particles and a triton would, although occurring rarely, be of considerable interest because the only particle escaping detection is a neutron; and it is therefore possible, in principle, to make a complete investigation of the energy and momentum balance.

The possibility of identifying such a reaction is complicated by the difficulty of establishing whether ejected particles of charge $|e|$ are protons or heavier hydrogen nuclei; but if a track is of sufficient length, identification is possible by measuring its grain-density, and the scattering of the particle. If, further, a particular disintegration is correctly represented by equation (6), there must be a consistency between the values of the energy and momenta of the unobserved neutron as determined by two independent methods:—(*a*) from an application of the principle of the conservation of energy, the energy of the ejected charged particles being known; and (*b*) by determining the resultant of the momenta of the three charged particles, and, hence, the momentum and energy of the neutron.

In view of this possibility, a complete analysis was made of 13 σ-disintegrations, of the type under consideration in which all the tracks end in the emulsion, and details are given in Table XII. In two cases, the mass of the particle of charge $|e|$, as determined by observations on the grain density along the track, appeared to be greater than that of a proton. Making the tentative assumption that all the particles of charge $|e|$ are tritons, values of their energy and momentum have been determined from their observed range. The corresponding values of the total energy of the particles in each star, and the vector sum of their momenta are given in cols. 3 and 4, respectively of Table XII., while col. 5 gives the momentum of the neutron assumed to carry the remaining available energy. The limits of error indicated include those due to straggling, to lack of precise knowledge regarding the shrinkage factor of the emulsion, and to errors in the measurement of the lengths and directions of the tracks. All errors have been considered for the most unfavourable cases, and are therefore much greater than the probable errors.

TABLE XII.

Energies of particles in the star	Evidence about nature of the particle of charge $\lvert e \rvert$	Total kinetic † energy of three charged particles (MeV.)	Total momentum † of the three charged particles ($\sqrt{2mE}$)	Calculated † momentum of the neutron $=\sqrt{2(140-Q-\Sigma E_{kin})}$
α_1 : 3·3 MeV. α_2 : 6·5 MeV. p : 83 μ	?	14·5±1·3	4·6±0·9	13·8±0·2
α_1 : 4·4 MeV. α_2 : 2·3 MeV. p : 168 μ	?	14·2±1·3	6·5±0·4	13·8±0·2
α_1 : 1·8 MeV. α_2 : 1·7 MeV. p : 1232 μ	Identified as proton by scattering and grain density	27·5±1·7	5·4±2·9	12·7±0·3
α_1 : 9·4 MeV. α_2 : 7·0 MeV. p : 220 μ	?	24·4±1·0	7·9±3·5	13·1±0·1
α_1 : 5·6 MeV. α_2 : 5·6 MeV. p : 165 μ	?	20·7±1·5	10·2±1·4	13·5±0·2
α_1 : 4·2 MeV. α_2 : 3·5 MeV. p : 66 μ	?	12·0±1·3	7·1±1·1	14·0±0·2
α_1 : 11·6 MeV. α_2 : 14·0 MeV. p : 330 μ	Identified as proton	38·7±1·1	24±12	12·0±0·02
α_1 : 2·4 MeV. α_2 : 11·6 MeV. p : 945 μ	Identified as proton	35±1·4	16·9±5·0	12·2±0·2
α_1 : 3·5 MeV. α_2 : 0·5 MeV. p : 1425 μ	Identified as proton	31·3±1·6	17·7±1·8	12·5±0·2
α_1 : 5·1 MeV. α_2 : 5·8 MeV. p : 110 μ	* ?	16·5±1·3	14·3±1·0	13·7±0·2
α_1 : 2·0 MeV. α_2 : 5·8 MeV. p : 315 μ	* Identified as proton	18·8±1·3	14·7±1·0	13·5±0·1
α_1 : 3·4 MeV. α_2 : 9·0 MeV. p : 116 μ	* ?	18·3±1·0	12·4±6·0	13·1±0·2
α_1 : 4·0 MeV. α_2 : 7·9 MeV. p : 65 μ	* Grain density indicates triton possible	15·6±1·2	13·5±2·5	13·7±0·2
α_1 : 13·0 MeV. α_2 : 10·5 MeV. p : 74 μ	* Grain density indicates triton possible	28·2±1·0	14±6	12·8±0·2

† These columns have been computed, assuming that the particle of charge $\lvert e \rvert$ is a triton.

* In these cases, energy and momentum balance considerations seem to justify the assumption that the particle of charge $\lvert e \rvert$ is a triton.

From these observations, it may be concluded, first, that if tritons of energy 30 MeV. are somtimes produced as a result of the capture of π^--particles by carbon nuclei, they are rare. Second, in five of the disintegrations referred to in Table XII., there is a consistency between the balance of energy and of momentum, if the particle of charge $|e|$ is assumed to be a triton. In one of these examples, however, the particle of charge $|e|$ can be identified as a proton so that the apparent consistency between the momentum and energy balance in the star must be regarded as fortuitous. In two of the remaining four examples, the grain-densities in the tracks are consistent with the view that the particles of charge $|e|$ are more massive than protons. For these four cases the average energy of the neutron required to provide the balance of energy and momentum is 85 MeV., and the neutron–triton model appears to give a satisfactory description of the disintegrations.

The above results suggest that in a small proportion of the disintegrations of carbon nuclei, the transmutation can be correctly represented by equation (6). Many of the other examples of which the details are included in Table XII. may be attributed to an interaction with an α-cluster in which its disintegration is more complete than that suggested by the neutron–triton model. In a few cases, however, the following analyses suggest that the primary interaction is not confined to a single α-cluster.

The energy of the particles observed in the $2a+1p$ stars has been plotted in a triangular energy diagram ; see fig. 6. In this diagram the three coordinates are (*a*) the total energy of the two α-particles ; (*b*) the energy of the particle of charge $|e|$, assumed to be a proton ; and (*c*) the remaining available energy which represents the energy carried by the three neutrons. The sum of the three coordinates of any point in this diagram is 100 MeV. This value has been chosen because it is nearly equal to the difference between the rest-energy of the π-meson and Q value of the reaction ${}^{12}_{6}C \rightarrow 2\alpha+1p+3n$.

It will be seen that the points in fig. 6 are grouped together in a region corresponding to small values of the α-particle and proton energies, but that there are some points widely displaced from it. These correspond to disintegrations in which the α-particles carry away most of the rest-energy of the meson. The effect is particularly marked for the two examples described below ; the letter α_1 and α_2 refer to the two α-particles, and p to the proton.

Case 1 : α_1 24 MeV., stays in emulsion ;
α_2 : 19 MeV., stays in emulsion ;
angle between α_1 and α_2 153° ;
p : leaves the emulsion after traversing a path length of 100μ.

*Case 2 : α_1 ; 21·5 MeV., stays in emulsion ;

---

* This star was found recently by Dr. D. H. Perkins, who kindly directed our attention to it.

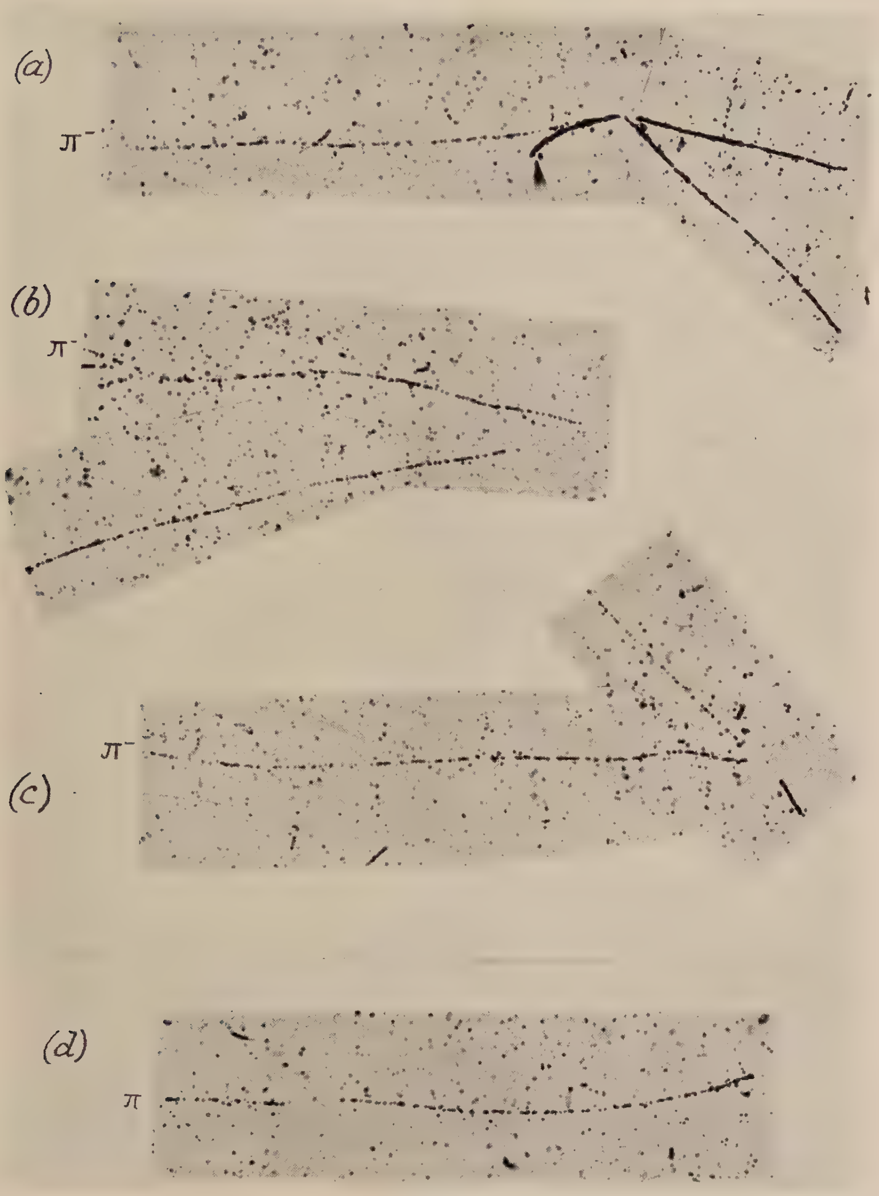

CAPTIONS FOR PLATES.

Plate XVIII.

(*a*), (*b*), (*c*). Three typical examples of disintegrations observed in the "sandwich-plates". A meson is captured by a light element and produces a star whose centre is absent because it is located in the layer of pure gelatine $5\,\mu$ thick.

(*d*) Meson showing a "blob". Events of this type are sometimes observed when negative mesons come to the end of their range in the emulsion and do not produce a star.

Plate XIX.

(*a*) Sigma-star accompanied by a slow electron. (Auger effect in heavy nuclei.)

(*b*) Energetic "$2\alpha+1p$" star identified as the disintegration of a ^{12}C nucleus. Two alpha-particles of 24 and 19 MeV. respectively, are emitted at an angle of 153° to each other.

This star represents a possible case in which the capture process leads directly to the total disruption of a light nucleus.

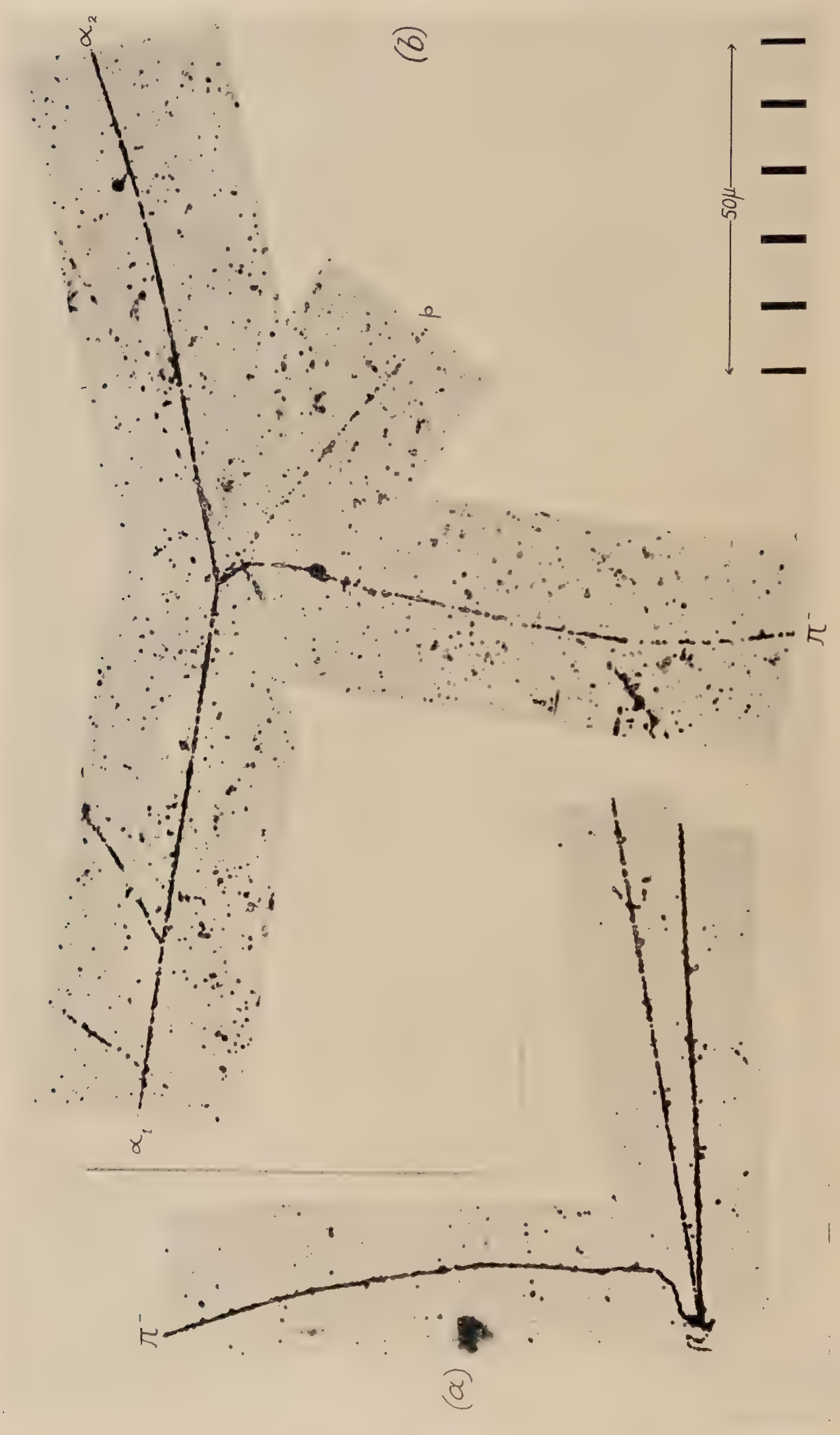
(b)
α_2
p
π^-
50μ
α_1
π^-
(a)

α_2 : 5·4 MeV., stays in emulsion;
p : leaves the emulsion after a path length of 3250μ; energy from grain-count and multiple scattering 28 ± 3 MeV.; angle between α_1 and $p = 180°$.

A photo-micrograph of case 1 is shown in Pl. XIX.

Fig. 6.

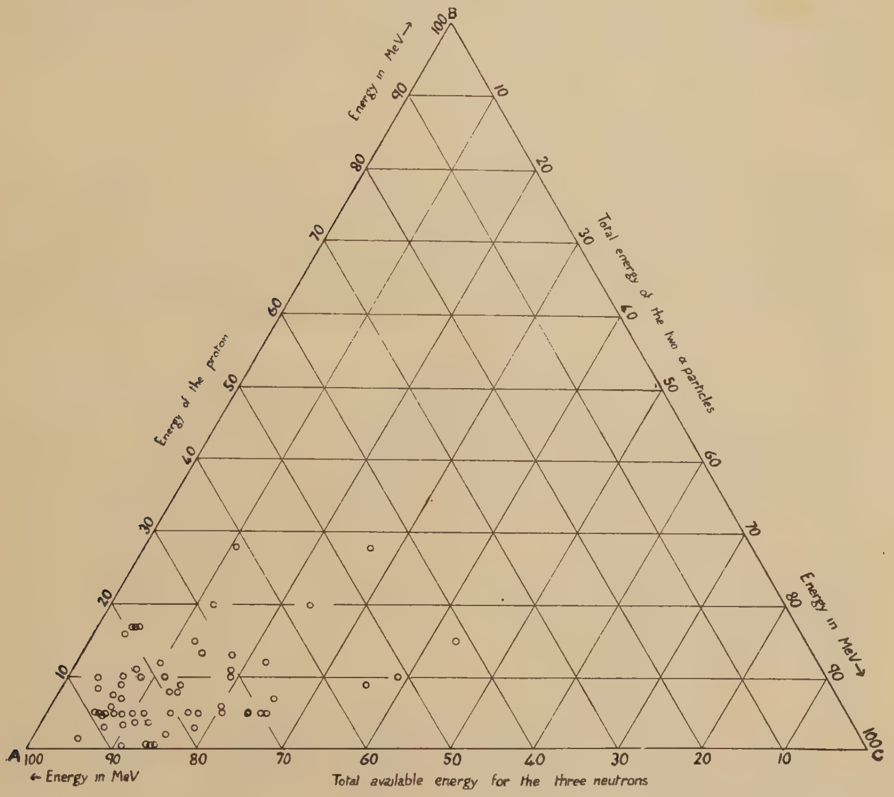

Distribution of the available energy amongst the disintegration fragments resulting from the disintegration of $^{12}_{6}C$.

The total energy of the two α-particles is constant along lines parallel to AB. Similarly, the energy of the proton and total available energy for the 3 neutrons is constant along lines parallel to AC and CB respectively.

These disintegrations appear to indicate that a larger part of the nucleus can sometimes take part in the primary interaction, and that the α-particles can interact as a whole group in the distribution of energy. It would seem, therefore, that the distance between the α-particle groups in a carbon nucleus is sufficiently small to permit this interaction to compete with the disintegration of a single α-cluster.

§ 19. COMPARISON OF THE DISINTEGRATIONS OF LIGHT AND HEAVY NUCLEI.

The present observations give support to the conclusion reached by previous observers that " radiative " capture, or the emission of neutrettos, rarely or never accompanies the capture of π^--particles by nuclei of charge number greater than six. It follows that several nucleons are involved in the primary act and one can, as a rough approximation, assume that all the nucleons situated within a certain distance of the interacting proton will be involved in the interaction. This distance may be computed, for instance, by applying the uncertainty relation (Bruno 1949)

$$\Delta r=c\Delta\tau \quad \text{with} \quad \Delta\tau\times\Delta E=\hbar \quad \text{and} \quad \Delta E=140 \text{ MeV.};$$

the result is $r=1{\cdot}35\ 10^{-13}$ cm.

There is, therefore, on this view, a certain volume of nuclear matter influenced by the primary interaction, and the dimensions of this volume are more or less constant and independent of the size of the nucleus. The difference between the characteristics of the disintegrations produced in light and heavy nuclei can then be explained qualitatively in the following terms :—

In heavy nuclei the primary interaction is confined to a relatively small part of the nucleus, and most of the fast nucleons originating from it lose their energy in the surrounding mass of the nucleus. When the interaction takes place near the edge of the nucleus, however, a nucleon may sometimes escape, either directly or after making one collision with a nucleon. Apart from these fast particles, the disintegration of the nucleus is independent of the precise characteristics of the primary process and takes place many nuclear periods afterwards, as a result of the rise in " temperature " of the nucleus.

In light nuclei the primary process involves a much larger part of the nucleus. The observed disintegration is likely to be much more dependent upon particular characteristics of the primary process, and especially on the number and the nature of the fragments which take part in the initial sharing of energy. This explains the occurrence of stars, originating from nuclei of the same type, which show wide variations in the total energy represented by the ejected charged particles. Owing to their strong cohesion the α-groups are likely to participate as a whole in the interaction, a fact which may explain the low probability of observing fast isolated protons from the disintegration of light nuclei.

CONCLUSIONS.

(*a*) The separation of σ-stars produced in light (C, N, O) and heavy (Ag, Br) nuclei in photographic emulsions has been carried out using three different methods. The results indicate that 46 ± 5 per cent of all visible σ-stars are due to the interaction of the π^--mesons with light nuclei, and 54 ± 5 per cent with heavy nuclei. 28 ± 2 per cent of all the π^--mesons absorbed suffer capture without producing any visible star.

(*b*) The relative frequency with which the disintegrations are accompanied by the emission of different numbers of charged particles has been determined separately for light and heavy nuclei. For light nuclei there is a maximum in the distribution at a point corresponding to the emission of three charged particles. For heavy nuclei, on the other hand, there is a rapid fall as the number of emitted particles increases, disintegrations with no charged particles emitted occurring most frequently.

(*c*) Nuclear reactions produced by the capture of π^--mesons in heavy nuclei exhibit characteristics most of which are in good accord with the general predictions of the Weisskopf evaporation theory. The average number of prongs observed per heavy nucleus is $1{\cdot}1 \pm {\cdot}15$. The α/p ratio, the ratio of the number of emitted α-particles to the number of protons, is $0{\cdot}30 \pm 0{\cdot}04$. The absence of any appreciable motion of the centre-of-mass system commonly prevents the observation of the recoil nuclei. The energy spectrum of the ejected protons has the characteristic Maxwellian form for particles of energy up to 20 MeV., and is consistent with an average excitation energy of 109 MeV. This value is in good accord with the observed prong distribution and α/p ratio.

The energy spectrum of the ejected protons departs from a Maxwellian distribution at high energies. $21{\cdot}4 \pm 2{\cdot}5$ per cent of the σ-stars in heavy nuclei have an associated fast particle of charge $|e|$ with an energy greater than 30 MeV. An interpretation is offered according to which these protons represent, " primary " protons resulting from the distribution of the rest-energy of the π^--mesons among three or more nucleons, or charged secondaries produced in the collisions with protons in the nucleus of fast " primary " neutrons.

(*d*) By applying the principle of the conservation of charge it has been found possible to identify the parent nucleus in about half the stars due to light elements ; and to study in particular the disintegration of ^{12}C and ^{14}N.

The nuclear reactions produced by the capture of π^--mesons in light elements show the following characteristics :—

(1) The rest-energy of the meson is not dispersed symmetrically amongst the products of the disintegration. In the majority of cases the primary interaction results in one or two fast neutrons and an excited residual nucleus.

(2) In the case of the disintegration of the $^{14}_{7}$N nucleus the states of excitation of the residual $^{12}_{6}$C nucleus into 3α particles have been measured.

(3) The presence in a few stars of high energy α-particles with energies exceeding 20 MeV. indicate that these particles may occasionally take part as a whole in the initial distribution of the rest-energy of the mesons.

(4) No tritons with energy $\sim$30 MeV., such as would result from the interaction of the π^--meson with an α-particle group on the neutron–triton model, have been observed. The occurrence of slow tritons from such a process, though unlikely, is not excluded.

(5) Particles of charge $|e|$ with energies greater than 30 MeV. have been observed in $4{\cdot}9 \pm 1{\cdot}5$ per cent of all the σ-stars produced in light nuclei.

ACKNOWLEDGMENTS.

We have pleasure in thanking Professor C. F. Powell, F.R.S., for his continued interest and encouragement during the course of the work. We are especially grateful to Dr. E. Gardner and Professor C. M. G. Lattes for arranging exposures of our plates in the Berkeley cyclotron, to Dr. H. Heitler for technical assistance and Mr. C. Waller of Ilford Ltd., for supplying us with the sandwich plates used in this investigation. We should also like to thank Professor H. Fröhlich and his group at the University of Liverpool and Mr. U. Camerini of this Laboratory, for helpful discussions.

One of us (O.R.) would like to take this opportunity to express his gratitude to the British Council for the award of a scholarship which has enabled him to pursue research at Bristol.

REFERENCES.

ADELMAN and JONES, 1949, *Phys. Rev.*, **75,** 1468 (A).
BRUECKNER and POWELL, 1949, *Phys. Rev.*, **75,** 1274.
BRUNO, 1948, *Ark. f. Mat. Astro. Fys.*, A. **36,** 1 ; 1949, *Ark. f. Fys.*, **1,** 19.
CHESTON and GOLDFARB, 1950, *Bull. Amer. Phys. Soc.*, **25** (1) (Abstract D 5).
CLEMENTEL and PUPPI, 1949, *Nuovo Cim.*, **6,** 1.
COSYNS, DILWORTH, OCCHIALINI, SCHOENBERG and PAGE, 1949, *Proc. Phys. Soc.* A, **62,** 801.
FERMI and TELLER, 1947, *Phys. Rev.*, **72,** 399.
FOWLER, 1950, *Phil. Mag.*, **41,** 169.
FRANZINETTI, 1950, *Phil. Mag.*, **41,** 86.
FUJIMOTO, HAYAKAWA and YAMAGUCHI, 1949, *Prog. Theor. Phys.*, **4,** 576.
FUJIMOTO and YAMAGUCHI, 1949, *Prog. Theor. Phys.*, **4,** 468.
GOLDBERGER, 1948, *Phys. Rev.*, **74,** 1269.
GOWARD, TITTERTON and WILKINS, 1950, *Proc. Phys. Soc.* A, **63,** 172.
HANNI, TELEGDI and ZUNTI, 1948, *Helv. Phys. Acta.*, **21,** 203.
HARDING, 1949, *Phil. Mag.*, **40,** 530.
HEIDMANN and LEPRINCE-RINGUET, 1948, *Comptes Rendus*, **226,** 1716.
HEISENBERG, 1937, *Leipziger Ber.*, **89,** 369.
LATTES and OCCHIALINI, 1947, *Nature, Lond.*, **159,** 331.
LE COUTEUR, 1950, *Proc. Phys. Soc.* A, **63,** 259.
MARSHAK, 1949, *Phys. Rev.*, **76,** 114.
MARSHAK and WHITMAN, 1950, *Bull. Amer. Phys. Soc.*, **25** (3) (Abstract M 6).
PANOFSKY, 1950, New York Meeting of the Amer. Phys. Soc.
PERKINS, 1948, *Nature, Lond.*, **161,** 487 ; 1949, *Phil. Mag.*, **40,** 601 ; 1950, *Ibid.*, **41,** 138.
OCCHIALINI and POWELL, 1948, *Nature, Lond.*, **162,** 168.
ROSENFELD, 1948, *Nuclear Forces* (Amsterdam : North Holland Publishing Co.), pp. 266.
RUDDLESDON and CLARK, 1949, *Nature, Lond.*, **164,** 487.
TAMOR, 1950, *Phys. Rev.*, **77,** 412.

LV. *Notices of New Books and Periodicals received.*

The Nature of Physical Theory. By P. W. Bridgman. (Dover Publications, Inc.). 1949.

The presentation of physical theory now generally accepted errs, according to Professor Bridgman, because interest centres on the mathematical equations summarizing physical knowledge, whilst inadequate attention is paid to the context within which these equations take on their significance—the context of the methodology of experimental physics. The "operational" viewpoint, first expounded in the author's earlier 'The Logic of Modern Physics', is extended in 'The Nature of Physical Theory' to more metaphysical, and therefore more controversial aspects of the subject, only briefly touched upon in his earlier work. It is to be hoped that, when discerning readers disagree with some of the arguments of the book, as is inevitable in so subtle and neglected a subject, they will thereby be stimulated to further thought upon it. Unquestionably, Professor Bridgman's critical examination of the principal physical theories makes it evident that they possess disquieting features of which most physicists will be surprised to learn. The book has a particularly important bearing on the validity of the rapidly developing subject of cosmology. W. R. H.

Electronic Engineering Master Index, 1947–48. Editor, John F. Rider. Price $19.50.

This is a most useful bibliography covering publications in electronics and allied subjects in the two years 1947 and 1948. It includes also patent specifications, and gives titles, authors and sources of the articles listed, but no abstracts. There is a cross index which refers also to previous editions. It might be criticized in its attempt to cover some subjects—for example, the entries headed "Nucleonics" comprise only about a page and seem to be chosen in an entirely arbitrary manner, but in the field of electrical communication and the more closely allied subjects, the entries appear to be very well classified and easy to locate. D. F. G.

Numerical Calculus. By W. E. Milne. [Pp. x+393; $6\frac{1}{4}'' \times 9\frac{1}{4}''$.] (Princeton University Press; London: Geoffrey Cumberlege, 1949.) English price 21*s*. net.

This book aims to bridge the gap between formal pure mathematics and detailed numerical answers. It covers the solution of simultaneous equations, approximation, interpolation, finite differences, numerical integration and differentiation, solution of differential equations, and curve-fitting by least squares. The book is essentially practical, and numerous examples are worked by methods best adapted to machine computation. While essential theory is given, proofs are often omitted or only briefly indicated; the method for finding complex roots could have been explained in more detail.

The book is clearly written and is thoroughly recommended both as a text for undergraduate courses in numerical methods and for scientists who are forced to seek numerical solutions. The casual user will find the classified guide to formulæ and methods in appendix C particularly useful when searching for a formula or method suited to a particular problem.

The text has been photographically reproduced from typescript and contains a number of trivial errors which could have been removed before printing. J. K. M.

Photoelasticity. By H. T. Jessop and F. C. Harris. (Cleaver-Hume Press Ltd.)

This is a good text-book for those wishing to learn the potentialities of the photoelastic method of stress analysis, as well as for those engaged in photoelastic work. It answers many of the questions which are often asked by those beginning to study the subject, and the principles are clearly explained without recourse to difficult mathematics. The book contains much helpful guidance in experimental methods, the fruits of many years' experience. As an example, the chapters on elementary optics and on the optical systems used in photoelasticity should be valuable to anyone setting up a photoelastic bench or wishing to improve the efficiency of an existing one. Consideration is given to the comparatively recent "frozen stress" method of three-dimensional stress analysis, of which the usefulness and limitations are discussed. A number of examples of the application of photoelastic methods to specific problems are given and the book includes tables of the mechanical and photoelastic properties of the materials used. The addition of a bibliography would have been useful to those wishing to make a more detailed study of the subject. C. A.

Tables of Inverse Hyperbolic Functions. By The Staff of the Computation Laboratory. [Pp. xx+290; $8\frac{1}{4}'' \times 10\frac{3}{4}''$.] (Harvard University Press; London: Geoffrey Cumberlege, 1949.). English price 55*s*. net.

The tables form volume 20 of "The Annals of the Computation Laboratory of Harvard University", and required a mere twelve days for computing and printing by the Automatic Sequence Controlled Calculator. They contain tables of the inverse hyperbolic sine, cosine, and tangent to nine decimal places, together with first and second forward differences; the interval in each part of the tables is chosen so that second-order interpolation gives the full nine decimal accuracy over almost the whole of the tables.

There are four tables: Table I. gives $\tanh^{-1} x$ for $x=0(0{\cdot}001-0{\cdot}00001)0{\cdot}99999$; Table II. gives $\sinh^{-1} x$ for $x=0(0{\cdot}002, 0{\cdot}005)3{\cdot}495$; Table III. gives $\cosh^{-1} x$ for $x=1{\cdot}00000(0{\cdot}00001-0{\cdot}002)3{\cdot}498$; Table IV. gives $\sinh^{-1} x$ and $\cosh^{-1} x$ for $x=3{\cdot}5(0{\cdot}005-20)22{,}980$, while for larger values of x these two functions differ from $\log_e 2x$ by less than the round-off error in the tables. The error in the tables is estimated to be less than 0·6 unit in the ninth decimal in Table I. and less than 0·9 unit in the ninth decimal in the other tables.

These tables are quite unique and should be of great use to physicists, statisticians, engineers and applied mathematicians generally. J. K. M.

The Variational Principles of Mechanics. By Cornelius Lanczos. (Toronto University Press. London: Geoffery Cumberleye.) [Pp. 307.] Price 42*s*.

It is stated in the preface that "the present treatise on the variational principles of mechanics should not be regarded as competing with the standard text-books on advanced mechanics . . . the author feels that there is room for monographs which exhibit the fundamental skeletons of the exact sciences in an elementary and philosophically orientated fashion". This statement is probably the simplest summary of a work which, starting from the principle of virtual work and D'Alembert's principle, derives the variational principles of Gauss, Hamilton, Jacobi and Least Action, and goes on to determine Lagrange's equations, and the canonical equations of motion and to discuss canonical transformations and the Hamilton–Jacobi equation. Although the present reviewer's view-point differs in some fundamental points from the author's, he found that the author's obvious enthusiasm had made the work eminently readable and likely to provide the student of the subject with a useful exposition. L. H.

[*The Editors do not hold themselves responsible for the views expressed by their correspondents.*]

α U. of Haw. Ca